

AD _____

AWARD NUMBER: DAMD17-03-1-0100

TITLE: Transcriptional Regulation by KLF6, A Novel Tumor Suppressor Gene in Prostate Cancer, Through Interaction with HATS and HDACS

PRINCIPAL INVESTIGATOR: Scott L. Friedman M.D.

CONTRACTING ORGANIZATION: Mount Sinai School of Medicine
New York, New York 10029-6574

REPORT DATE: March 2006

TYPE OF REPORT: Annual

PREPARED FOR: U.S. Army Medical Research and Materiel Command
Fort Detrick, Maryland 21702-5012

DISTRIBUTION STATEMENT: Approved for Public Release;
Distribution Unlimited

The views, opinions and/or findings contained in this report are those of the author(s) and should not be construed as an official Department of the Army position, policy or decision unless so designated by other documentation.

REPORT DOCUMENTATION PAGE

Form Approved
OMB No. 0704-0188

Public reporting burden for this collection of information is estimated to average 1 hour per response, including the time for reviewing instructions, searching existing data sources, gathering and maintaining the data needed, and completing and reviewing this collection of information. Send comments regarding this burden estimate or any other aspect of this collection of information, including suggestions for reducing this burden to Department of Defense, Washington Headquarters Services, Directorate for Information Operations and Reports (0704-0188), 1215 Jefferson Davis Highway, Suite 1204, Arlington, VA 22202-4302. Respondents should be aware that notwithstanding any other provision of law, no person shall be subject to any penalty for failing to comply with a collection of information if it does not display a currently valid OMB control number. **PLEASE DO NOT RETURN YOUR FORM TO THE ABOVE ADDRESS.**

1. REPORT DATE (DD-MM-YYYY) 01-03-2006			2. REPORT TYPE Annual		3. DATES COVERED (From - To) 1 Mar 2005 – 28 Feb 2006	
4. TITLE AND SUBTITLE Transcriptional Regulation by KLF6, A Novel Tumor Suppressor Gene in Prostate Cancer, Through Interaction with HATS and HDACS					5a. CONTRACT NUMBER	
					5b. GRANT NUMBER DAMD17-03-1-0100	
					5c. PROGRAM ELEMENT NUMBER	
6. AUTHOR(S) Scott L. Friedman M.D. E-Mail: Scott.Friedman@mssm.edu					5d. PROJECT NUMBER	
					5e. TASK NUMBER	
					5f. WORK UNIT NUMBER	
7. PERFORMING ORGANIZATION NAME(S) AND ADDRESS(ES) Mount Sinai School of Medicine New York, New York 10029-6574					8. PERFORMING ORGANIZATION REPORT NUMBER	
9. SPONSORING / MONITORING AGENCY NAME(S) AND ADDRESS(ES) U.S. Army Medical Research and Materiel Command Fort Detrick, Maryland 21702-5012						
12. DISTRIBUTION / AVAILABILITY STATEMENT Approved for Public Release; Distribution Unlimited					10. SPONSOR/MONITOR'S ACRONYM(S)	
					11. SPONSOR/MONITOR'S REPORT NUMBER(S)	
13. SUPPLEMENTARY NOTES						
14. ABSTRACT KLF6 is a zinc finger transcription factor mutated in more than 50% of sporadic prostate cancers. Our studies have explored the role of acetylation of KLF6, and how its abrogation by mutation in human cancer may contribute to its dysregulation and emergence of prostate cancer. The KLF6 tumor suppressor protein normally inhibits cell growth by upregulating p21(WAF1/CIP1) independent of p53, whereas most tumor derived mutations are no longer growth-suppressive (Narla et al, Science 294:2563,2001). We have demonstrated by chromatin that transactivation of p21 by KLF6 occurs through its direct recruitment to the p21 promoter and requires acetylation by histone acetyltransferase activity. Based on these data we have extended findings to uncover additional cancers in which KLF6 is dysregulated and have defined a novel pathway of KLF6 dysregulation through generation of dominant negative alternative splice forms that are overexpressed in many cancers. These data suggest that multiple mechanisms including loss of acetylation contribution to KLF6 dysregulation that contributes to carcinogenesis in prostate and other cancers.						
15. SUBJECT TERMS Tumor suppressor gene in prostate cancer; transcriptional regulation; histone acetyltransferase, histone deacetylase						
16. SECURITY CLASSIFICATION OF:				17. LIMITATION OF ABSTRACT	18. NUMBER OF PAGES	19a. NAME OF RESPONSIBLE PERSON USAMRMC
a. REPORT U	b. ABSTRACT U	c. THIS PAGE U	19b. TELEPHONE NUMBER (include area code)			

Table of Contents

Cover	1
SF 298	2
Introduction	4
Body	4-6
Key Research Accomplishments	6
Reportable Outcomes	6
Conclusions	7
References	7
Appendices	8-80

INTRODUCTION

We have comprehensively addressed the role of Kruppel-like factor 6 (KLF6) as a new tumor suppressor gene mutated in a majority of human prostate cancers (1) and have extended these studies to include not only those aspects proposed in the original application, but have explored its role in a number of other tumors.

We have established key functional properties of KLF6. While wild-type KLF6 transactivates the cyclin-cdk inhibitor p21 (Waf1/Cip1) in a p53-independent manner and significantly reduces cell proliferation, tumor-derived KLF6 mutants do not(1). We have defined the impact of tumor derived mutations of KLF6 by specifically examining whether loss of lysines, a key acetylation site, contribute to its loss of KLF6 function in prostate cancer (2). We have established that KLF6 is an acetylated protein in vivo, and in vitro it can be acetylated by CBP and PCAF. Importantly, we have characterized in detail the acetylation pattern and biological activities of wild type and mutant KLF6 in order to understand the biologic function of this important tumor suppressor gene. Finally, in work supported by DOD we have also broadened our understanding of KLF6 dysregulation in human cancer by defining the presence of splice variants that antagonize the growth suppressor activity of wild type KLF6, and are over-expressed in several human cancers(3).

BODY

The studies completed are detailed in a series of publications in which support by DOD was acknowledged (note that in earlier publications the incorrect grant number was cited as “PC02770” rather than “DAMD17-03-01-0100”). All data summarized in earlier annual reports are now contained entirely within the cited publications, in particular publications #'s 1 & 2. These **publications** are attached as appendices #1 - 7 (see pages 8-80) and briefly summarized here:

1. Li D, Yea S, Cooreman MP, Li S, Narla G, Laborda J Banck M, Friedman SL (corresponding author) and Walsh MJ. KLF6 promotes preadipocyte differentiation through histone deacetylase 3 (HDAC3)-dependent repression of *Dlk1* . **Journal of Biological Chemistry**, 280(29): 26941-52, 2005.

This study documented the role of acetylation in of KLF6 by HDACs in promoting differentiation, a function hypothesized to extend to its role in prostate differentiation.

2. Li D, Yea S, Dolios D, Martignetti JA, Narla G, Wang R, Walsh MJ and Friedman SL. Regulation of Krüppel-like factor 6 tumor suppressor activity by acetylation. **Cancer Research**, 65(20):9216-9225, 2005.

This study defined the specific functional importance of lysine mutations found in prostate cancer that specifically affect the transactivating function of KLF6 through altered acetylation.

3. Kimmelman A, Qiao RF, Narla G, Bos P, Sanfiz A, Lau N, Li D, Eng FJ, Liang BC, Guha A, Martignetti JA, Friedman SL and Chan AML. Suppression of

Friedman, SL, Award No. DAMD17-03-01-0100-FINAL
glioblastoma tumorigenicity by the Kruppel-like transcription factor, KLF6.
Oncogene, 23:5077-83, 2004.

This publication extended the original studies in prostate cancer to another malignancy, glioblastoma, establishing a novel pathway of tumor suppression through antagonism of PDGF mediated transformation.

4. Rubinstein M, Idelman G, R Plymate SR, Narla G, Friedman SL, and Werner H. Transcriptional activation of the IGF-I receptor gene by the KLF6 tumor suppressor: potential interactions between KLF6 and p53. **Endocrinology**, 145(8): 3769-77, 2004.

This work defines an important interaction between KLF6 and p53 in regulating IGF receptor gene expression, a key pathway in prostate carcinogenesis.

5. Kremer-Tal S, Reeves HL, Narla G, Thung SN, Schwartz M, Difeo A, Katz A, Bruix J, Bioulac-Sage B, Martignetti JA, Friedman SL. Frequent inactivation of the tumor suppressor Kruppel like factor 6 (KLF6) in hepatocellular carcinoma. **Hepatology**, 40:1047-1052, 2004.

Studies in this manuscript further established the role of KLF6 as a tumor suppressor in yet another primary cancer. DOD support was instrumental in performing biology analysis of KLF6 activity in HCC lines (Figure 2 in attached manuscript), since this utilized reagents and methodology also applied to our studies of prostate cancer.

6. Narla G, Difeo A, Yao S, Banno A, Hod E, Reeves H, Qiao RF, Camacho-Vanegas O, Levine A, Kirschenbaum A, Chan AM, Friedman SL*, and Martignetti JA* (*shared senior authorship). Targeted inhibition of the KLF6 splice variant KLF6SV1 suppresses prostate cancer growth and spread. **Cancer Research**, 65(13): 5761-5768, 2005.

This work defined a novel pathway of KLF6 inactivation through generation of dominant negative alternative splice products, further underscoring the role of KLF6 dysregulation of prostate carcinogenesis, which was the major theme of the DOD funded studies.

7. Narla G, Kremer-Tal S, Matsumoto N, Zhao X, Yao S, Kelley K, Tarocchi M, and Friedman SL. *In vivo* regulation of p21 by the KLF6 tumor suppressor gene in mouse liver and human hepatocellular carcinoma. Invited resubmission to **Oncogene**, currently under re-review.

This study extends the findings characterized in manuscript #1 (above) exploring mechanisms of p21 regulation by KLF6 and thus drew upon studies funded by DOD.

List of Personnel Receiving Pay from the Research Effort:

Friedman, Scott (MD)
Narla, Goutham (MD, PhD)
Katz, Amanda (BS)
Veal, Nary (PhD)
Loke, Johnny (MS)
Marcos, Luis (MD)
Yea, Steven (MD, PhD, 2008)

KEY RESEARCH ACCOMPLISHMENTS

The following are key accomplishments as detailed in the preceding section:

- **Acetylation of KLF6 is a major mode of regulating its activity as a trans-repressor factor and tumor suppressor**
- **CBP and PCAF synergize with KLF6 in transactivating p21 and KLF6 is acetylated in vitro by CBP and PCAF, and is acetylated in vivo**
- **Loss of lysines in prostate cancer -derived KLF6 mutations leads to impaired repressive function of KLF6 and enhanced growth**
- **An additional pathway of KLF6 inactivation in prostate cancer is through the generation of dominant negative isoforms that antagonize full length KLF6.**
- **Dysregulation of KLF6 as originally discovered in prostate cancer also extends to other major tumors, including HCC glioblastoma**
- **KLF6 interacts with p53, a major tumor suppressor, in regulating IGF receptor gene expression, a prominent pathway in prostate carcinogenesis.**

REPORTABLE OUTCOMES:

Manuscripts: See above for published manuscripts,1-6 (attached as Appendix)

Patents: US Patent pending. *A germline DNA polymorphism enhances alternative splicing of the KLF6 tumor suppressor gene and is associated with increased cancer risk.*
Inventors: John A. Martignetti, M.D., PhD, Goutham Narla and Scott L. Friedman, M.D.

Degrees obtained: Goutham Narla, Ph.D. (awarded May 2006)
Steven Yea, Ph.D. (expected May 2008)

Licenses: none

Training supported by this award:

Goutham Narla – PhD Thesis studies
Steven Yea – PhD Thesis studies
Luis Marcos MD – postdoctoral research studies

CONCLUSIONS

The findings in aggregate confirmed our hypothesis that acetylation of KLF6 is an important post-translational modification of the wild type protein, which when abrogated through mutation, led to loss of protein function and lack of growth suppression. These findings explain how mutations of lysine residues, which we have identified in primary prostate cancers, lead to loss of KLF6 tumor suppressor function. Additional studies have defined new pathways of KLF6 inactivation in prostate cancer, and have unearthed evidence of functional interactions of KLF6 with p53, a major tumor suppressor in prostate carcinogenesis. Finally, methods and reagents used to define KLF6's role as a tumor suppressor in prostate cancer were applied to the study of other major cancers, broadening and solidifying the evidence of a widespread role of KLF6 as a tumor suppressor in a number of tumors beyond prostate, including glioblastoma, and primary hepatocellular carcinoma.

REFERENCES

1. Narla G, Heath KE, Reeves HL, Li D, Giono LE, Kimmelman AC, Glucksman MJ, et al. KLF6, a candidate tumor suppressor gene mutated in prostate cancer. *Science* 2001;294:2563-2566.
2. Li D, Yea S, Dolios G, Martignetti JA, Narla G, Wang R, Walsh MJ, et al. Regulation of Kruppel-like factor 6 tumor suppressor activity by acetylation. *Cancer Res* 2005;65:9216-9225.
3. Narla G, DiFeo A, Yao S, Banno A, Hod E, Reeves HL, Qiao RF, et al. Targeted inhibition of the KLF6 splice variant, KLF6 SV1, suppresses prostate cancer cell growth and spread. *Cancer Res* 2005;65:5761-5768.

Krüppel-like Factor-6 Promotes Preadipocyte Differentiation through Histone Deacetylase 3-dependent Repression of DLK1*

Received for publication, January 13, 2005, and in revised form, May 9, 2005
Published, JBC Papers in Press, May 25, 2005, DOI 10.1074/jbc.M500463200

Dan Li,^a Steven Yea,^{a,b} Side Li,^c Zhu Chen,^d Goutham Narla,^a Michaela Banck,^a Jorge Laborda,^e Song Tan,^{f,g} Jeffrey M. Friedman,^d Scott L. Friedman,^{a,h} and Martin J. Walsh^c

From the ^aDivision of Liver Diseases, Department of Medicine, Mount Sinai School of Medicine, New York, New York 10029, the ^bDepartment of Inorganic and Organic Chemistry and Biochemistry, Molecular Biology Branch, Medical School, University of Castilla-La Mancha, 02071 Albacete, Spain, the ^cDepartment of Pediatrics, Mount Sinai School of Medicine, New York, New York 10029, ^dHoward Hughes Medical Institute, Laboratory of Molecular Genetics, Rockefeller University, New York, New York 10021, and the ^eCenter for Gene Regulation, the Department of Biochemistry and Molecular Biology, Pennsylvania State University, University Park, Pennsylvania 16802

Preadipocyte differentiation occurs during distinct periods of human development and is a key determinant of body mass. Transcriptional events underlying adipogenesis continue to emerge, but the link between chromatin remodeling of specific target loci and preadipocyte differentiation remains elusive. We have identified Krüppel-like factor-6 (KLF6), a recently described tumor suppressor gene, as a repressor of the proto-oncogene Delta-like 1 (*Dlk1*), a gene encoding a transmembrane protein that inhibits adipocyte differentiation. Forced expression of KLF6 strongly inhibits *Dlk1* expression in preadipocytes and NIH 3T3 cells *in vivo*, whereas down-regulation of KLF6 in 3T3-L1 cells by small interfering RNA prevents adipogenesis. Repression of *Dlk1* requires HDAC3 deacetylase activity, which is recruited to the endogenous *Dlk1* promoter where it interacts with KLF6. Our studies identify the interaction between HDAC3 and KLF6 as a potential mechanism underlying human adipogenesis, and highlight the role of KLF6 as a multifunctional transcriptional regulator capable of mediating adipocyte differentiation through gene repression.

Adipocyte differentiation requires coordinated expression of general and tissue-specific regulatory proteins in a defined sequence (1, 2). A critical regulator of adipogenesis is *Dlk1*,¹ also called preadipocyte factor-1, whose sustained expression prevents differentiation of 3T3-L1 preadipocytes into adipocytes (3). *Dlk1* encodes DLK1, a transmembrane epidermal

growth factor repeat domain-containing protein highly expressed in preadipocytes and other cells (4). The abrupt down-regulation of *Dlk1* following hormonal stimulation in preadipocytes is an early and necessary event in the phenotypic conversion to fat cells. Forced expression of *Dlk1* prevents adipogenesis, whereas enforced down-regulation enhances adipocyte differentiation. Following the reduction in DLK1, rapid induction of adipogenic transcription factors, including SREBP1, C/EBP β/γ then C/EBP α , and PPAR γ 2, leads to terminal differentiation of adipocytes, and expression of adipocyte proteins, including leptin and adiponectin (1, 2).

Our previous work (5) has explored the activity of a transcription factor, KLF6 (also known as Zf9 or CPBP), a ubiquitously expressed 283-amino acid Krüppel-like zinc finger protein and a member of a growing family of related transcriptional regulators. KLF6 contains an 82-amino acid C-terminal DNA-binding domain identical to other Krüppel-like factors, and a 201-amino acid N-terminal activation domain, whose only homology is to KLF7 in its N-terminal 41 amino acids (6). KLF6 was originally identified as a rapidly induced mRNA following activation of hepatic stellate cells, a mesenchymal liver cell, during liver injury (7). Most interestingly, stellate cells harbor many features of adipocytes, including the storage of lipids as vitamin A esters (retinoids), the production of leptin, and phenotypic plasticity in defined biologic contexts (8). Transcriptional targets of KLF6 include transforming growth factor- β 1 and its receptors (9), urokinase-type plasminogen activator (10), and the human immunodeficiency virus-long terminal repeat (11). Recently, we have established Krüppel-like factor 6 (KLF6) as a novel tumor suppressor gene frequently mutated in human prostate and colon cancers (12, 13). A key mechanism of tumor suppression by KLF6 is the transcriptional up-regulation of p21^{waf1,cdi} a cyclin-dependent kinase inhibitor whose induction also accounts for the growth suppressive activity of the tumor suppressor p53 (12).

Although many studies have described down-regulation of *Dlk1* during adipocyte differentiation, the underlying mechanisms regulating this event have not been well characterized. The phenotype resemblance of hepatic stellate cells (the original source of KLF6) to adipocytes led us to explore a potential role of KLF6 in adipogenesis, particularly because stellate cell activation in liver injury is also accompanied by KLF6 induction (7, 8). In fact, previous studies have documented the induction of KLF6 during adipocyte differentiation, but its role in this process has been unclear (14).

Our preliminary experiments, using a commercial membrane array (Clontech), identified *Dlk1* as a strongly repressed

* This work was supported in part by United States Public Health Service Awards DK37340 (to S. L. F.), DK56621 (to S. L. F.), HL67099 (to M. J. W.), CA98552 (to M. J. W.), and DK41096 (to J. M. F.) from the National Institutes of Health and Department of Defense Grant DAMD 17-03-01-0100 (to S. L. F.). The costs of publication of this article were defrayed in part by the payment of page charges. This article must therefore be hereby marked "advertisement" in accordance with 18 U.S.C. Section 1734 solely to indicate this fact.

^b Performed this work as a Medical Student Research Fellow of the Howard Hughes Medical Institute.

^g Pew Scholar in the Biomedical Sciences.

^h To whom correspondence may be addressed: Box 1123, Mount Sinai School of Medicine, 1425 Madison Ave., Rm. 11-70C, New York, NY 10029. Tel.: 212-659-9501; Fax: 212-849-2574; E-mail: scott.friedman@mssm.edu.

¹ The abbreviations used are: *Dlk1*, Delta-like 1; KLF6, Krüppel-like factor 6; TSA, trichostatin A; shRNA, short hairpin ribonucleic acid; HDAC, histone deacetylase; ChIP, chromatin immunoprecipitation; siRNA, small interfering RNA; PPAR, peroxisome proliferator-activated receptor; PBS, phosphate-buffered saline; TEV, tobacco etch virus; Rb, retinoblastoma.

mRNA following induction of *KLF6* in fibroblasts (data not shown). The aim of the present study was to investigate whether *Dlk1* is a transcriptional target of *KLF6* and, if so, to elucidate the mechanism of *Dlk1* gene regulation by *KLF6*. Our data demonstrate that *KLF6* promotes adipocyte differentiation by transcriptionally repressing *Dlk1* expression, and this repression specifically requires the deacetylase activity of HDAC3.

MATERIALS AND METHODS

Expression Plasmids—PCIneo-KLF6 (human) expression plasmid was constructed as described previously (7, 8). pCDNA3-HDAC3-FLAG and pCDNA3-HDAC3 (15) constructs were gifts from Dr. Eric Verdin (Gladstone Institute for Virology and Immunology at University of California, San Francisco). The tetracycline-inducible expression system constructs pTet-splice and pTet-tTAK were purchased from Invitrogen. Expression plasmids pVgRXR and pIND for the ecdysone-inducible mammalian expression system were purchased and prepared for cloning (Invitrogen). The expression plasmid pVgRXR (Invitrogen) was used to establish 3T3-L1 cells under Zeocin™ selection (600 µg/ml) to produce a stable transcriptional transactivator 3T3-L1 cell line following the manufacturer's procedures (Invitrogen). Insertion of the FLAG-HDAC3 fragment into the pIND expression vector was by digesting pCDNA3-HDAC3-FLAG with EcoRI and NotI. The resulting HDAC3-containing DNA fragment was then ligated into the EcoRI site of pIND. The cDNA insert was confirmed by DNA sequence analysis. Cell culture and differentiation of preadipocytes.

Tissue and Cell Culture—3T3-L1, NIH 3T3, HeLa, 293 and 293T cell lines were obtained from the American Tissue Culture Collection (ATCC). 3T3-L1 cells were grown in Dulbecco's modified Eagle's medium, supplemented with 10% calf serum (Invitrogen), 100 units/ml penicillin and 100 units/ml streptomycin, and 2 mM L-glutamine (Invitrogen). NIH 3T3, 293, and 293T cells were cultured in Dulbecco's modified Eagle's medium, supplemented with 10% fetal bovine serum (Hyclone), 100 units/ml penicillin and 100 units/ml streptomycin, and 2 mM L-glutamine. For induction of adipocyte differentiation, 3T3-L1 and Balb/c 3T3 cells were cultured in the presence of 4 µM biotin (Sigma) until the day of induction. Cells were re-incubated in medium containing 10% calf serum, 4 µM biotin, 0.5 mM isobutylmethylxanthine, 1 µM dexamethasone (Sigma), and 1 µM insulin (Sigma). Culture medium was changed every 3 days. For histology, cells were fixed with 2% formaldehyde, 0.2% glutaraldehyde in PBS for 15 min, rinsed in PBS, and stained with Oil Red O (0.6% in 60% isopropyl alcohol for 25 min).

Transfection Assays—Transient transfections were performed using Lipofectamine 2000 reagent (Invitrogen). For luciferase assay, 3T3-L1 cells or HeLa cells cultured in 10-cm plates (Corning Glass) were transfected with 10 µg of pCIneo empty vector or pCIneo-KLF6, with or without pCDNA3-HDAC3, as indicated in the text, together with the *Dlk1* promoter-luciferase construct. Five ng of pRL-TK plasmid (Promega) were co-transfected in each dish as a control for transfection efficiency. Forty eight hours after transfection, cells were washed three times with cold PBS and cell lysates prepared using dual-luciferase reporter assay system (Promega). The luciferase activity in 10 µl of lysate was determined using the dual-luciferase reporter assay system and a Dynex luminometer. Transfection efficiency was normalized to *Renilla* luciferase activity measured in the same lysate.

Stable Transfection and Tetracycline-inducible Expression of *KLF6* in Cultured Cells—To establish cell lines stably expressing *KLF6*, 3T3-L1 cells were transfected with 10 µg of pCIneo-KLF6. Ten µg of pCIneo was transfected separately as a control. Two days after transfection, cells were selected with 600 µg/ml geneticin (Invitrogen). Individual colonies resistant to the selective medium were transferred to new plates for expansion.

A tetracycline-inducible system for regulated expression of *KLF6* was established as described (16), with modification. Briefly, pTet-KLF6 was constructed by inserting the rat *KLF6* cDNA into AccI/EcoRV sites of pTet-splice vector (Invitrogen). A tetracycline-inducible cell line expressing *KLF6* was established by co-transfecting pTet-KLF6 and pBpuro into NIH 3T3 cells line that expressed pTet-pTAK, followed by selection with histidine-deficient Dulbecco's modified Eagle's medium (Irvine Scientific) containing 2 µg/ml puromycin (Sigma) in the presence of 2 µg/ml tetracycline (Sigma). For induction of *KLF6*, cells were washed three times with serum-free Dulbecco's modified Eagle's medium and changed to medium without tetracycline.

Stable Transfection and Ponasterone A-inducible Expression of FLAG-tagged HDAC3 in 3T3-L1 Preadipocytes—Following the inser-

tion of FLAG-tagged HDAC3 into expression vector pIND (see above), stable transfectants of 3T3-L1 cells carrying the pVgRXR transgene under Zeocin™ drug selection were used following transfection of the pIND-FLAG/HDAC3 construct. After 48 h, transfected 3T3-L1 cells were placed under growth selection with 400 µg/ml G418 (geneticin, Invitrogen) and 400 µg/ml Zeocin™ for 2 weeks to select for both transgenes and individual populations of stably transfected 3T3-L1 cells. Individual clones were then selected for the induction of the FLAG-tagged HDAC3 target gene following treatment with ponasterone A (5 µM) (Sigma) and analyzed by immunoblot studies.

Northern Blot Analysis—Cells were washed twice with cold PBS, and total RNA was isolated using TRIzol Reagent (Invitrogen) according to the manufacturer's instructions. Ten micrograms of total RNA from each sample was electrophoresed in 1% formaldehyde-agarose gel, stained with ethidium bromide, and transferred to Hybond N+ (Amersham Biosciences). After UV cross-linking, filters were prehybridized overnight at 42 °C in 50% formamide, 5× SSC, 2.5× Denhardt's solution, 0.1% SDS, and 100 µg/ml herring sperm DNA. Membranes were hybridized overnight at 42 °C with ³²P-labeled cDNA probes for *Dlk1* and glyceraldehyde-3-phosphate dehydrogenase. After hybridization, blots were washed three times with 2× SSC, 0.1% SDS, 20 min each wash, followed by exposure to Kodak MS film at -80 °C.

Real Time Reverse-Transcription-PCR of Total RNA—3T3-L1 cells were grown on 10-cm plastic plates, induced to differentiate into adipocytes, as described above, and then harvested at 100% confluency. Total cellular RNA was extracted using Trizol reagent® and chloroform extraction. RNA concentration was measured by spectrophotometry. Synthesis of cDNA was performed on 2 µg of total RNA per sample with random primers using reagents contained in the reverse transcription system kit according to the manufacturer's protocol (Promega Corp., Madison, WI). The reverse transcriptase product was diluted 20-fold in nuclease-free H₂O, and 5 µl of each sample were loaded into 96-well plates for real time PCR in an ABI Prism 7700 sequence detection system (Applied Biosystems). β-Actin was used as a housekeeping gene for normalization, and H₂O was used as negative control. Amplifications were performed using oligonucleotide primers for murine *KLF6* (upper, 5'-GAGTTCCTCCGTCATTTCCA-3', and lower, 5'-GTCGC-CATTACCCTTGTCAC-3'), murine *Dlk1* (upper, 5'-TGTCAGGAGTCTGCAAGG-3', and lower, 5'-TCGTAAGTGGCCTTTCTCCAG-3'), and β-actin (upper, 5'-GATGAGATTGGCATGGCTTT-3', and lower, 5'-AGAGGTGGGGTGGCTT-3'), platinum Taq polymerase, and SYBR Green as fluorescent DNA-binding dye. Fluorescence signals were analyzed during each of 40 cycles (denaturation, 15 s at 95 °C; annealing, 15 s at 56 °C; and extension, 40 s at 72 °C). Detection of the PCR products by agarose gel electrophoresis confirmed the homogeneity of the DNA products. Relative quantitation was calculated using the comparative threshold cycle (C_T) method as described in the User Bulletin 2, ABI PRISM 7700 sequence detection system. C_T indicates the fractional cycle number at which the amount of amplified target genes reaches a fixed threshold within the linear phase of gene amplification and is inversely related to the abundance of mRNA transcripts in the initial sample. Mean C_T of duplicate measurements was used to calculate ΔC_T as the difference in C_T for target and reference. ΔC_T for each sample was compared with the corresponding C_T at day 0 and expressed as $\Delta \Delta C_T$. Relative quantitation was expressed as fold change of the gene of interest compared with the starting condition (day 0), according to the formula $2^{-\Delta \Delta C_T}$.

Taqman Quantitative PCR—Quantitative reverse transcription-PCR was performed by the Taqman system (Applied Biosystems) according to the manufacturer's instructions. Oligonucleotides were designed by the PrimerExpress software. C_T for the internal control (cyclophilin) and target genes were determined from raw fluorescence. The amount of each gene was derived from its C_T and normalized with the amount of cyclophilin. Samples are in duplicate.

Sequences of the Taqman primers and probes are as following: cyclophilin-F, 5'-TGTGCCAGGGTGGTACTT-3'; cyclophilin-R, 5'-TCA-AATTCTCTCCGTAGATGGACTT-3'; cyclophilin probe, 5'-ACACGC-CATAATGGCACTGGTGG-3'; aP2-F, 5'-CACCGCAGACGACAGGAA-G-3'; aP2-R, 5'-GCACCTGCACCAGGGC-3'; aP2 probe, 5'-CCGCCAT-CTAAGGTTATGATGCTCTTCA-3'; PPAR-γ2-F, 5'-CCATTCTGGCC-CACCAAC-3'; PPAR-γ2-R, 5'-AATGCGAGTGGCTCTCCATCA-3'; PPAR-γ2 probe, 5'-TCGGAATCAGCTCTGTGACCTCTCC-3'; C/EBPα-F, 5'-TCTGCGAGCAGCAGACGTC-3'; C/EBPα-R, 5'-AACTCGTGGTTG-AAGGCGG-3'; C/EBPα probe, 5'-AGACATCAGCGCCTACATCGACC-CG-3'; SCD-1-F, 5'-GCGCTTTGCAAGGTAATGTG-3'; SCD1-R, 5'-CC-TTTCAGCAGCACTGTACCAC-3'; and SCD1 probe, 5'-CCTGCC-TGCATGGATCAGCCAAAG-3'.

Electrophoretic Mobility Shift Assays—Gel shift assays were per-

formed using a commercial gel shift assay system (Promega). The oligonucleotide sequences from the *Dlk1* promoter were as follows (with putative KLF6-binding site underlined, and mutated position(s) indicated): wild type, sense, 5'-CGCGAGGGCGTGGGCGTGGGCGGGGGC-3'; antisense, 5'-GCCCCCGCCACGCCACGCCCTCGCG-3'; mutant, sense, 5'-CGCGAAAAATGAAAATGAAAAGGGGC-3'; antisense, 5'-GCCCCTTTTCATTTTCATTTTTCGCG-3'.

Single-stranded oligonucleotides (Genelink) were labeled with [γ -³²P]ATP using T4 polynucleotide kinase. Double-stranded oligonucleotide probes were created by annealing complementary single-stranded oligonucleotides. Nuclear extracts from 3T3-L1 preadipocytes (Geneka) were used for gel shift. DNA-binding reactions were performed with 10 μ g of 3T3-L1 nuclear extract incubated for 10 min at room temperature with 1 \times gel shift binding buffer containing 4% glycerol, 1 mM MgCl₂, 0.5 mM EDTA, 0.5 mM dithiothreitol, 50 mM NaCl, 10 mM Tris-HCl (pH 7.5), and 50 μ g/ml poly(dI-dC), with or without unlabeled competitor oligonucleotides.

A monoclonal antibody was generated for use in supershift assays. To do so, the N terminus of KLF6 (amino acids 1–200) was expressed as a recombinant glutathione *S*-transferase fusion protein in *Escherichia coli*, purified, and inoculated into BALB/c mice. Hybridomas were screened by enzyme-linked immunosorbent assay. The monoclonal antibody "2A2" was found to be suitable for KLF6 detection in Western blot and supershift. For supershift, 1.5 μ g of monoclonal anti-KLF6 antibody was incubated with the above nuclear extract in the presence of 1 \times gel shift binding buffer for 1 h at room temperature. Next, 1 μ l (~20,000 cpm/ μ l) of radiolabeled probe was added, and the mixture was incubated for an additional 20 min at room temperature. The DNA-protein complexes were separated through a 4.5% nondenaturing polyacrylamide gel for 2.5 h at 250 V, at room temperature. Gels were dried and exposed to Kodak MS film for 5 h to overnight at -80 °C with an intensifying screen.

Chromatin Immunoprecipitation Assay—Chromatin immunoprecipitation assays were performed using a commercial kit following the manufacturer's instructions (Upstate Biotechnologies, Inc.). Briefly, 2 \times 10⁶ 3T3-L1 cells at the 5th day of differentiation were cross-linked with 1% formaldehyde for 10 min at 37 °C, followed by cell lysis and sonication fracture of the DNA into 200–1000-bp fragments. Proteins cross-linked to DNA were immunoprecipitated with 10 μ g of anti-Zf9/KLF6 antibody (R-173) (Santa Cruz Biotechnology) or two different anti-HDAC3 antibodies (a gift from Dr. Eric Verdin, and anti-HDAC3 antibody from Upstate Biotechnology, Inc., respectively) and 40 μ l of salmon sperm DNA/protein-A-agarose beads. The protein-A-agarose-antibody-protein complexes were washed extensively and eluted, according to the manufacturer's recommendations. The cross-link was reversed by heating at 65 °C for 4 h, and proteins were digested by proteinase K for 1 h at 45 °C. DNA was recovered by phenol/chloroform extraction and ethanol precipitation in the presence of 10 μ g/ml yeast tRNA carrier and used as a template for PCRs. Genomic sequence primers encompassing the promoter region -481 to -283 upstream of transcriptional start site were used to amplify immunoprecipitated DNA: forward, 5'-GTGGTTTTCGTGTGTCATC-3'; reverse, 5'-GCGTCTCAGGCCGC-3'.

Immunoprecipitation and Western Blotting—For co-immunoprecipitation assay, 293T cells were transfected with 20 μ g of plasmid DNA. Thirty six hours after transfection, cells were washed twice with cold PBS and lysed on ice for 20 min using IP lysis buffer containing 0.5% Nonidet P-40, 50 mM Tris-Cl (pH 7.4), 120 mM NaCl, and protease inhibitors (Complete Protease Inhibitor Mixture Tablets, Roche Applied Science). The cell lysate was precipitated for 30 min at 14,000 \times *g* at 4 °C. The supernatant was immunoprecipitated at 4 °C for 1 h using 4 μ g of anti-Zf9/KLF6 antibody (R-173) (Santa Cruz Biotechnology) or 4 μ g of anti-HDAC3 antibody (Upstate Biotechnology, Inc.) with 50 μ l of protein-G beads (Pierce) or using 50 μ l of M2 anti-FLAG-agarose (Sigma). The beads were subsequently washed three times with 800 μ l of IP wash buffer (0.5% Nonidet P-40, 50 mM Tris-HCl (pH 7.4), and 500 mM NaCl), solubilized in Laemmli sample buffer (Sigma) containing 5% β -mercaptoethanol, boiled, and subjected to SDS-PAGE followed by Western blotting as described below. As a negative control, immunoprecipitation was conducted using control rabbit or mouse IgG (Sigma). For immunoprecipitations and immunoblotting procedures with the various antibodies against HDAC1–5 and -7, the antibodies were obtained from various sources and described in the Fig. 6 legend.

For Western blotting, cell extracts were harvested in RIPA buffer (Santa Cruz Biotechnology, standard protocol). Protein samples (30 μ g/sample) were separated on SDS-polyacrylamide gel and transferred to a nitrocellulose membrane (Bio-Rad). The membranes were blocked in 5% milk in 10 mM Tris-Cl (pH 8.0), 150 mM NaCl, and 0.1% Tween 20

(1 \times TBS-T) for 1 h at room temperature. The membrane was incubated with primary antibody (anti-Zf9/KLF6 (R-173) 1:2,000, Santa Cruz Biotechnology; anti-HDAC3 1:250, Upstate Biotechnology, Inc.). Secondary antibody (horseradish peroxidase-conjugated anti-rabbit or anti-mouse IgG; Amersham Biosciences) was used according to manufacturer's instructions at 1:2,000 dilution, followed by enhanced chemiluminescence protocol (Amersham Biosciences).

Bicistronic Bacterial Expression System for Direct Protein-Protein Interaction Analysis—KLF6 containing an N-terminal combination hexahistidine-thioredoxin-TEV protease site tag was co-expressed with HDAC3 in BL21(DE3) *E. coli* cells by bicistronic expression (17). Cleared extracts in 50 mM sodium phosphate (pH 7.0), 100 mM NaCl, 1 mM benzamidine, and 5 mM 2-mercaptoethanol (P100 buffer) were prepared from cells induced at 18 °C for 12–15 h, and the hexahistidine-tagged components were purified by Talon cobalt metal affinity chromatography using P100 buffer with 100 mM imidazole to elute. Similar procedures were used for untagged HDAC3 expressed on its own under identical conditions.

In Vitro HDAC Assay—Histone deacetylase activity was assayed essentially as described (18) with 50 μ l of crude cell extract and then immunoprecipitated with rabbit polyclonal anti-KLF6 antibody for 2.5 h at 37 °C. Immunoprecipitates of human KLF6 were washed three times at 4 °C in a low stringency wash containing 0.1% Nonidet P-40 in phosphate-buffered saline. Pretreatment of immunoprecipitates with 100 ng/ml trichostatin A (TSA) was performed for 30 min at 4 °C before addition of the peptide substrate. The synthetic peptide substrate was purchased (Accurate Chemical, Westbury, NY) and corresponds to the first 24 residues of the N-terminal domain of bovine histone H4. Immunoprecipitates were then incubated with 2.5 mg (60,000 dpm) of acid-soluble peptide for 30 min at 37 °C. The reaction was terminated with acetic acid and HCl. Released [³H]acetic acid was obtained by extraction with ethyl acetate and quantified by liquid scintillation counting. Samples were assayed in triplicate (in four separate experiments), and the nonenzymatic release of label was subtracted to obtain the final value.

HDAC Pre-absorption Deacetylase Assays—Cultures of 293T cells were transfected with FLAG-tagged KLF6 expression vector in 100-mm² dishes as described above. Approximately, 5 \times 10⁶ cells were harvested 48 h following transfections, and nuclear extracts were prepared as described above. Nuclear extracts were pre-cleared (pre-absorbed) of HDAC3 or HDAC2 protein using a rabbit polyclonal anti-human HDAC3 antiserum or HDAC2 antiserum (and compared with rabbit preimmune serum) followed by precipitation with protein-A-Sepharose (Amersham Biosciences), and supernatants were transferred into separate tubes. Nuclear extracts were resuspended in 50 μ l of HDAC buffer (50 mM Tris (pH 8.0), 150 mM NaCl, 5 mM EDTA, 0.5% Nonidet P-40 (v/v), 0.2 mM phenylmethylsulfonyl fluoride) with 150,000 cpm of ³H-labeled and -acetylated H4 peptide. Nuclear extracts, pre-absorbed of HDAC3 or HDAC2 protein, were then used in an anti-FLAG (M2)-agarose (Sigma) immunoprecipitation followed by an HDAC assay as briefly described here. In a separate experiment, nuclear extracts were pre-cleared (pre-absorbed) of pRb110 (C15, Santa Cruz Biotechnology) followed by precipitation with protein A-Sepharose (Amersham Biosciences). Supernatants were then transferred to new tubes and used further in HDAC assays following immunoprecipitation of FLAG epitope-tagged KLF6 with anti-FLAG (M2)-agarose (Sigma). Reactions were incubated at 37 °C for 3 h with gentle mixing. Deacetylation reactions were terminated by the addition of 50 μ l of an acid termination mixture (1 N HCl, 0.16 M glacial acetic acid). 500 μ l of ethyl ether was added to each reaction tube and vigorously mixed for 30 s with a vortex. Organic and aqueous phases were separated by centrifugation at 12,000 rpm for 1 min. 400 μ l of the organic phase containing ethyl acetate was removed and mixed with 1 ml of scintillant (OCS, Amersham Biosciences). Release of [³H]acetic acid from the histone H4 peptide was measured in counts/min using a scintillation counter (model 1216 LKB-Wallac).

Inputs of each of the nuclear extracts used in the deacetylase assays were evaluated using immunoblot analysis to determine the presence or absence of specific HDAC protein in the nuclear extracts used in the HDAC assays. Equivalent amounts of nuclear extract were loaded onto 12.5% SDS-polyacrylamide gels and separated by electrophoresis. Separated proteins were then transferred onto polyvinylidene difluoride membranes and blotted with rabbit anti-human HDAC3 and HDAC2 antiserum. Membranes were visualized using ECL by the manufacturer's instructions (Amersham Biosciences).

siRNA KLF6 Silencing—pSuperRetro-KLF6 used to down-regulate KLF6 expression was constructed similarly as described using pSuperRetro vector (19). To insert the targeting sequence, DNA oligonucleo-

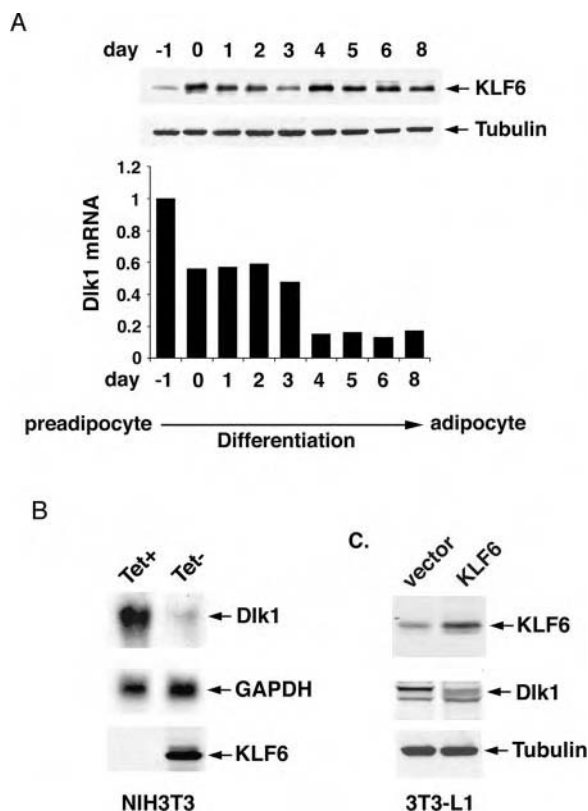


FIG. 1. KLF6 represses DLK1 expression. A, expression of KLF6 and *Dlk1* during 3T3-L1 preadipocyte differentiation. 3T3-L1 cells were differentiated into adipocytes following incubation with a differentiation mixture (see “Materials and Methods”). KLF6 protein levels were determined by SDS-PAGE/Western analysis using cells lysates from days 0 to 8 during differentiation. *Dlk1* mRNA expression was determined by real time quantitative reverse transcription-PCR. B, KLF6 represses *Dlk1* gene expression in tetracycline-regulated NIH 3T3 cells. Northern blot demonstrates that upon KLF6 induction through tetracycline withdrawal, *Dlk1* mRNA level is markedly diminished. *GAPDH*, glyceraldehyde-3-phosphate dehydrogenase. C, KLF6 represses *Dlk1* gene expression in 3T3-L1 preadipocytes. Western analysis demonstrates that expression of KLF6 via stable transfection in 3T3-L1 cells reduces the level of endogenous DLK protein.

tides (Alt-KLF6 (1)F, GATCCCGGAGAAAAAGCCTTACAGATttcaagagaATCTGTAAGGCTTTTCTCCTTTTTGGAAA; Alt-KLF6 (1)-R, AGCTTTTCCAAAAGGAGAAAAGCCTTACAGATtctcttgaaATCT-GTAAGGCTTTTCTCCTCGG) were designed and cloned into the BglII-HindIII sites of the pSuper vector. To establish 3T3-L1 cell lines with reduced KLF6 expression, 10 μ g of pSuper-KLF6 plasmid was transfected with pCIneo in 10:1 ratio into 3T3-L1 cells. Two days after transfection, cells were selected with 600 μ g/ml geneticin (G418, Invitrogen). Individual colonies resistant to the selective medium were transferred to new plates for expansion.

RNA Interference of HDAC3 mRNA—Specific short double-stranded RNA directed against human and mouse HDAC3 mRNA was purchased as a kit (SmartpoolTM-RPD3-2A) from the manufacturer (Dharmacon). RNA-mediated interference was conducted within stably transfected 3T3-L1 cells bearing the pVgRXR and pIND-FLAG/HDAC3 transgenes using specific short RNA oligonucleotide acid duplexes following the manufacturer’s instructions (Dharmacon) using Oligofectamine (Invitrogen) (20, 21).

RESULTS

KLF6 Represses DLK1 Expression—We examined KLF6 and *Dlk1* expression during differentiation of 3T3-L1 cells from preadipocytes into adipocytes following stimulation with a defined hormonal mixture that includes dexamethasone, insulin, and isobutylmethylxanthine (1, 3, 22) (Fig. 1A). Following the onset of differentiation by hormonal stimulation, KLF6 was induced in a biphasic pattern, with a transient induction immediately following adipogenic stimulation on day 0, followed

by a sustained expression accompanying terminal differentiation, between days 4 and 8. Each peak of KLF6 protein at days 0 and 4 was followed by an abrupt decrease of *Dlk1* mRNA as assessed by real time PCR, first by \sim 40% and then by more than 80%. To examine whether KLF6 transcriptionally represses *Dlk1*, we studied *Dlk1* mRNA levels in a 3T3 fibroblast line with tetracycline-regulated KLF6 expression (12), and we examined DLK protein levels in 3T3-L1 cells with forced expression of KLF6 following stable transfection. As shown in Fig. 1, B and C, KLF6 markedly reduced *Dlk1* expression in both KLF6 tetracycline-regulated NIH 3T3 cells and in 3T3-L1 preadipocytes stably transfected with KLF6.

DLK1 Is a Direct Transcriptional Target of KLF6—To establish *Dlk1* as a potential target of KLF6 transactivation/repression, electrophoretic mobility shift assays were performed using nuclear extracts from 3T3-L1 preadipocytes and an oligonucleotide corresponding to the region of the *Dlk1* promoter between -78 and -53 bp upstream of the transcriptional start site, a region containing a GC box to which KLF6 binds (Fig. 2A). Fig. 2B shows that the binding complex was supershifted by an anti-KLF6 monoclonal antibody directed to the N terminus of the protein, confirming a direct interaction between KLF6 and one of the GC boxes in the *Dlk1* promoter.

Silencing of KLF6 Results in Sustained DLK1 Expression and Impaired Adipogenesis—If KLF6 promotes adipocyte differentiation through repression of *Dlk1*, then diminished expression of KLF6 should lead to a decrease of adipogenesis through sustained *Dlk1* (or DLK) expression and concomitant reduced expression of downstream adipogenic markers. To test this prediction, we studied the effects of KLF6 silencing on adipocyte differentiation of 3T3-L1 cells using retroviral gene transduction (Fig. 3), as well as stable gene expression via liposome-mediated transfection (data not shown). KLF6-specific gene silencing was accomplished by RNA interference targeting the partial sequence in exons 2 and 3 of the KLF6 genomic sequence (Fig. 3A). Retroviral gene transduction of the pSuperRetro vector containing the target KLF6 sequence generated cells with reduced expression of endogenous KLF6 compared with the control cell line infected only with the pSuperRetro control vector (Fig. 3B). We then evaluated the impact of retroviral siRNA-mediated down-regulation of KLF6 on expression of *Dlk1* and other downstream adipogenic markers, including C/EBP α , PPAR γ , adiponin, aP2, and steroyl-CoA desaturase-1 (SCD1) following induction of adipocyte differentiation. As shown in Fig. 3, B and C, the level of *Dlk1* failed to decrease in cells in which KLF6 had been silenced compared with vector-infected control cells, whose *Dlk1* level markedly diminished during adipocyte differentiation. As predicted, the expression of key adipogenic mRNAs was significantly attenuated in siRNA-KLF6 cell lines but not in control cells (Fig. 3C). To evaluate the degree of differentiation toward terminal adipocytes, cells in the 7th day of differentiation were stained with Oil Red O to reveal fat droplet content. As shown in Fig. 3D, there were significantly fewer terminally differentiated adipocytes in cultures in which KLF6 had been silenced than in control cultures. These data further confirm a role of KLF6 in promoting adipocyte differentiation through repression of *Dlk1*.

The Repression of DLK1 by KLF6 Requires HDAC Activity—Because gene repression is often associated with the activity of histone deacetylases (HDACs), we examined whether the repression of *Dlk1* by KLF6 was affected by the presence of the HDAC inhibitor TSA (23) (Fig. 4A). TSA completely abolished KLF6-dependent repression of *Dlk1*, indicating that HDAC activity is required for *Dlk1* repression by KLF6.

The studies using TSA suggested that HDAC activity was

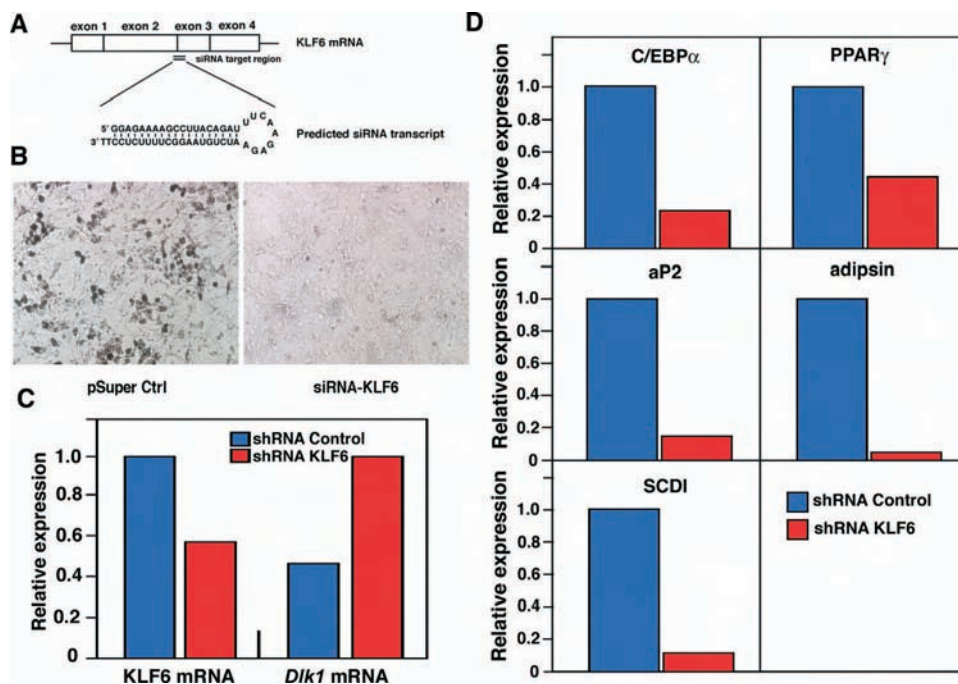


FIG. 3. **KLF6 silencing leads to reduced level of adipocyte differentiation.** A, the target sequence and structure of the antisense shRNA-KLF6. B, Oil Red O staining of the fat droplets on day 7 of the differentiating cells. C, comparative profiles of the relative mRNA levels of downstream markers for differentiation of 3T3-L1 cells transduced with retroviral shRNA vectors for KLF6 and a standard control mRNA. The differentiation markers shown include the following: C/EBP α , PPAR γ , aP2, adipsin, and SCD1 using Taqman quantitative-PCR. D, the relative mRNA levels of KLF6 and *Dlk1* following 7 days post-transduction from retroviral vectors containing antisense KLF6 shRNA and control shRNA are shown.

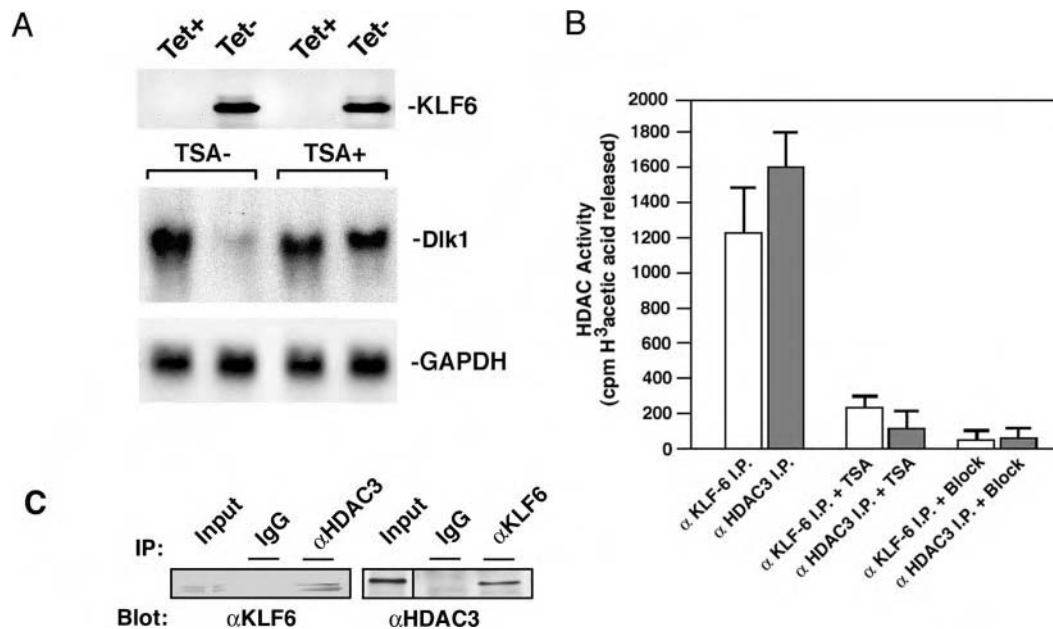


FIG. 4. **Repression of *DLK1* expression by *KLF6* is associated with HDAC activity.** A, repression of *Dlk1* expression by *KLF6* is reversed by HDAC inhibitor TSA. Northern blot analysis was performed in tetracycline-regulable NIH 3T3 cells expressing *KLF6*. Upon induction of *KLF6* through tetracycline withdrawal, *Dlk1* mRNA level was markedly diminished. However, in the presence of TSA (200 nM), the repression of *Dlk1* expression was completely abolished. B, *KLF6* is associated with HDAC activity *in vivo*. pCIneo-KLF6 was transfected into 293 cells; 36 h later, the *KLF6* complex was immunoprecipitated (IP) using anti-KLF6 antibody and incubated with ³H-labeled and -acetylated histone H4 peptides. *KLF6*-associated HDAC activity was examined by counting the released [³H]acetic acid within the supernatant of the reaction. +TSA indicates that the anti-KLF6 immunoprecipitates were pretreated with 100 ng/ml TSA for 30 min at 4 °C before being assayed for HDAC activity. +block indicates that the anti-KLF6 antibodies were pre-absorbed with recombinant *KLF6* proteins. *KLF6*-associated HDAC activity was blocked ~80% by the addition of the HDAC inhibitor TSA. Purified human HDAC3 (Biomol) was used as a positive control. C, HDAC3 is associated with endogenous *KLF6* in 3T3-L1 adipocytes following differentiation. Approximately 3×10^6 post-induced 3T3-L1 mouse cells were collected and prepared as nuclear extract (see "Materials and Methods"). Nuclear extracts were immunoprecipitated with anti-HDAC3 and anti-KLF6 antisera and immunoblotted with either anti HDAC3 or anti-KLF6 antisera.

panel, lane 8). Because bacterial co-expression of HDAC3 and *KLF6* is sufficient for complex formation, our results suggest that HDAC3 can interact directly with *KLF6* without other

accessory or intermediate eukaryotic factors.

HDAC3 Is Essential for *KLF6*-associated HDAC Activity—To determine whether HDAC3 is essential for the deacetylation

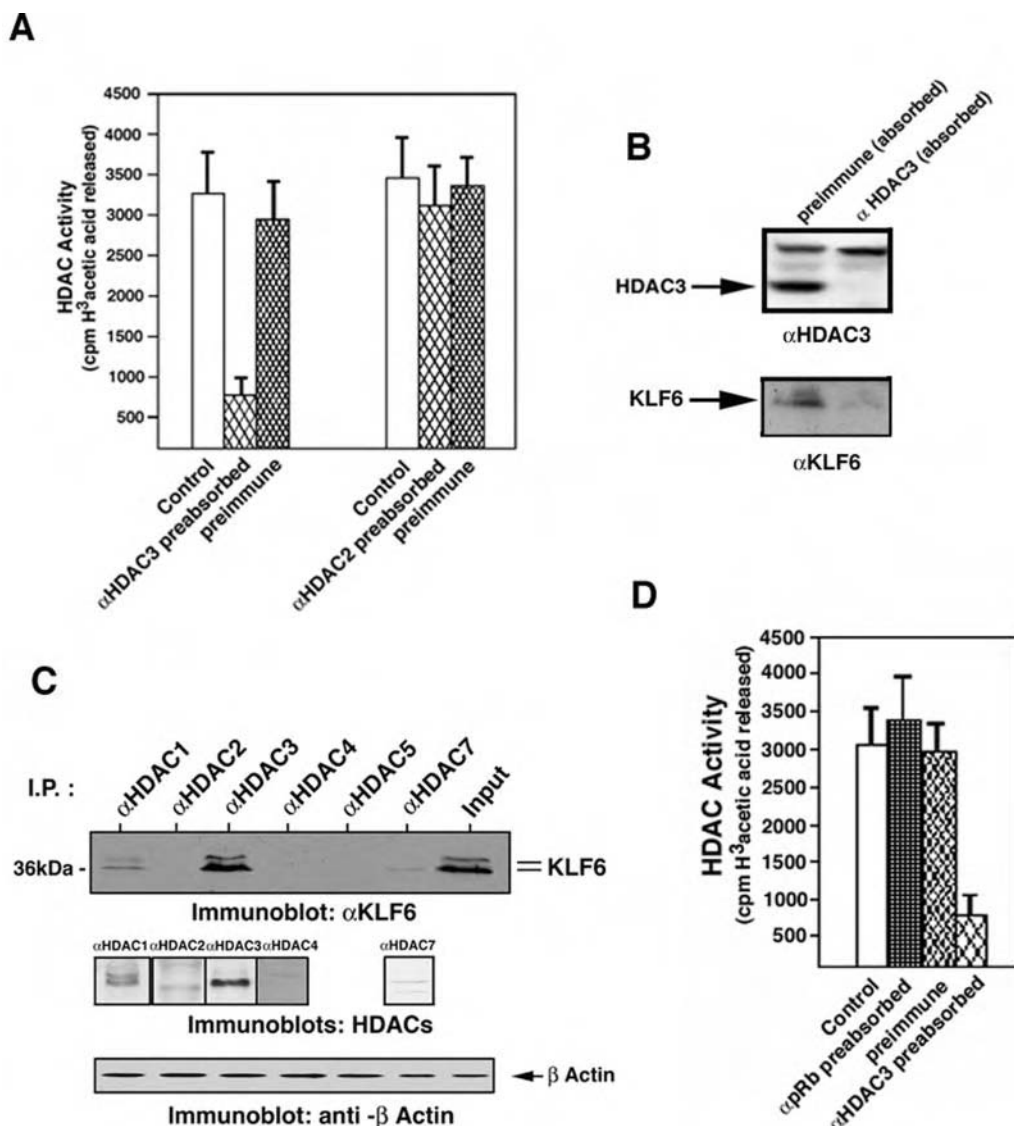


FIG. 6. HDAC3 catalytic activity is specifically associated with KLF6 and independent of pRb. Nuclear extracts immunodepleted of HDAC3 or HDAC2 proteins were used to identify specific HDAC protein activity associated with KLF6. *A*, anti-FLAG (M2) agarose-bound protein was assayed for deacetylase activity following pre-absorption of specific HDAC3 and HDAC2 proteins. Preimmune serum was used to determine background levels of nonspecific protein absorption. Release of tritiated acetate was measured by scintillation counting. *B*, immunoblot analysis of nuclear lysate precleared of HDAC3. *C*, the specific association of KLF6 with the various endogenous classes I and II HDACs were evaluated in 3T3-L1 cell nuclear lysates following the differentiation protocol that was described ("Materials and Methods"). Antibodies against the various HDACs from the class I and II families (α HDAC1, α HDAC2, α HDAC3, α HDAC4, α HDAC5, and α HDAC7) were used to react with specific HDAC proteins from 3T3-L1 cell nuclear lysates, followed by precipitation with protein-A-agarose. Samples were then blotted with anti-KLF6 antisera (α KLF6). To monitor the levels of endogenous class I and class II HDACs, immunoblots were performed for each of the same HDACs with specific antibodies, with significant expression only of HDAC3 (HDAC5 was not detected in nuclear lysates-not shown). *D*, HDAC activity was measured, as described above, following the pre-absorption of pRb by immunodepletion of nuclear extracts using rabbit polyclonal antibody against pRb (C15, Santa Cruz Biotechnology). *IP*, immunoprecipitation.

pRb110 did not reduce HDAC activity associated with KLF6 (Fig. 6D), indicating that the HDAC activity associated with KLF6 is independent of pRb110-associated HDAC activity.

HDAC3 Mediates the Repression of Endogenous *DLK1* through *KLF6*—Our data indicate that KLF6 associates *in vivo* with HDAC3 to form a stable complex repressing *Dlk1* expression. However, they do not establish the relative contribution of this complex to occupancy of the native *Dlk1* promoter during adipocyte differentiation. To address this issue, we performed chromatin immunoprecipitation assays to verify that KLF6 recruits HDAC3 to the endogenous *Dlk1* promoter (Fig. 7A). Immunoprecipitation of chromatin using polyclonal antisera against either KLF6 or HDAC3 was performed on nuclear extracts from 3T3-L1 cells undergoing differentiation cross-linked with formaldehyde. Following reversal of the formalde-

hyde cross-links and proteinase K digestion, a fragment corresponding to -481 through -283 of the mouse *Dlk1* promoter was amplified by PCR. Our results confirmed that the endogenous *Dlk1* promoter was occupied by full-length but not mutant ($\Delta 128$) KLF6, together with HDAC3, following differentiation of 3T3-L1 cells (Fig. 7, A and B).

To determine the relative contribution of HDAC3 to transcriptional repression of *Dlk1*, an ecdysone/ponasterone-regulated system was used to control the induction of HDAC3 in 3T3-L1 cells. In 3T3-L1 preadipocytes stably expressing both the pVgRXR transactivator and pIND-FLAG/HDAC3 target transgenes, stimulation of HDAC3 expression *in vivo* by ponasterone A led to down-regulation of endogenous DLK1 protein, which was partially reversed by silencing of HDAC3 expression using either trichostatin A or HDAC3 siRNA (Fig. 7C). Fur-

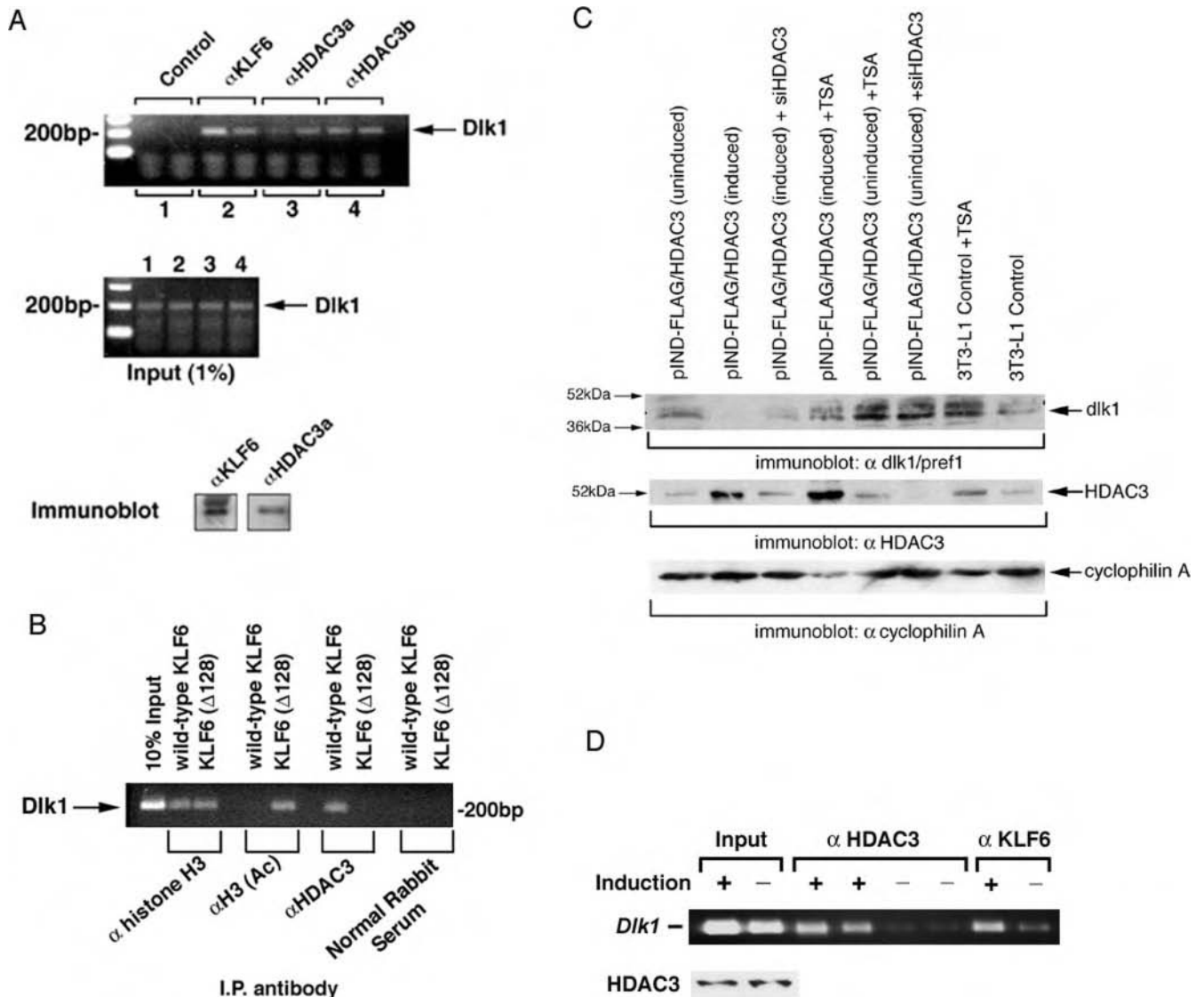


FIG. 7. KLF6 and HDAC3 occupy the DLK1 locus and correspond to the loss of DLK1 expression *in vivo*. *A*, upper panel, anti-KLF6 antibody and two different antibodies against HDAC3 (labeled as anti-HDAC3a and anti-HDAC3b) were used for immunoprecipitation. PCRs for ChIP assay were performed using primers positioned at -481 and -283 bp upstream of the mouse *Dlk1* promoter transcriptional start site. *Middle panel*, prior to each immunoprecipitation, 1% volume of each cell lysate was analyzed by PCR to determine the input signals from the *Dlk1* promoter. *Lower panel*, to demonstrate the presence of KLF6 and HDAC3 in the anti-KLF6 and anti-HDAC3 immunoprecipitates, respectively, one-half of each of anti-KLF6 and anti-HDAC3a immunoprecipitates was subjected to SDS-PAGE/Western analysis, blotted with anti-KLF6 antibody or anti-HDAC3a antibody, respectively. *B*, ChIP analysis was conducted with NIH 3T3 cells stably transfected with pcDNA3.1/HDAC3 under G418 selection. After three serial passages under G418 selection (600 μ g/ml), both wild-type KLF6 and deletion mutant of KLF6 (Δ 128) were transiently transfected into the HDAC3 expression system as indicated above the image. After 48 h, cells ($\sim 5 \times 10^6$ cells) were fixed with formaldehyde, and chromatin was prepared for chromatin immunoprecipitation assays. ChIPs were performed with anti-histone H3 (Upstate Biotechnology, Inc.), anti-acetyl histone H3 (Upstate Biotechnology, Inc.), anti-HDAC3, and normal rabbit serum as a negative control as indicated below the image. *C*, stably transfected 3T3-L1 cells were used to induce the expression of HDAC3 *in vivo* by an ecdysone-inducible mammalian system (Invitrogen) with ponasterone A. RNA interference was conducted with siRNA duplexes directed against HDAC3 (Dharmacon). Transfection of siRNA into stably transfected 3T3-L1 cells was performed under induced and uninduced states of HDAC3 expression. Stably transfected 3T3-L1 cells were then monitored for the expression of HDAC3 by immunoblot analysis with rabbit antiserum against mammalian HDAC3, and input levels were monitored by parallel immunoblot analysis of cyclophilin A as a control. Levels of *Dlk1/pref1* were analyzed by immunoblot studies conducted with rabbit anti-mouse *Dlk1/pref1* antiserum. *D*, chromatin immunoprecipitation studies were performed on chromatin from pre- and post-induced (as indicated - and +, respectively) state of differentiation in 3T3-L1 cells. Mouse preadipocyte 3T3-L1 cells were cultured under selective conditions (see “Materials and Methods”) to induce cell differentiation. On day 0 (-) of induction, 5×10^6 3T3-L1 cells were fixed with formaldehyde and used in the ChIP experiments as shown. Following 8 days of induction (+), the same number of cells was recovered from formaldehyde fixation and used in the ChIP experiments. Immunoprecipitation (IP) of sonicated chromatin lysates was performed with polyclonal rabbit antisera as indicated. An approximate amount of 10% of the total input was used to monitor equivalent levels of chromatin used in the PCR from the sheared DNA templates. The levels of pre (-) and post (+)-induced 3T3-L1 cells from the chromatin input were monitored for HDAC3 protein by immunoblot analysis.

thermore, from these experiments we conclude that HDAC3 is a direct mediator of *Dlk1* repression *in vivo*.

To determine whether recruitment of HDAC3 is mediated directly by KLF6 recruitment to the *Dlk1* locus, we established a stably transfected NIH 3T3 cell line that constitutively over-expresses HDAC3. These cells were transiently transfected

with either the wild-type KLF6 plasmid or the KLF6 deletion mutant (Δ 128) expression construct (which lacks part of the activation domain and the entire DNA-binding domain) in order to examine their respective ability to recruit HDAC3 to the *Dlk1* promoter. Based on chromatin immunoprecipitation analysis (Fig. 7B), there was a direct correlation between wild-type

KLF6 expression and HDAC3 recruitment to the endogenous *Dlk1* promoter. In contrast, under identical conditions, the KLF6 ($\Delta 128$) deletion mutant failed to recruit HDAC3 to the same *Dlk1* promoter element, further indicating that full-length KLF6 mediates the interaction of HDAC3 within the *Dlk1* promoter.

To confirm additionally the requirement for KLF6 and HDAC3 to occupy the *Dlk1* locus during adipogenesis, chromatin immunoprecipitation analysis was performed using extracts of 3T3-L1 cells isolated before or after induction of adipogenesis. Although minimal HDAC3 occupied the endogenous *Dlk1* locus prior to induction of adipogenesis, the HDAC3-*Dlk1* promoter occupancy was clearly demonstrable following adipogenic induction (Fig. 7D). Moreover, although KLF6 was also detectable prior to induction, its association with the promoter was also increased upon adipogenesis. These data support the conclusion that both HDAC3 and KLF6 co-occupy the *Dlk1* promoter, but only in mature adipocytes and not preadipocytes.

DISCUSSION

Our data support a role for KLF6 in adipocyte differentiation. HDAC3 activity is specifically recruited to the transactivation domain of KLF6, which together directly bind to the *Dlk1* promoter to achieve repression, leading to induction of key regulators of adipocyte differentiation. Silencing of KLF6 mRNA using either retroviral infection or stable transfection of KLF6 siRNA blocks 3T3-L1 cell differentiation, indicating that KLF6 function is necessary, albeit not sufficient, to direct preadipocytes into mature adipocytes. In fact, forced expression of KLF6 in the absence of a full differentiation mixture does not induce adipogenesis in 3T3-L1 cells (data not shown). Although several factors and upstream pathways converge to promote differentiation of adipocytes, there are no previous examples where direct transcriptional repression of a regulatory protein (DLK1) controls this process. A potential contribution of KLF6 was suggested by an earlier report (14) in which murine KLF6/Zf9 was associated with adipogenesis immediately following the induction of 3T3-L1 cells with adipogenic hormones, but neither its activity nor regulatory targets were clarified.

KLF6 Is a Novel Transcriptional Repressor of *DLK1* and Modulates Adipocyte Differentiation—Our data identify a novel transcriptional repressor function of KLF6 in promoting adipocyte differentiation, whereas previous studies have focused on its role as a transcriptional activator in tumor suppression (12, 28, 29) and other biologic contexts (8, 30, 31). Transactivation by KLF6 may be coupled with co-activator activities (32); however, our findings indicate a more complex transcriptional model for KLF6-mediated repression. Specifically, transcriptional repression by KLF6 is associated with HDAC3 activity in both 3T3-L1 and 293T cells. Other Krüppel-like factors may function as either transcriptional activators or repressors (33, 34), but none has been linked to cell type-specific transcriptional co-factors in this manner. Most interestingly, two recent studies (35, 36) implicate other Krüppel-like factors in mediating adipocyte differentiation through multiple and discrete transcriptional mechanisms.

In support of the data shown in Fig. 2, we performed ChIP shown in Fig. 7. Although there is a discrepancy between the DNA elements bound by KLF6 *in vitro* (Fig. 2) and the choice of genomic sequences used to amplify by PCR following ChIP (Fig. 7), these results are due to the inability to identify optimal primer sequences for PCR overlapping the KLF6-binding site of the *Dlk1* promoter. To address this issue, a region proximal to the KLF6-binding site was selected both for optimal conditions for PCR and the capacity to detect the occupation of KLF6 within a proximal region of *Dlk1*. We account for this discrepancy because a consequence of shearing chromatin within

~500 bp to 1 kb will allow retention of the target sequences following the immunoprecipitation step. Therefore, amplification of the genomic region overlapping the putative KLF6 binding is capable of generating a signal during the PCR procedure.

HDAC3 as a Critical Co-repressor in Adipocyte Differentiation—The architecture of chromatin has a fundamental role regulating gene transcription *in vivo*. The relationship between KLF6 and the remodeling of chromatin structure via the modification of nucleosomal histones has not been studied previously. We demonstrate that KLF6 incorporates histone-modifying activity through the recruitment of HDAC3 (Figs. 4 and 5). HDAC3 is a member of the class I *Rpd* 3-like histone deacetylases (37–40) that has activities clearly distinct from those of HDAC1 and -2 (37, 41). A role for HDAC3 in cell differentiation has been suggested based on its functional relationship to signaling mechanisms directing a number of crucial cell fate decisions (37, 42, 43). The evidence that KLF6 is a true HDAC3-associated protein is supported by its co-purification using a bicistronic bacterial expression system able to identify direct protein-protein interactions under native conditions (Fig. 5D). Furthermore, immunodepletion experiments also demonstrate that HDAC3 is responsible for the majority of the deacetylase associated with KLF6 (Fig. 6). These results indicate that HDAC3 is a specific co-factor for KLF6 activity during 3T3-L1 adipogenic differentiation. Our findings also exclude participation of other HDACs, including HDAC2, in cooperating with KLF6, a surprising finding, considering that several proteins that bind HDAC1/2 also partner with HDAC3 (44).

Our results further indicate that KLF6 complexes directly with HDAC3 (Fig. 5D). KLF6 appears to recruit directly HDAC3 to the endogenous *Dlk1* promoter, and the induction of HDAC3 expression correlates directly with a decrease of DLK1 levels in 3T3-L1 (Fig. 7). These data demonstrate that one potential mechanism directing repression of *Dlk1* involves recruitment of HDAC3 through interaction with KLF6. Several previous studies indicate that HDAC3 participates in transcriptional repression through either direct interactions with transcriptional co-repressor molecules NCoR and SMRT to form stable ternary complex(es) (15, 37, 42, 45–47) or through binding to pRb (44). However, our experiments demonstrate that KLF6 complexes with HDAC3 independently of these co-repressors or pRb (Figs. 5D and 6D, and data not shown). The lack of NCoR/SMRT participation in directing complex formation between KLF6 and HDAC3 (Fig. 5D) suggests that KLF6 utilizes mechanism(s) of transcriptional repression independent of those associated with nuclear hormone receptor signaling that require NCoR/SMRT, receptors that contribute important permissive signals during adipocyte differentiation (41). Thus, HDAC3 is a nexus for multiple converging mechanisms that drive terminal differentiation of adipocytes, among which is its interaction with KLF6. Moreover, KLF6 represents one of only a few transcription factors utilizing HDAC3 in repressing transcription. Because our studies exclude the participation of some other class I and class II HDACs in this repression (Fig. 6, A and B), HDAC3 may be the only deacetylase activity recruited by KLF6 during adipogenesis, further reinforcing the central importance of HDAC3.

The outcome of the interaction between HDAC3 and KLF6 is the repression of *Dlk1*, a gene encoding an epidermal growth factor-like homeotic transmembrane protein whose down-regulation is required for adipocyte differentiation (48). Similarly, HDAC3 has been assigned recently a role in repressing PPAR γ function by interacting with hypophosphorylated Rb (24). Combined with previous studies by Fajas *et al.* (24), our results indicate that HDAC3 appears to function as a central mediator

46. Li, J., Wang, J., Nawaz, Z., Liu, J. M., Qin, J., and Wong, J. (2000) *EMBO J.* **19**, 4342–4350
47. Kao, H. Y., Downes, M., Ordentlich, P., and Evans, R. M. (2000) *Genes Dev.* **14**, 55–66
48. Laborda, J. (2000) *Histol. Histopathol.* **15**, 119–129
49. Ferreira, R., Naguibneva, I., Pritchard, L. L., Ait-Si-Ali, S., and Harel-Bellan, A. (2001) *Oncogene* **20**, 3128–3133
50. Wade, P. A. (2001) *Hum. Mol. Genet.* **10**, 693–698
51. Hansen, J. B., Petersen, R. K., Larsen, B. M., Bartkova, J., Alsner, J., and Kristiansen, K. (1999) *J. Biol. Chem.* **274**, 2386–2393
52. Richon, V. M., Lyle, R. E., and McGehee, R. E., Jr. (1997) *J. Biol. Chem.* **272**, 10117–10124
53. Classon, M., Kennedy, B. K., Mulloy, R., and Harlow, E. (2000) *Proc. Natl. Acad. Sci. U. S. A.* **97**, 10826–10831

Regulation of Krüppel-like Factor 6 Tumor Suppressor Activity by Acetylation

Dan Li,¹ Steven Yea,¹ Georgia Dolios,² John A. Martignetti,² Goutham Narla,¹ Rong Wang,² Martin J. Walsh,³ and Scott L. Friedman¹

¹Division of Liver Diseases, Department of Medicine; and Departments of ²Human Genetics and ³Pediatrics, Mount Sinai School of Medicine, New York, New York

Abstract

Krüppel-like factor 6 (KLF6) is a zinc finger transcription factor and tumor suppressor that is inactivated in a number of human cancers by mutation, allelic loss, and/or promoter methylation. A key mechanism of growth inhibition by wild-type KLF6 is through p53-independent up-regulation of p21^{WAF1/cip1} (CDKN1A), which is abrogated in several tumor-derived mutants. Here we show by chromatin immunoprecipitation that transactivation of p21^{WAF1/cip1} by KLF6 occurs through its direct recruitment to the p21^{WAF1/cip1} promoter and requires acetylation by histone acetyltransferase activity of either cyclic AMP-responsive element binding protein-binding protein or p300/CBP-associated factor. Direct lysine acetylation of KLF6 peptides can be shown by mass spectrometry. A single lysine-to-arginine point mutation (K209R) derived from prostate cancer reduces acetylation of KLF6 and abrogates its capacity to up-regulate endogenous p21^{WAF1/cip1} and reduce cell proliferation. These data indicate that acetylation may regulate KLF6 function, and its loss in some tumor-derived mutants could contribute to its failure to suppress growth in prostate cancer. (Cancer Res 2005; 65(20): 9216-25)

Introduction

Krüppel-like factor 6 (KLF6) is an ubiquitously expressed zinc finger protein belonging to the KLF family of transcription factors (1, 2). These proteins are DNA-binding transcriptional regulators that serve myriad roles in differentiation and development (3, 4). All KLF members possess a distinct NH₂ terminus activation domain and a highly conserved COOH terminus zinc finger DNA-binding domain that interacts with "GC box" or "CACCC" DNA motifs in responsive promoters (3, 4). In contrast to the conserved DNA-binding domain among KLFs, the divergent activation domain of each family member accounts for their diverse biological activities.

KLF6 has broad activity in regulating cell growth, tissue injury, and differentiation. Its transcriptional targets include a placental glycoprotein (5), HIV-1 (6), collagen α_1 (I) (2), transforming growth factor β 1 (TGF β 1), types I and II TGF β receptors (7), nitric oxide synthase (8), and urokinase type plasminogen activator (9). It is also an immediate early gene up-regulated in hepatic stellate cells during acute liver injury (1) and during the differentiation of preadipocytes into adipocytes (10), suggesting a generalized function of KLF6 in different biological contexts.

KLF6 has recently been identified as a tumor suppressor gene that is inactivated in primary prostate (1, 11), colon (12) nasopharyngeal (13), glial (14), and hepatocellular (15) cancers and is down-regulated in lung and prostate cancers (16, 17). Decreased *KLF6* mRNA expression correlates with clinical outcome in prostate cancer (17). Somatic loss of heterozygosity (LOH) and DNA mutations result in functional deletion of the *KLF6* gene in ~60% of prostate and 45% of colon tumors (1, 11, 12). *KLF6* promoter silencing by methylation also has been uncovered in esophageal cancer cell lines (18).

One mechanism by which KLF6 reduces cell proliferation is through up-regulation of p21^{WAF1/cip1}, a key cyclin-dependent kinase (cdk) inhibitor. This induction does not require p53, a well-established transactivator of p21^{WAF1/cip1}, because p21^{WAF1/cip1} induction by KLF6 is preserved in p53-null cells (1). The molecular requirements for p21^{WAF1/cip1} up-regulation by KLF6 have not been defined, and information about transcriptional coactivators within KLF6 transcriptional complexes is limited. Heterologous interaction of KLF6 with KLF4 or Sp1 is required for keratin (19) or endoglin gene expression (20), respectively, but potential interacting proteins in that context have not been explored.

Coactivators, specifically histone acetyltransferases (HAT), contribute to the transcriptional activity of other tumor suppressors (e.g., p53), where recruitment of HATs is vital to its function (21). HATs are chromatin-modifying proteins that directly regulate transcription through interaction with transcription factors (22), including p53 (23, 24), pRb (25), and BRCA1 (26), as well as the zinc finger transcription factors Sp1 (27) and EKLF (28, 29). Altered interactions between HATs and transcription factors may contribute to tumorigenesis. For example, disruption of the p300-p53 interaction may underlie the mechanism by which the viral oncoprotein E1A induces cell transformation (23, 24, 30).

In vivo, HATs function as part of large protein complexes that share a highly conserved acetyl-CoA binding motif but have different substrate specificities. Among the best studied HATs, cyclic AMP-responsive element binding protein-binding protein (CBP) and p300/CBP-associated factor (PCAF) modulate gene transcription through the acetylation of specific lysine residues on chromatin, and function as coactivators for a number of transcription factors regulating cell growth and development (31–34). In addition, acetylation of nonhistone proteins has emerged as a novel mechanism of posttranslational modification (35, 36).

Our identification of a KLF6 lysine-to-arginine mutation in primary prostate cancer raised the prospect that mutation of an acetylation substrate site might contribute to the loss of growth suppressive activity through the abrogation of p21^{WAF1/cip1} transactivation. In the present study, we have explored the role of CBP and PCAF in up-regulating p21^{WAF1/cip1} gene expression by KLF6. Loss of lysine through mutation impairs KLF6's capacity to transactivate the p21^{WAF1/cip1} promoter or up-regulate endogenous

Requests for reprints: Scott L. Friedman, Mount Sinai School of Medicine, Box 1123, 1425 Madison Avenue, Room 11-70C, New York, NY 10029-6574. Phone: 212-659-9501; Fax: 212-849-2574; E-mail: Scott.Friedman@mssm.edu.
©2005 American Association for Cancer Research.
doi:10.1158/0008-5472.CAN-05-1040

p21^{WAF1/cip1}. These findings suggest that acetylation of KLF6 plays a critical role in its regulation of target gene expression. Given its role as a tumor suppressor, loss of KLF6 acetylation may be associated with tumorigenesis.

Materials and Methods

Expression plasmids. PCIneo-KLF6 (human; previously known as "Zf9") expression plasmid was constructed as previously described (1). HA-CBP was a gift from Dr. R.H. Goodman, Vollum Institute, Oregon Health Sciences University, Portland, OR (37). PCI-PCAF plasmid was a gift from Dr. Yoshihiro Nakatani, Department of Cancer Biology, Dana-Farber Cancer Institute, Boston, MA (38). p21^{WAF1/cip1} promoter-luciferase construct was a gift from Dr. Toru Ouchi, Department of Oncological Sciences, Mount Sinai School of Medicine, New York, NY (39). pRL-TK Vector used as a control for transfection efficiency was from Dual-luciferase Reporter Assay System (Promega, Madison, WI).

Site-directed mutagenesis. A lysine-to-arginine point mutant of KLF6 (pCIneoK209R) was constructed using Quick-Change site-directed mutagenesis kit (Stratagene, La Jolla, CA), as described below. pCIneo-KLF6 (human) was used as the template for the mutagenesis. The primers used for mutagenesis were K209R sense, 5'-CCACTTTAACGGCTGCAGGAGAGTTTACACCAAAGC-3' and K209R antisense, 5'-GCTTTTGGTGTAACCTCTCTGCAGCCGTTAAAGTGG-3'. All mutated constructs were sequenced on both strands to verify these mutations and to confirm that no other alterations were introduced.

Cell culture. Prostate cancer 3 (PC3M) cells, 293 cells, and 293T cells were obtained from the American Type Culture Collection (Manassas, VA). Cells were grown in DMEM supplemented with 10% fetal bovine serum (Hyclone, Logan, UT), 100 units/mL penicillin and 100 units/mL streptomycin, and 2 mmol/L L-glutamine (Life Technologies, Gaithersburg, MD). Treatment with trichostatin A (Sigma-Aldrich, St. Louis, MO) and suberoylaniline hydroxamic acid (Biomol, Plymouth Meeting, PA) was used at a final concentration of 0.5 μ mol/L. Cells were recovered 8 to 12 hours following treatment with individual histone deacetylase (HDAC) inhibitors.

Transfection and luciferase reporter assays. Transient transfections were done using Lipofectamine 2000 reagent (Invitrogen, Carlsbad, CA). For analyzing transfected protein using Western blot, PC3M cells cultured in 10-cm plates (Corning, Acton, MA) were transfected with 10 μ g pCIneo empty vector, pCIneoKLF6, or the pCIneoK209R mutant; cells were lysed 36 hours later for Western blot analysis. For luciferase assay, PC3 cells were transfected with pCIneo-KLF6 (1 μ g), HA-CBP (5 μ g), pCI-PCAF (5 μ g), respectively or together, as indicated in text, together with the p21^{WAF1/cip1} promoter-luciferase construct. Five nanograms of pRL-TK plasmid (Promega) were cotransfected in each transfection as a control for transfection efficiency. Forty-eight hours after transfection, cells were washed thrice with cold PBS and cell lysates prepared using Dual-luciferase reporter assay system (Promega). The luciferase activity in 10 μ L lysate was determined using Dual-luciferase reporter assay system and luminometer (Dynex Technologies, Worthing, West Sussex, United Kingdom). Transfection efficiency was normalized by *Renilla* luciferase activity measured concurrently in the same lysate. Stable cell lines were generated by cotransfecting the appropriate expression constructs (pCIneo empty vector, KLF6 full length, and KLF6 full length with K209R mutation) with a puromycin expressing plasmid in a 10:1 ratio. Transfected cells were selected with 2.5 μ g/mL of puromycin, and pooled clones of cells were used in subsequent experiments.

Chromatin immunoprecipitation assays. Chromatin immunoprecipitation assays were done as previously described (40) with minor modifications described here. Briefly, 293 cells (4×10^6) were transfected with pCIneoKLF6 or pSG4 + Sp1 (gift from R. Tijan, University of California at Berkeley and G. Gill, Harvard University, Boston, MA). Thirty-six hours after transfection, cells were cross-linked with 1% formaldehyde for 10 minutes at 37°C followed by cell lysis and sonication of DNA into 200- to 1,000-bp fragments. Proteins cross-linked to DNA were immunoprecipitated with 10 μ g anti-Zf9/KLF6 antibody (R-173; Santa

Cruz Biotechnology, Santa Cruz, CA) or anti-Sp1 antibody (Upstate Biotechnology Charlottesville, VA) and 60 μ L salmon sperm DNA/protein A agarose beads. Antisera against histone H3 (Upstate Biotechnology) was used as an input control for chromatin in each assay as shown. The protein A agarose/antibody/protein complexes were washed extensively and eluted following the manufacturer's instruction. The cross-linking was reversed by heating at 65°C for 4 hours and proteins were digested by proteinase K for 1 hour at 45°C. DNA was recovered by phenol/chloroform extraction and ethanol precipitation in the presence of 10 μ g/mL yeast tRNA carrier and used as a template for PCR reactions. Genomic sequence primers encompassing the p21^{WAF1/cip1} promoter region -150 to -3 bp upstream of transcriptional start site were used to amplify immunoprecipitated DNA as template: -150F, 5'-GCTGGCAGCCAGGAGCCTG-3'; -3R, 5'-CTGCTCACCTCAGCTGGC-3'.

Immunoprecipitation and Western blotting. For coimmunoprecipitation assays, 293T cells were transfected with 20 μ g of plasmid DNA. Thirty-six hours after transfection, cells were washed twice with cold PBS and lysed on ice for 20 minutes using immunoprecipitation lysis buffer containing 0.5% NP40, 50 mmol/L Tris-HCl (pH 7.4), 120 mmol/L NaCl, and protease inhibitors (Complete Protease Inhibitor Cocktail Tablets, Roche, Nutley, NJ). The cell lysate was precipitated for 30 minutes at 14,000 $\times g$ at 4°C. The supernatant was immunoprecipitated at 4°C for 1 hour using 4 μ g of anti-Zf9/KLF6 antibody (R-173; Santa Cruz Biotechnology), or 4 μ g of anti-HA antibody (Mount Sinai Hybridoma Center, New York, NY) with 50 μ L of protein-G beads (Pierce, Rockford, IL), or using 50 μ L of M2 anti-agarose (Sigma, St. Louis, MO). For coimmunoprecipitation of endogenous KLF6 and CBP, monoclonal anti-KLF6 antibody was cross-linked to agarose beads using ImmunoPure Protein G IgG Plus Orientation Kit (Pierce). NIH 3T3 cells (1×10^8) were lysed and precipitated, as described above. The supernatant was immunoprecipitated using cross-linked anti-KLF6 agarose. The beads were subsequently washed thrice with 800 μ L immunoprecipitation wash buffer [0.5% NP40, 50 mmol/L Tris-HCl (pH 7.4), and 500 mmol/L NaCl], solubilized in Laemmli sample buffer (Sigma) containing 5% β -mercaptoethanol, boiled, and separated by SDS-PAGE followed by Western blotting as described below. As a negative control, immunoprecipitation was done using control rabbit or mouse IgG (Sigma).

For Western blotting, cell extracts were harvested in radioimmunoprecipitation assay buffer (Santa Cruz Biotechnology, standard protocol). Protein samples (30 μ g per sample) were separated on SDS-polyacrylamide gel (6% for CBP and 10% for KLF6 and PCAF) and transferred to a nitrocellulose membrane (Bio-Rad, Hercules, CA). The membranes were blocked in 5% dried milk in 10 mmol/L Tris-HCl (pH 8.0), 150 mmol/L NaCl, and 0.1% Tween 20 (1 \times TBS-T) for 1 hour at room temperature. The membrane was incubated with primary antibody: anti-Zf9/KLF6 (R-173), 1:2,000 (Santa Cruz Biotechnology); anti-p21^{WAF1/cip1} (H-164), 1:250 (Santa Cruz Biotechnology); anti-CBP-NT, 1:1,000 (Upstate Biotechnology); anti-PCAF, 1:1,000 (Upstate Biotechnology); anti-acetyl-lysine antibody, 1:1,000 (Cell Signaling, Beverly, MA). Secondary antibody (horseradish peroxidase-conjugated anti-rabbit or anti-mouse IgG (Amersham Biosciences, Piscataway, NJ) was used according to manufacturer's instruction at 1:2,000 dilution followed by enhanced chemiluminescence protocol (Amersham Pharmacia).

In vitro protein acetyltransferase assay. Protein acetyltransferase reactions were done with *in vitro* translated KLF6 protein and synthesized by using the TNT *in vitro* transcription and translation system (Promega) either in the absence of radioisotope or in the presence of [¹⁴C]-leucine (50 μ Ci/mmol, Perkin Elmer, Boston, MA). For acetyltransferase reactions, ~1 μ g of *in vitro* translated KLF6 and 100 ng of immunoprecipitated HA or FLAG-tagged proteins of CBP (wild type), CBP (HAT-; kind gifts from Dr. R.H. Goodman), or PCAF (wild type) were incubated with [¹⁴C]-acetyl-CoA (55 μ Ci/mmol, New England Nuclear) for 1 hour at 30°C. After acetyltransferase reactions, KLF6 protein was immunoprecipitated with anti-Zf9/KLF6 antibody (R-173, Santa Cruz Biotechnology). The entire reaction mixture was separated by 10% SDS-PAGE. Gels containing [¹⁴C]-labeled proteins were stained and fixed with 10% glacial acetic acid and 40% methanol for 1 hour, soaked in Amplify (Amersham

Pharmacia) for 40 minutes, and exposed to X-ray film for autoradiography for ~10 minutes.

Analysis of proliferation. Proliferation was determined by estimating ^3H -thymidine incorporation. BPH1 and PC3M cell lines stably expressing the appropriate expression vectors were plated at a density of 50,000 cells per well in 12-well dishes. Twenty-four hours after plating, 1 $\mu\text{Ci}/\text{mL}$ ^3H -thymidine (Amersham, Biosciences) was added. After 2 hours, cells were washed four times with ice-cold PBS and fixed in methanol for 30 minutes at 4°C . After methanol removal and cell drying, cells were solubilized in 0.25% sodium hydroxide/0.25% SDS. After neutralization with hydrochloric acid (1 N), disintegrations per minute were estimated by liquid scintillation counting. This process was repeated at 48 and 72 hours.

Tumor samples. The preparation of tumor samples was as previously described (1). Briefly, 5- μm sections stained with H&E were used as an accurate histologic reference for normal and tumor-derived tissue. Microdissection was done on sequential 20- μm sections and DNA subsequently extracted (Ambion paraffin block isolation kit, Austin, TX). DNA was isolated by proteinase K digestion overnight at 37°C incubator followed by heat inactivation at 95°C for 10 minutes. KLF6 sequence analysis of tumor samples was done as previously described (1).

Peptide acetylation assay. Four peptides were synthesized using commercially available resources (Invitrogen) covering the majority of lysine residues within the KLF6 molecule. The peptides' sequences are as follows: (a) h68-87 ILAREKKEESELKISSPPE, (b) h115-134 SSEELSP-TAKFTSDPIGEVL, (c) h204-223 FNGCRKYTKSSHLKAHQRT, and (d) h248-267 TRHFRKHTGAKPFKCSHCDR. For peptide acetylation assay, 5 ng of peptide were incubated at 30°C for 1.5 hours with 5 ng CBP or PCAF, 10 μL of 1 mmol/L acetyl CoA, 5 μL of 0.1 mol/L sodium butyrate, in the presence or absence of 10 μL ^3H -acetyl CoA (0.5 $\mu\text{Ci}/\mu\text{L}$, Amersham Pharmacia), in $1\times$ HAT assay buffer (Upstate Biotechnology). Following the reaction, the mixture was analyzed by scintillation counting to confirm ^3H incorporation followed by mass spectrometry (MS) analysis. To assess ^3H incorporation, 5 μL of reaction mixture were spotted onto a small square of filter paper followed by washing with 50 mmol/L Na_2HPO_4 (pH 9.0), then the filter paper was placed into scintillation fluid overnight for counting the next day.

Mass spectrometry analysis. KLF6 peptides and their acetylation products (1 pmol) were isolated and purified using Poros 20 R2 beads (Applied Biosystems, Foster City, CA) and ZipTip_{C18} pipette tip (Millipore, Bedford, MA) following the manufacturer's protocol. Molecular masses of the synthetic peptides before and after acetylation reaction were accurately measured by matrix-assisted laser desorption ionization-MS (MALDI-MS) using a QSTAR XL hybrid quadrupole time-of-flight mass spectrometer (Applied Biosystems). α -Cyano-4-hydroxy-cinnamic acid was used as matrix for sample preparation. To determine the acetylation site(s), fragment spectra of peaks corresponding to acetylated peptides were collected and analyzed by MALDI tandem MS (MS/MS) experiment using the same mass spectrometer.

Results

KLF6 targets the p21^{WAF1/cip1} (CDKN1A) locus and is associated with hyperacetylation of histone H3. To determine if KLF6 interacts directly with the endogenous p21^{WAF1/cip1} (CDKN1A) promoter, we used chromatin immunoprecipitation (Fig. 1). PCR reactions were carried out using primers encompassing -150 to -3 bp upstream of the start site of p21^{WAF1/cip1} transcription as shown (Fig. 1A), which contains multiple GC boxes predicted by sequence homology to interact with KLF6 and related family members. Chromatin immunoprecipitation analysis confirmed that KLF6 binds to this region of the endogenous p21^{WAF1/cip1} promoter, establishing p21^{WAF1/cip1} as a transcriptional target of KLF6 (Fig. 1B). Interestingly, we were unable to show the binding of Sp1 to the same region despite reports to the contrary based on electromobility shift assay (41). To confirm the ability of the Sp1 antibody to recognize Sp1 in the chromatin immunoprecipitation

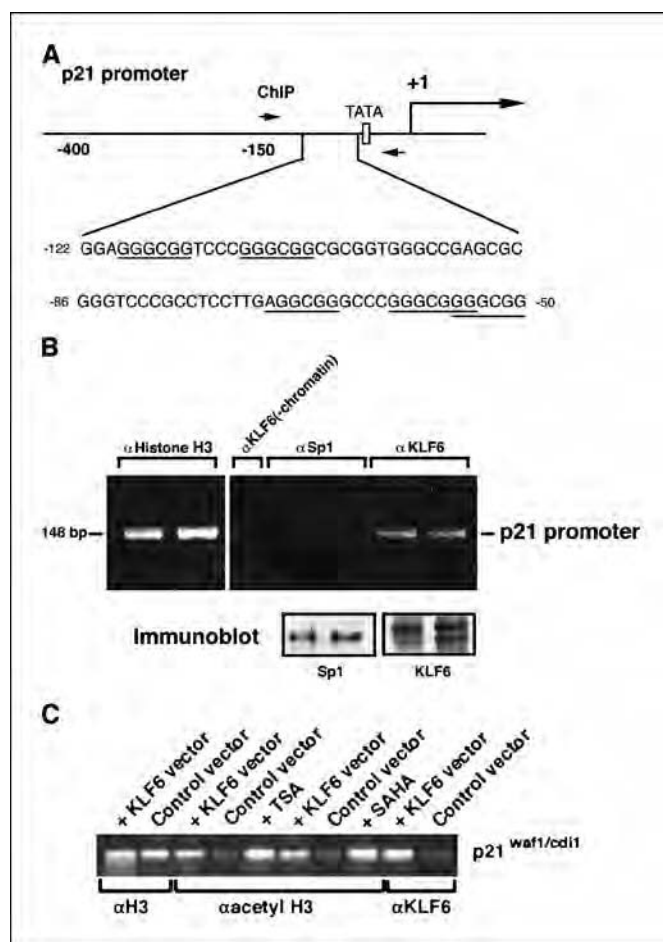


Figure 1. KLF6 is directly associated with the p21^{WAF1/cip1} (CDKN1A) locus and deposition of acetylated histone H3. **A**, schematic representation of p21^{WAF1/cip1} promoter. PCR for chromatin immunoprecipitation (ChIP) assay was done using primers (small arrows) positioned at -150 and -3 bp upstream of transcriptional start site of p21^{WAF1/cip1} promoter. This GC-rich region contains five putative binding sites for KLF6 as well as for Sp1, all of which are between -102 and -30 bp region, as shown in (A). **B**, chromatin immunoprecipitation assay at p21^{WAF1/cip1} promoter in 293 cells. Anti-KLF6 antibody (α KLF6) was used for immunoprecipitation. Anti-histone H3 (α Histone H3) antibody was used as a positive control. The binding of Sp1 to p21^{WAF1/cip1} promoter is also examined using anti-Sp1 antibody (α Sp1). **C**, acetylation of the p21^{WAF1/cip1} (CDKN1A) locus within the gene promoter was monitored upon transfection with a KLF6 expression vector by chromatin immunoprecipitation analysis. Input levels of chromatin for immunoprecipitation reactions were monitored for total histone H3. HDAC inhibitors trichostatin A (TSA) and suberoylanilide hydroxamic acid (SAHA) at a final concentration of 0.5 $\mu\text{mol}/\text{L}$ were used to compare acetylation of histone H3.

assay, a positive control was used to verify Sp1 on other loci (data not shown). Furthermore, ectopic expression of KLF6 showed increased recruitment of acetylated histone H3 encompassing the region between -150 to -3 of the KLF6 promoter when compared with the control expression vector (Fig. 1C).

KLF6 interacts with CBP and PCAF *in vivo*. Because CBP and PCAF interact with critical cellular proteins, including p53 (21) and E2F1 (42) leading to altered function, we examined whether KLF6 interacts with CBP and/or PCAF using a coimmunoprecipitation assay. As shown in Fig. 2A (top), CBP was associated with KLF6 when whole cell lysate of 293T cells expressing Flag-tagged KLF6 and HA-tagged CBP was immunoprecipitated using anti-Flag antibody and blotted with anti-HA antibody; this result was confirmed by reciprocal coimmunoprecipitation (Fig. 2A). To show the interaction between endogenous KLF6 and CBP, coimmunoprecipitation was

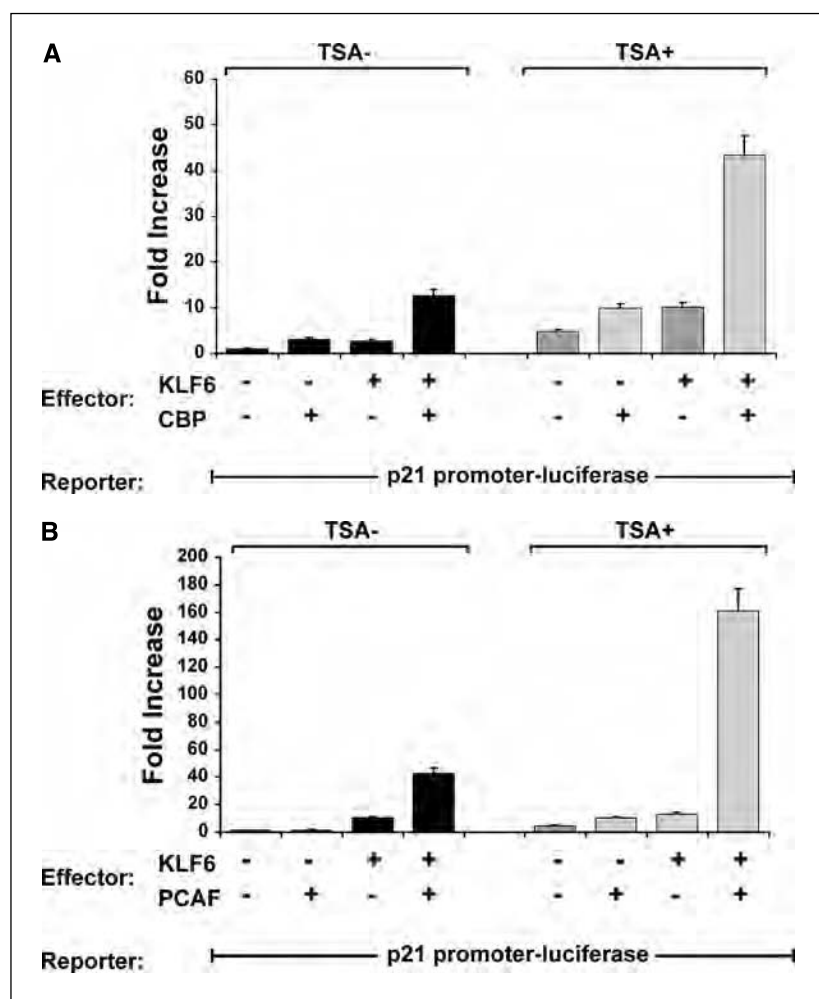


Figure 3. CBP and PCAF potentiate p21^{WAF1/cip1} up-regulation by KLF6, which is further enhanced by trichostatin A (TSA). **A**, CBP potentiates KLF6 in transactivating the p21^{WAF1/cip1} promoter. *Left columns*, PC3 cells were cotransfected with KLF6 and CBP constructs, along with a p21^{WAF1/cip1} promoter reporter. *Right columns*, the same cotransfection were done in the presence of an HDAC inhibitor, trichostatin A. **B**, PCAF potentiates KLF6 in transactivating p21^{WAF1/cip1} promoter. *Left columns*, PC3 cells were cotransfected with KLF6 and PCAF constructs, along with a p21^{WAF1/cip1} promoter reporter. *Right columns*, the same cotransfection were done in the presence of the HDAC inhibitor, trichostatin A. Transfection efficiencies were normalized using *Renilla* luciferase assay measured in the same lysate at the same time.

and a b-type fragment in the spectra. As shown in the fragment mass spectrum of 2,361.3 (nonacetylated form; Fig. 5E, top), a series of peaks were observed that corresponded to y-ion (y_4 - y_{11}). Acetylation of any of the three lysine residues was easily identified. In the fragment mass spectrum of 2,403.3 (singly acetylated form; Fig. 5E, middle), we observed two peaks corresponding to y_{11} ions. The major one (labeled with y_{11}^*) indicated the acetylation of Lys²¹³, and the minor one indicated the acetylation of 209, respectively. In the fragment mass spectrum of 2,445.3 (doubly acetylated form; Fig. 5E, bottom), we observed similar y-series peaks as in the singly acetylated peptide 3, which indicated the acetylation of Lys²⁰⁹ and Lys²¹³. Two additional y-ion peaks were also detected (labeled y_8^* and y_9^*) in the same spectrum. Because no mass shift was observed for peaks of y_6 and y_7 , we interpreted this observation to have resulted from acetylation of His²¹⁶, together with the acetylation of Lys²¹³ or Lys²⁰⁹ (most likely 213). Based on the mass spectrometric analysis, the data indicate that the acetylation accessibility of the three lysine residues on KLF6 peptide 3 is in the order of 213, 209, and 218. The histidine residue can also be acetylated by CBP.

A tumor-derived K-to-R mutant has impaired ability to up-regulate p21^{WAF1/cip1} and suppress growth. We have shown a high frequency of LOH and point mutations of *KLF6* in human prostate cancer (1). Importantly, in addition to the point mutants of *KLF6* originally identified from prostate cancer (1), several

additional lysine mutations were identified in prostate, colon, and hepatocellular cancers (11, 12, 15). Of these, we focused on a single new mutation not previously reported, K209R (Fig. 6A), to explore the potential effect of loss of an acetylation site on KLF6 function. Given that K209 can be acetylated by CBP as confirmed by MS (Fig. 5), a K209R mutation would be predicted to abrogate acetylation at this site. To assess the ability of K209R to transactivate the p21^{WAF1/cip1} promoter, we cotransfected the mutant with a p21^{WAF1/cip1} promoter reporter construct into PC3M cells. As shown in Fig. 6B, compared with wild-type KLF6, K209R completely lost the ability to transactivate the p21^{WAF1/cip1} promoter. To correlate this change with p21^{WAF1/cip1} expression *in vivo*, K209R was introduced into PC3 cells and the endogenous p21^{WAF1/cip1} level was assessed by Western blot. As shown in Fig. 6C, K209R lost the ability to up-regulate endogenous p21^{WAF1/cip1}.

Loss of growth suppression by the K209R mutant was also shown in stably transfected prostate cancer cell lines. K209R was stably expressed in both PC3M cells (a metastatic prostate cancer line) and BPH1 cells (a line derived from benign prostate). In contrast to cells expressing wild-type KLF6, the K209R mutant was unable to decrease cell proliferation in either BPH1 or PC3M cell lines (Fig. 6D). Moreover, in PC3M cells but not BPH cells, the K209R mutant actually increased proliferation when compared with cells stably expressing the pCneo empty vector. These results were validated in two independent sets of stable cell lines

for both BPH1 and PC3M cells. Collectively, these data suggest that the acetylation at K209 is necessary for KLF6 to up-regulate $p21^{WAF1/cip1}$ gene expression, which in turn can inhibit cellular proliferation.

Discussion

KLF6 has been established as a tumor suppressor gene involved in key intracellular pathways in a number of human cancers (1, 12, 14, 15, 43, 44). Among several target genes transcriptionally regulated by KLF6, $p21^{WAF1/cip1}$ has been particularly relevant to prostate cancer given $p21^{WAF1/cip1}$'s central role in growth regulation, especially as a mediator of p53-stimulated cell cycle arrest. The acetylation status of the human $p21^{WAF1/cip1}$ (*CDKN1A*) locus has been extensively characterized in cellular contexts that are tied to cancer development (45). These activities require specific GC-rich elements (46) in the $p21^{WAF1/cip1}$ promoter, which are consensus target sequences for KLF6 binding (1). However, little is known about either the biochemical requirements for transcriptional activity of KLF6, or the complexes through which KLF6 regulates target gene activity.

An important goal in studying KLF6 has been to understand the physiologic significance of protein complexes that modify its function in regulating the activity of its target genes. Recently, we showed that KLF6 sequesters cyclin D1 to reduce cyclin D/cdk4 interactions and enhance the phosphorylation of pRb, thereby promoting G₁ cell cycle arrest (47). This activity alters the equilibrium of $p21^{WAF1/cip1}$ levels, with induction and titration onto cdk2 complexes and further growth suppression (47). These

findings suggest that covalent modifications may differentially regulate KLF6 activity.

Despite clear evidence that KLF6 transcriptionally activates $p21^{WAF1/cip1}$ (1, 12), the biochemical mechanisms underlying this observation have not been clarified. Here, we establish that KLF6 activity is associated with increased complexing of acetylated histones within the $p21^{WAF1/cip1}$ (*CDKN1A*) locus. Furthermore, we show that KLF6 interacts with the CBP/p300 complex and its acetylation by CBP contributes to normal KLF6 activity. Moreover, MS shows acetylation of a specific lysine residue of KLF6 that is mutated in a primary prostate tumor. Collectively, the findings provide evidence that acetylation of KLF6 is biologically significant, and its dysregulation in human cancer may contribute to loss of KLF6's growth suppressive activity.

Our findings also provide an important functional link between protein acetyltransferases and KLF6 by showing that KLF6 recruits CBP and PCAF to the $p21^{WAF1/cip1}$ locus. In contrast to the evidence that KLF6 occupies the $p21^{WAF1/cip1}$ promoter using chromosomal immunoprecipitation, the lack of promoter occupation by Sp1 was unexpected. One potential explanation may be the weak affinity of different antisera used against Sp1 from cross-linked material to detect the protein in these experiments. Alternatively, Sp1 may represent a low-abundance protein involved primarily in stimulated rather than basal expression of $p21^{WAF1/cip1}$. This possibility is supported by studies showing that $p21^{WAF1/cip1}$ transactivation by Sp1 is greatly enhanced by TGF β signaling for example (48). Although our study does not exclude the possible participation of Sp1-like factors in regulating the expression of $p21^{WAF1/cip1}$ (49), it may indicate a greater role for KLF6 than Sp1 in regulating $p21^{WAF1/cip1}$ within this specific cellular context. Additionally, Sp1 may use different GC boxes in the $p21^{WAF1/cip1}$ promoter from those used by KLF6 under our experimental conditions. In other contexts, there may be cooperation between KLF6 and Sp1, as suggested by their transcriptional synergy in regulating the expression of TGF β and of endoglin, a TGF β -binding protein (20). Thus, there may be a precise stoichiometry between KLF6 and Sp1 that is promoter and context specific in regulating their target genes.

The identification of several point mutations of KLF6 in human cancer affecting lysine residues led us to explore the potential role of lysine modification in regulating KLF6 activity. These have included mutations in prostate (K186R; ref. 1), colon (K74R; ref. 12), and hepatocellular carcinoma (K182R; ref. 15). Here we tested the functional activity of an additional prostate cancer-derived mutant of KLF6, K209R, for its capacity to both transactivate the $p21^{WAF1/cip1}$ promoter, and to function as a substrate for protein acetyltransferase activity by CBP. Our findings indicate that acetylation of a specific Lys²⁰⁹ was closely linked with CBP-dependent activation of endogenous $p21^{WAF1/cip1}$ *in vitro*. Moreover, its mutation to arginine as seen in prostate cancer abrogated $p21^{WAF1/cip1}$ transactivation. Interestingly, this lysine is within the peptide consensus sequence for acetylation of p53 by p300/CBP (21, 50, 51), consistent with recent models proposed for acetylation of p53 (21). However, despite ample evidence that acetylation of p53 regulates several of its functions (52), the relative biological significance of p53 acetylation still remains uncertain. Because p53 has been one of the most thoroughly studied molecules that is covalently modified (52), more recent efforts have focused on the interdependence of its different covalent modifications, including phosphorylation, acetylation, methylation, ubiquitination, and sumoylation, and how they affect

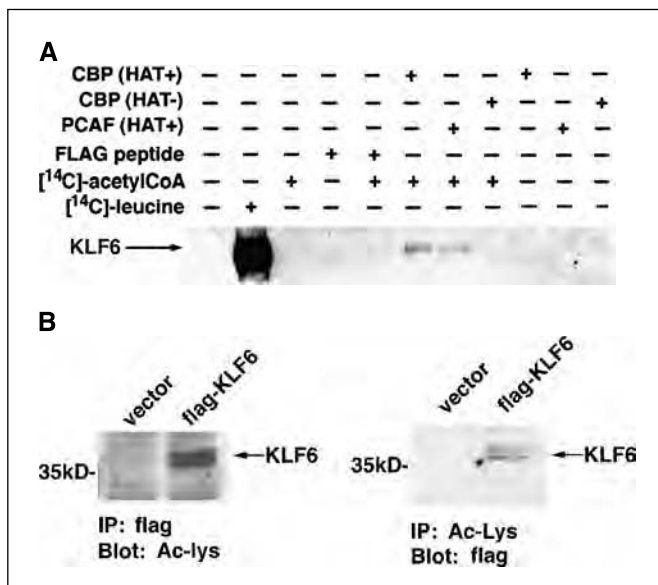


Figure 4. KLF6 is acetylated *in vitro* and *in vivo*. **A**, KLF6 is acetylated *in vitro* by CBP and PCAF. Equivalent molar amount of CBP (wild type), CBP (HAT-), and PCAF (wild type) were immunoprecipitated from cells expressing HA-tagged CBP, HA-tagged CBP (HAT-), and FLAG-tagged PCAF (wild type). *In vitro* translated KLF6 was incubated with immunoprecipitation-purified CBP (wild type), CBP (HAT-), and PCAF (wild type), together with [¹⁴C]-acetyl CoA. KLF6 was synthesized with [¹⁴C]-leucine *in vitro* and immunoprecipitated as a control. Immunoprecipitated products were resolved on SDS/PAGE followed by autoradiography. **B**, KLF6 is acetylated *in vivo*. 293T cells expressing FLAG-tagged KLF6 were immunoprecipitated with anti-FLAG agarose, followed by SDS-PAGE and Western blot analysis. Immunoprecipitated KLF6 was detected by anti-acetylated lysine antibody. Moreover, using lysates from the same cell line, FLAG-tagged KLF6 was immunoprecipitated by anti-acetylated lysine antibody and detected by anti-FLAG antibody using Western blot.

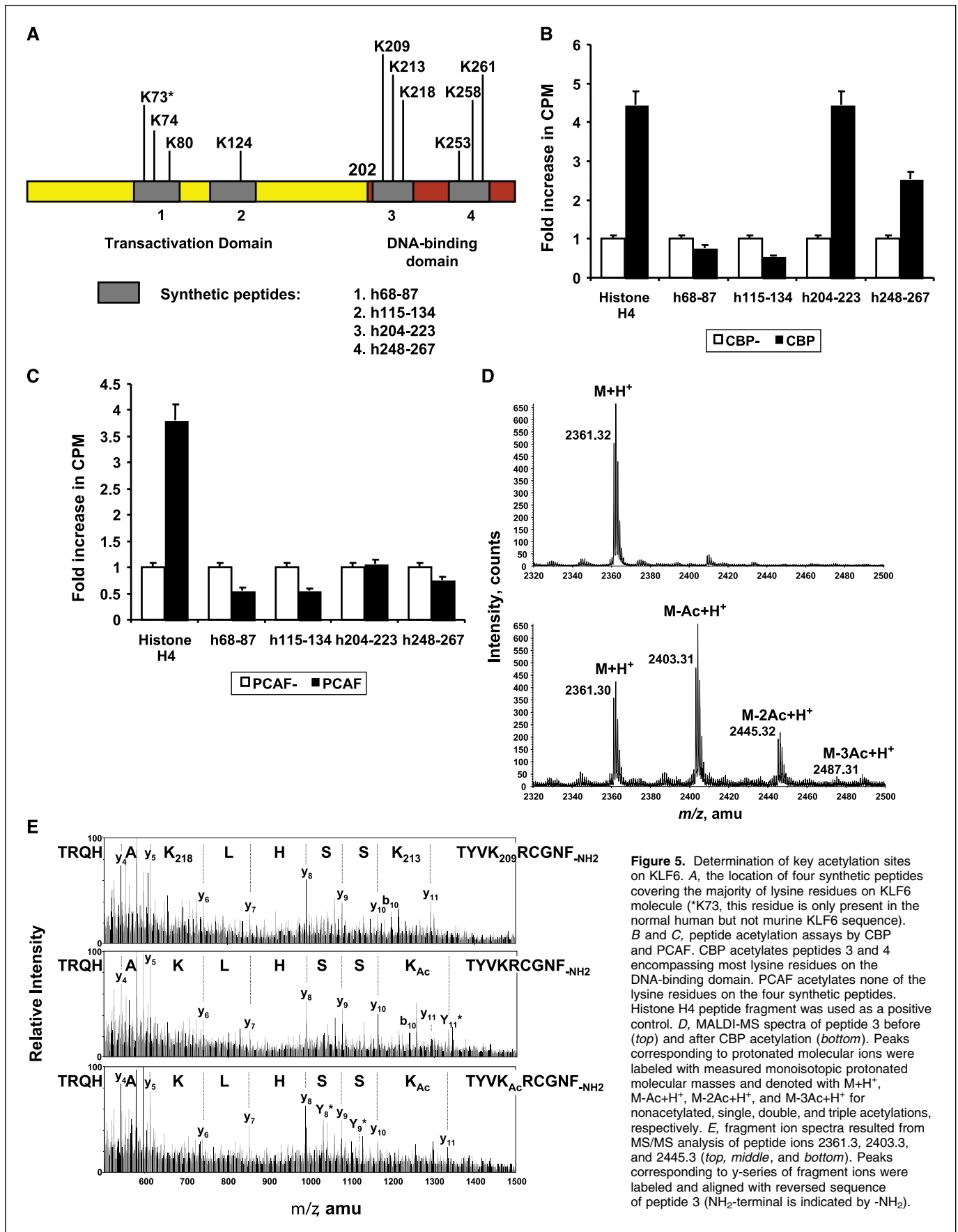


Figure 5. Determination of key acetylation sites on KLF6. *A*, the location of four synthetic peptides covering the majority of lysine residues on KLF6 molecule (*K73, this residue is only present in the normal human but not murine KLF6 sequence). *B* and *C*, peptide acetylation assays by CBP and PCAF. CBP acetylates peptides 3 and 4 encompassing most lysine residues on the DNA-binding domain. PCAF acetylates none of the lysine residues on the four synthetic peptides. Histone H4 peptide fragment was used as a positive control. *D*, MALDI-MS spectra of peptide 3 before (*top*) and after CBP acetylation (*bottom*). Peaks corresponding to protonated molecular ions were labeled with measured monoisotopic protonated molecular masses and denoted with $M+H^+$, $M-Ac+H^+$, $M-2Ac+H^+$, and $M-3Ac+H^+$ for nonacetylated, single, double, and triple acetylations, respectively. *E*, fragment ion spectra resulted from MS/MS analysis of peptide ions 2361.3, 2403.3, and 2445.3 (*top*, *middle*, and *bottom*). Peaks corresponding to y -series of fragment ions were labeled and aligned with reversed sequence of peptide 3 (NH_2 -terminal is indicated by $-NH_2$).

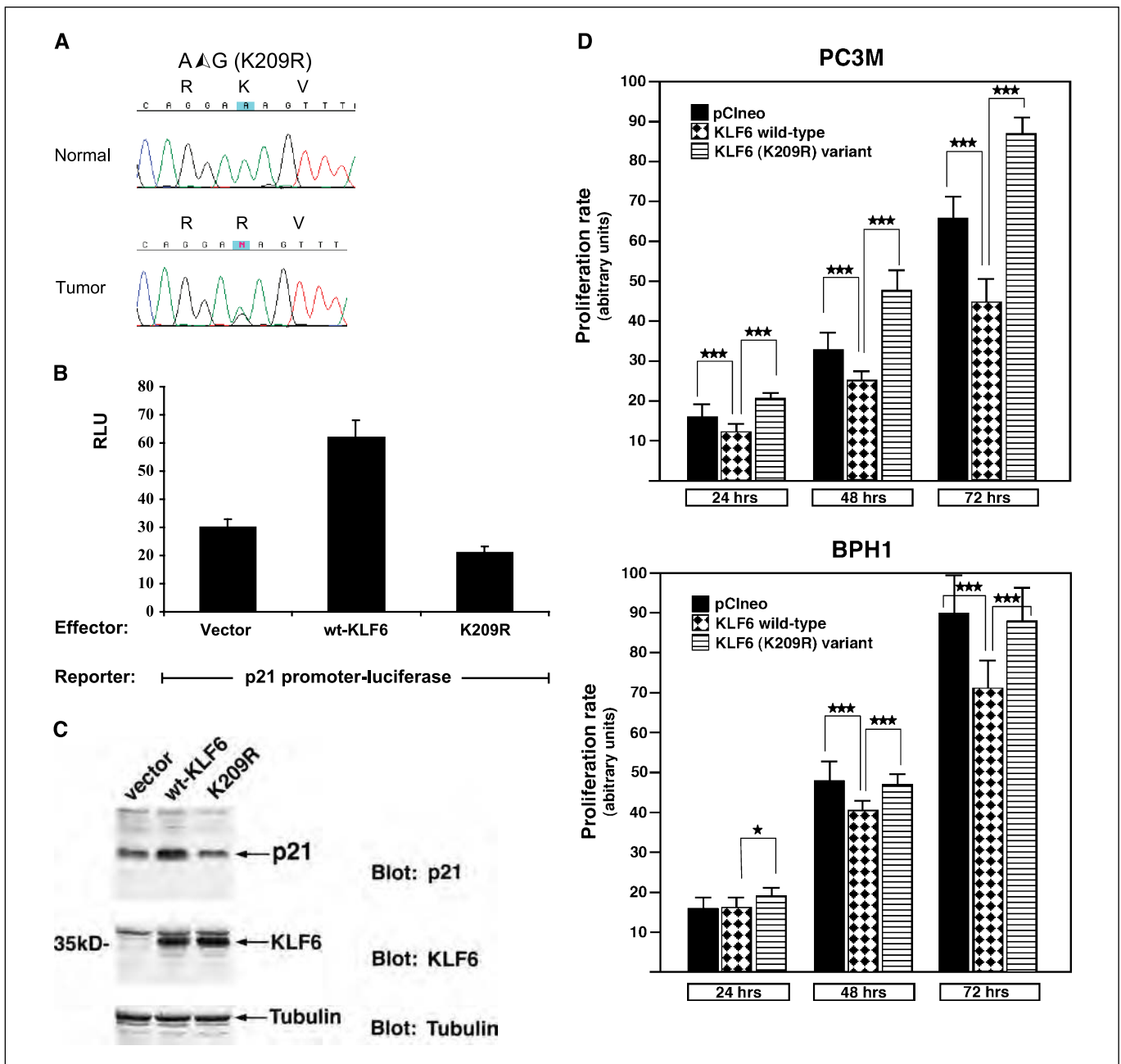


Figure 6. A lysine (K) to arginine (R) mutant (K209R) identified from prostate cancer has impaired ability to up-regulate p21^{WAF1/cip1} expression. **A**, a KLF6 mutation (K209R) affecting an acetylation site in primary prostate cancer. Sequencing chromatogram of DNA derived from microdissected primary prostate cancer is shown, along with normal sequence from the surrounding unaffected sequence. **B**, K209 tumor mutant has reduced ability to transactivate p21^{WAF1/cip1} promoter. Wild-type KLF6 and K209R were cotransfected with a p21^{WAF1/cip1} promoter reporter, respectively. Empty expression vector was transfected as a control for baseline luciferase activity. Transfection efficiencies were normalized using *Renilla* luciferase assay measured in the same lysate at the same time. **C**, K209R tumor mutant has reduced ability to up-regulate endogenous p21^{WAF1/cip1}. Wild-type KLF6 and K209R were transfected into PC3 cells, respectively. Thirty-six hours after transfection, cells were lysed and loaded onto SDS-PAGE followed by Western blot analysis. Anti-p21^{WAF1/cip1} antibody was used to detect the expression of endogenous p21^{WAF1/cip1} protein. The protein expression of transfected KLF6 and mutants constructed was detected by anti-KLF6 antibody. Tubulin was blotted as a control for protein loading. **D**, impaired growth suppression by K209R mutant in stable prostate cell lines. Both PC3M and BPH cell lines were stably transfected with either pCIneo empty vector, KLF6 wild type, or K209R mutant as described in Materials and Methods, and cell proliferation was assessed by estimating ³H-thymidine incorporation at 24, 48, and 72 hours after replating equal numbers of cells. The differences were statistically significant, as indicated by Ps. ★, *P*<0.05; ★★★, *P*<0.01.

p53's interaction with other cellular and viral factors, thereby altering protein p53 levels (52–55).

Acetylation of specific lysine residues by different acetyltransferases may lead to divergent functional outcomes. For example, acetylation of pRb at specific lysine residues by p300 has been

linked to inhibition of cell cycle progression (25), whereas acetylation of pRb by PCAF of key Lys^{873/874} near the COOH terminus correlates with cell differentiation (56). These divergent outcomes may also reflect differences between p300 and PCAF in promoting cell differentiation *in vivo* (57). It seems possible that similar, subtle

differences in KLF6 acetylation may also underlie functional differences as well, a possibility that merits further study. Interestingly, rodent and human KLF6 carry the consensus R-K-X-X-T-K sequence at residues 208 to 213, which is as a substrate site for p300/CBP in nuclear factor- κ B (relA)-mediated inflammation and interaction with I κ B α (58). Thus far, KLF5 and KLF13 are the only KLFs reported to be regulated by acetylation (59, 60).

In summary, our data establish a role of KLF6 in recruiting a specific coactivator complex containing CBP and PCAF to promote transcriptional activation of p21^{WAF1/cip1} and provide evidence that KLF6 serves as a substrate for CBP HAT activity. Combined with the loss of growth suppressive activity of a tumor-derived

lysine mutant of KLF6, these findings point to acetylation as a key modification in regulating its growth- and tumor-suppressive activities.

Acknowledgments

Received 3/29/2005; revised 7/31/2005; accepted 8/8/2005.

Grant support: Department of Defense grants DAMD17-03-1-0100 (S.L. Friedman), DAMD17-02-1-0720, and DAMD17-03-1-0129 (J.A. Martignetti); NIH grants DK37340 (S.L. Friedman), CA088325 (R. Wang), HL67099, and CA98552 (M.J. Walsh); Bendheim Foundation (S.L. Friedman); and Howard Hughes Medical Student Research Fellowships (S. Yea and G. Narla).

The costs of publication of this article were defrayed in part by the payment of page charges. This article must therefore be hereby marked *advertisement* in accordance with 18 U.S.C. Section 1734 solely to indicate this fact.

References

- Narla G, Heath KE, Reeves HL, et al. KLF6, a candidate tumor suppressor gene mutated in prostate cancer. *Science* 2001;294:2563-6.
- Ratziu V, Lalazar A, Wong L, et al. Zf9, a Kruppel-like transcription factor up-regulated *in vivo* during early hepatic fibrosis. *Proc Natl Acad Sci U S A* 1998;95:9500-5.
- Turner J, Crossley M. Mammalian Kruppel-like transcription factors: more than just a pretty finger. *Trends Biochem Sci* 1999;24:236-40.
- Bieker JJ. Kruppel-like factors: three fingers in many pies. *J Biol Chem* 2001;276:34355-8.
- Koritschoner NP, Bocco JL, Panzetta-Dutari GM, Dumur CI, Flury A, Patrito LC. A novel human zinc finger protein that interacts with the core promoter element of a TATA box-less gene. *J Biol Chem* 1997;272:9573-80.
- Suzuki T, Yamamoto T, Kurabayashi M, Nagai R, Yazaki Y, Horikoshi M. Isolation and initial characterization of GBF, a novel DNA-binding zinc finger protein that binds to the GC-rich binding sites of the HIV-1 promoter. *J Biochem (Tokyo)* 1998;124:389-95.
- Kim Y, Ratziu V, Choi SG, et al. Transcriptional activation of transforming growth factor β 1 and its receptors by the Kruppel-like factor Zf9/core promoter-binding protein and Sp1. Potential mechanisms for autocrine fibrogenesis in response to injury. *J Biol Chem* 1998;273:33750-8.
- Warke VG, Nambiar MP, Krishnan S, et al. Transcriptional activation of the human inducible nitric-oxide synthase promoter by Kruppel-like factor 6. *J Biol Chem* 2003;278:14812-9.
- Kojima S, Hayashi S, Shimokado K, et al. Transcriptional activation of urokinase by the Kruppel-like factor Zf9/COPEB activates latent TGF- β 1 in vascular endothelial cells. *Blood* 2000;95:1309-16.
- Inuzuka H, Wakao H, Masuho Y, Muramatsu MA, Tojo H, Nanbu-Wakao R. cDNA cloning and expression analysis of mouse zf9, a Kruppel-like transcription factor gene that is induced by adipogenic hormonal stimulation in 3T3-L1 cells. *Biochim Biophys Acta* 1999;1447:199-207.
- Chen C, Hyytinen ER, Sun X, et al. Deletion, mutation, and loss of expression of KLF6 in human prostate cancer. *Am J Pathol* 2003;162:1349-54.
- Reeves HL, Narla G, Oginbiyi O, et al. Kruppel-like Factor 6 (KLF6) is a tumor suppressor gene frequently inactivated in colorectal cancer. *Gastroenterology* 2004;126:1090-103.
- Chen HK, Liu XQ, Lin J, Chen TY, Feng QS, Zeng YX. Mutation analysis of KLF6 gene in human nasopharyngeal carcinomas. *Ai Zheng* 2002;21:1047-50.
- Jeng YM, Hsu HC. KLF6, a putative tumor suppressor gene, is mutated in astrocytic gliomas. *Int J Cancer* 2003;105:625-9.
- Kremer-Tal S, Reeves HL, Narla G, et al. Frequent inactivation of the tumor suppressor Kruppel-like factor 6 (KLF6) in hepatocellular carcinoma. *Hepatology* 2004;40:1047-52.
- Ito G, Uchiyama M, Kondo M, et al. Kruppel-like factor 6 is frequently down-regulated and induces apoptosis in non-small cell lung cancer cells. *Cancer Res* 2004;64:3838-43.
- Glinsky GV, Glinskii AB, Stephenson AJ, Hoffman RH, Gerald WL. Gene expression profiling predicts clinical outcome of prostate cancer. *J Clin Invest* 2004;113:913-23.
- Yamashita K, Upadhyay S, Osada M, et al. Pharmacologic unmasking of epigenetically silenced tumor suppressor genes in esophageal squamous cell carcinoma. *Cancer Cell* 2002;2:485-95.
- Okano J, Opitz OG, Nakagawa H, Jenkins TD, Friedman SL, Rustgi AK. The Kruppel-like transcription factors Zf9 and GKLF coactivate the human keratin 4 promoter and physically interact. *FEBS Lett* 2000;473:95-100.
- Botella LM, Sanchez-Elsner T, Sanz-Rodriguez F, et al. Transcriptional activation of endoglin and transforming growth factor- β signaling components by cooperative interaction between Sp1 and KLF6: their potential role in the response to vascular injury. *Blood* 2002;100:4001-10.
- Barlev N, Liu L, Chehab NH, et al. Acetylation of p53 activates transcription through recruitment of coactivators/histone acetyltransferases. *Mol Cell* 2001;8:1243-54.
- Narlikar GJ, Fan HY, Kingston RE. Cooperation between complexes that regulate chromatin structure and transcription. *Cell* 2002;108:475-87.
- Lill NL, Grossman SR, Ginsberg D, DeCaprio J, Livingston DM. Binding and modulation of p53 by p300/CBP coactivators. *Nature* 1997;387:823-7.
- Avantaggiati ML, Ogryzko V, Gardner K, Giordano A, Levine AS, Kelly K. Recruitment of p300/CBP in p53-dependent signal pathways. *Cell* 1997;89:1175-84.
- Chan HM, Krstic-Demonacos M, Smith L, Demonacos C, La Thangue NB. Acetylation control of the retinoblastoma tumour-suppressor protein. *Nat Cell Biol* 2001;3:667-74.
- Pao GM, Janknecht R, Ruffner H, Hunter T, Verma IM. CBP/p300 interact with and function as transcriptional coactivators of BRCA1. *Proc Natl Acad Sci U S A* 2000;97:1020-5.
- Doetzlhofer A, Rotheneder H, Lagger G, et al. Histone deacetylase 1 can repress transcription by binding to Sp1. *Mol Cell Biol* 1999;19:5504-11.
- Matsumoto N, Laub F, Aldabe R, et al. Cloning the cDNA for a new human zinc finger protein defines a group of closely related Kruppel-like transcription factors. *J Biol Chem* 1998;273:28229-37.
- Zhang W, Kadam S, Emerson BM, Bieker JJ. Site-specific acetylation by p300 or CREB binding protein regulates erythroid Kruppel-like factor transcriptional activity via its interaction with the SWI-SNF complex. *Mol Cell Biol* 2001;21:2413-22.
- Scolnick DM, Chehab NH, Stavridi ES, et al. CREB-binding protein and p300/CBP-associated factor are transcriptional coactivators of the p53 tumor suppressor protein. *Cancer Res* 1997;57:3693-6.
- Goodman RH, Smolik S. CBP/p300 in cell growth, transformation, and development. *Genes Dev* 2000;14:1553-77.
- Janknecht R, Hunter T. Transcription. A growing coactivator network. *Nature* 1996;383:22-3.
- Kouzarides T. Acetylation: a regulatory modification to rival phosphorylation? *EMBO J* 2000;19:1176-9.
- Shikama N, Lee CW, France S, et al. A novel cofactor for p300 that regulates the p53 response. *Mol Cell* 1999;4:365-76.
- Boyes J, Byfield P, Nakatani Y, Ogryzko V. Regulation of activity of the transcription factor GATA-1 by acetylation. *Nature* 1998;396:594-8.
- Liu L, Scolnick DM, Trievel RC, et al. p53 sites acetylated *in vitro* by PCAF and p300 are acetylated *in vivo* in response to DNA damage. *Mol Cell Biol* 1999;19:1202-9.
- Lundblad JR, Kwok RP, Laurance ME, Harter ML, Goodman RH. Adenoviral E1A-associated protein p300 as a functional homologue of the transcriptional coactivator CBP. *Nature* 1995;374:85-8.
- Jiang H, Lu H, Schiltz RL, et al. PCAF interacts with tax and stimulates tax transactivation in a histone acetyltransferase-independent manner. *Mol Cell Biol* 1999;19:8136-45.
- Ouchi T, Monteiro AN, August A, Aaronson SA, Hanafusa H. BRCA1 regulates p53-dependent gene expression. *Proc Natl Acad Sci U S A* 1998;95:2302-6.
- Nishio H, Walsh MJ. CCAAT displacement protein/cut homolog recruits G9a histone lysine methyltransferase to repress transcription. *Proc Natl Acad Sci U S A* 2004;101:11257-62.
- Gartel AL, Tyner AL. Transcriptional regulation of the p21(WAF1/CIP1) gene. *Exp Cell Res* 1999;246:280-9.
- Martinez-Balbas MA, Bauer UM, Nielsen SJ, Brehm A, Kouzarides T. Regulation of E2F1 activity by acetylation. *EMBO J* 2000;19:662-71.
- Kimmelman AC, Qiao RF, Narla G, et al. Suppression of glioblastoma tumorigenicity by the Kruppel-like transcription factor KLF6. *Oncogene* 2004;23:5077-83.
- Wang SP, Chen XP, Qiu FZ. A candidate tumor suppressor gene mutated in primary hepatocellular carcinoma: Kruppel-like factor 6. *Zhonghua Wai Ke Zhi* 2004;42:1258-61.
- Fang JY, Lu YY. Effects of histone acetylation and DNA methylation on p21(WAF1) regulation. *World J Gastroenterol* 2002;8:400-5.
- Archer SY, Hodin RA. Histone acetylation and cancer. *Curr Opin Genet Dev* 1999;9:171-4.
- Benzene S, Narla G, Allina J, et al. Cyclin-dependent kinase inhibition by the KLF6 tumor suppressor protein through interaction with cyclin D1. *Cancer Res* 2004;64:3885-91.
- Pardali K, Kurisaki A, Moren A, ten Dijke P, Kardassis D, Moustakas A. Role of Smad proteins and transcription factor Sp1 in p21(Waf1/Cip1) regulation by transforming growth factor- β . *J Biol Chem* 2000;275:29244-56.
- Xiao H, Hasegawa T, Isobe K. Both Sp1 and Sp3 are responsible for p21waf1 promoter activity induced by histone deacetylase inhibitor in NIH3T3 cells. *J Cell Biochem* 1999;73:291-302.

50. Mujtaba S, He Y, Zeng L, et al. Structural mechanism of the bromodomain of the coactivator CBP in p53 transcriptional activation. *Mol Cell* 2004; 13:251-63.
51. Wang YH, Tsay YG, Tan BC, Lo WY, Lee SC. Identification and characterization of a novel p300-mediated p53 acetylation site, lysine 305. *J Biol Chem* 2003;278:25568-76.
52. Haupt Y, Robles AI, Prives C, Rotter V. Deconstruction of p53 functions and regulation. *Oncogene* 2002; 21:8223-31.
53. Minamoto T, Buschmann T, Habelhah H, et al. Distinct pattern of p53 phosphorylation in human tumors. *Oncogene* 2001;20:3341-7.
54. Nakamura S, Roth JA, Mukhopadhyay T. Multiple lysine mutations in the C-terminus of p53 make it resistant to degradation mediated by MDM2 but not by human papillomavirus E6 and induce growth inhibition in MDM2-overexpressing cells. *Oncogene* 2002;21:2605-10.
55. Chao C, Hergenbahn M, Kaeser MD, et al. Cell type- and promoter-specific roles of Ser¹⁸ phosphorylation in regulating p53 responses. *J Biol Chem* 2003; 278:41028-33.
56. Nguyen DX, Baglia LA, Huang SM, Baker CM, McCance DJ. Acetylation regulates the differentiation-specific functions of the retinoblastoma protein. *EMBO J* 2004;23:1609-18.
57. Puri PL, Sartorelli V, Yang XJ, et al. Differential roles of p300 and PCAF acetyltransferases in muscle differentiation. *Mol Cell* 1997;1:35-45.
58. Chen LF, Mu Y, Greene WC. Acetylation of RelA at discrete sites regulates distinct nuclear functions of NF- κ B. *EMBO J* 2002;21:6539-48.
59. Matsumura T, Suzuki T, Aizawa K, et al. The deacetylase HDAC1 negatively regulates the cardiovascular transcription factor Kruppel-like factor 5 through direct interaction. *J Biol Chem* 2005;280:12123-9.
60. Song CZ, Keller K, Chen Y, Stamatoyannopoulos G. Functional interplay between CBP and PCAF in acetylation and regulation of transcription factor KLF13 activity. *J Mol Biol* 2003;329:207-15.

Suppression of glioblastoma tumorigenicity by the Kruppel-like transcription factor *KLF6*

Alec C Kimmelman¹, Rui F Qiao¹, Goutham Narla², Asoka Banno¹, Nelson Lau³, Paula D Bos¹, Nelson Nuñez Rodriguez¹, Bertrand C Liang⁴, Abhijit Guha³, John A Martignetti^{1,5,6}, Scott L Friedman² and Andrew M Chan^{*,1}

¹The Derald H Ruttenberg Cancer Center, The Mount Sinai School of Medicine, New York, NY 10029, USA; ²Division of Liver Diseases, Department of Medicine, The Mount Sinai School of Medicine, New York, NY 10029, USA; ³Division of Neurosurgery, Toronto Western Hospital, 399 Bathurst Street, Toronto, Ontario, Canada M5T 2S8; ⁴Biogen Idec, 10996 Torreyana Road, San Diego, CA 92121, USA; ⁵Department of Human Genetics, The Mount Sinai School of Medicine, New York, NY 10029, USA; ⁶Department of Pediatrics, The Mount Sinai School of Medicine, New York, NY 10029, USA

The Kruppel-like transcription factor *KLF6* is a novel tumor-suppressor gene mutated in a significant fraction of human prostate cancer. It is localized to human chromosome 10p14–15, a region that displays frequent loss of heterozygosity in glioblastoma multiforme (GBM). Indeed, mutations of the *KLF6* gene have recently been reported in this tumor type. In this study, we report that the expression of *KLF6* is attenuated in human GBM when compared with primary astrocytes. Expression of *KLF6* in GBM cells reverts their tumorigenicity both *in vitro* and *in vivo*, which is correlated with its transactivation of the p21/CIP1/WAF1 promoter. Additionally, *KLF6* inhibits cellular transformation induced by several oncogenes (*c-sis*/PDGF-B, *v-src*, H-Ras, and EGFR) that are components of signaling cascades implicated in GBM. Our results provide the first evidence of functional tumor suppression by *KLF6*, and its loss may contribute to glial tumor progression.

Oncogene (2004) 23, 5077–5083. doi:10.1038/sj.onc.1207662
Published online 5 April 2004

Keywords: glioblastoma; tumor suppressor; *KLF6*; Kruppel; transcription factor

Introduction

KLF6 is a novel member of the Kruppel-like family initially isolated as an upregulated gene in activated stellate cells of the liver (Ratziu *et al.*, 1998). Kruppel-like transcription factors (KLFs) contain a shared DNA-binding domain containing three C2H2 zinc-fingers (Turner and Crossley, 1999). A growing list of KLF target genes has been identified. For example,

GKLF (*KLF4*) activates p21(WAF1/Cip1) through a specific Sp1-like *cis*-element in the p21(WAF1/Cip1) proximal promoter and can form a complex with the tumor suppressor p53 (Zhang *et al.*, 2000). *KLF6* transactivates the promoters of collagen $\alpha 1(I)$ (Ratziu *et al.*, 1998), urokinase type plasminogen activator (Kojima *et al.*, 2000), TGF- $\beta 1$, TGF- $\beta 1$ receptors, and endoglin (Botella *et al.*, 2002).

KLF6 also plays a role in human cancer, since this gene is mutated in a significant fraction of human prostate carcinomas (Narla *et al.*, 2001). Moreover, prostate cancer-derived mutations leading to disruption of *KLF6* function enhance the growth of cultured cells, supporting its role as a *bona fide* tumor suppressor (Narla *et al.*, 2001). This growth suppressing activity has been attributed in part to promoter transactivation of the cyclin-dependent kinase inhibitor, p21. Interestingly, this transcriptional activity of *KLF6* is p53-independent (Narla *et al.*, 2001). As expected, tumor-associated mutations in *KLF6* abolish its ability to transactivate the p21 promoter. Thus, *KLF6* represents member of a novel tumor-suppressor pathway whose inactivation in certain tumors may occur independent of the loss of p53.

The high incidence of *KLF6* inactivation in prostate cancer is consistent with its localization to chromosome 10p15, a region frequently deleted in this malignancy (Narla *et al.*, 2001). Similarly, high frequency of loss of 10p15 has also been reported in glioblastoma multiforme (GBM) (Kimmelman *et al.*, 1996; Voesten *et al.*, 1997; Kon *et al.*, 1998; Harada *et al.*, 2000). Malignant neoplasms of the brain, the majority of which are of glial origin, cause an average of more than 13 000 deaths annually. GBM is the most aggressive and prevalent of these glial tumors (Holland, 2000). The prognosis of patients with GBM is extremely poor despite multimodality treatment, including surgical resection, radiation therapy, and chemotherapy. The median survival is approximately less than 1 year, and with only a 2% 5-year survival (Kleihues and Cavenee, 2000).

We and others have previously demonstrated that the short arm of chromosome 10 (10p14–15) may harbor

*Correspondence: AM Chan, Cancer Center, Mt Sinai School of Medicine, One, Gustave Levy Place, Box #1130, New York, NY 10029, USA; E-mail: Andrew.Chan@mssm.edu

Received 28 September 2003; revised 18 February 2004; accepted 18 February 2004; published online 5 April 2004

one or more tumor-suppressor loci involved in glioma progression (Kimmelman *et al.*, 1996). *KLF6* is mapped to this region between two microsatellite repeat markers, D10S533 and D10S591. Genomic loss between these two markers has been reported in 10–50% of glial tumors of low and high grade (Kimmelman *et al.*, 1996). The hypothesis that *KLF6* can be a glial tumor suppressor was further strengthened by the recent finding of tumor-associated *KLF6* mutations in primary glioblastomas (Jeng and Hsu, 2003). However, evidence that *KLF6* does indeed possess the biological attributes of a tumor suppressor is still lacking. Here, we provide the first demonstration that *KLF6* suppresses several biological properties of glioblastomas both *in vitro* and *in vivo*.

Results

Expression of *KLF6* in human glioblastomas

In order to investigate the possible role of *KLF6* in glial tumor progression, the expression level of this transcription factor was analyzed in a panel of glial tumor cell lines. The normal counterparts of these tumors were obtained from primary astrocytes derived from both human and mouse brains. An additional control was provided by a neural-derived cell line, DI TNC1. It is a rat astrocyte cell line established from a newborn rat brain and retains the characteristics of type I astrocytes (Radany *et al.*, 1992). As shown in Figure 1a, both primary astrocytes, and DI TNC1 expressed readily detectable levels of *KLF6*, which migrates as doublets of variable intensity within a size range of 35–43 kDa. The level of *KLF6* expression was higher in DI TNC1 than the two primary astrocyte cultures. To ascertain the molecular weight of human *KLF6*, a human *KLF6* cDNA was ectopically overexpressed in PC3 prostate cancer cell line. Under this condition, human *KLF6* was expressed as a doublet of 37 and 40 kDa in size. This doublet and its variable mobility among different cells are likely due to various phosphorylation states of *KLF6* (S Friedman, unpublished data).

When a panel of human glial tumor cell lines was examined by Western blot analysis, *KLF6* expression was reduced in eight of nine samples when compared to primary human astrocytes (Figure 1a). Apart from the cell line A2782, *KLF6* levels were attenuated from 1.5- to 8.0-fold in the remaining tumor lines. Next, to examine if this low level of *KLF6* expression in established cultures was also manifested in primary tumors, Western blot analysis was performed with total cell lysates derived from 13 randomly selected GBM surgical specimens. Using actin as a loading control, four out of 13 samples (1136, 1152, 1192, 1035) (~31%) displayed greater than 85% reduction in *KLF6* expression when compared to primary human astrocytes. Moderate levels were, however, detected in six tumor specimens (1046, 1052, 1133, 1176, 1181, 1209) while three samples (1066, 1089, 1123) possessed higher levels of *KLF6* expression. Interestingly, these tumor samples

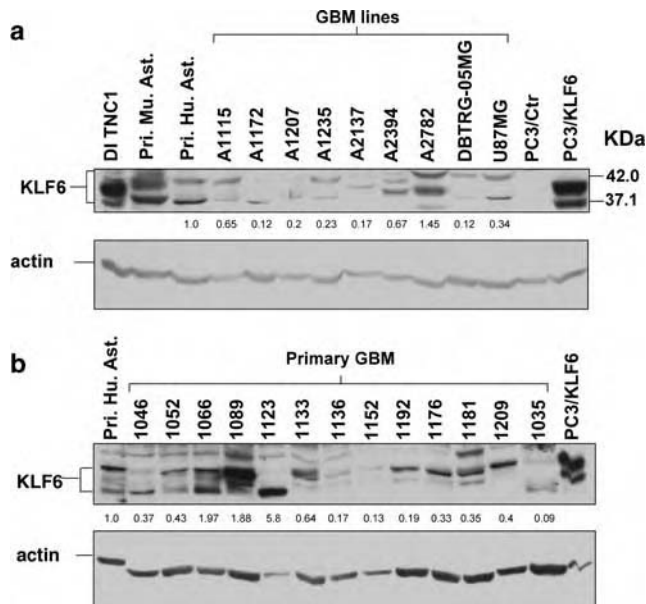


Figure 1 (a) Expression of *KLF6* in human gliomas. *KLF6* levels were determined using total cell extracts derived from a panel of nine GBM cell lines. Control lysates from primary mouse (Mu) and human (Hu) astrocytes (Ast), and DI TNC1 are included (upper panel). Cell lysates derived from PC3 cells transfected with control (Ctr) or *KLF6* expression plasmids are used to ascertain the size of the *KLF6* protein species. The doublets characteristic of endogenous *KLF6* are bracketed. A parallel filter was probed with an antibody to actin as a control for sample loading (lower panel). Numbers in the middle are relative densitometric values of *KLF6* normalized with actin. (b) Expression of *KLF6* in primary GBM was examined by Western blot analysis as described in (a)

displayed a varying pattern of *KLF6* isoforms, with several samples possessing only the lower molecular weight species (for example, 1046, 1123). This data implies that full-length *KLF6* expression may be lost or attenuated in a significant fraction of both primary tumors and established GBM cell lines.

KLF6 suppresses glioblastoma tumorigenicity and growth properties *in vitro*

To further study the importance of *KLF6* in the biology of glial tumors, *KLF6* was introduced through retroviral-mediated gene transfer in the DBTRG-05MG glioblastoma cell line. As shown in Figure 2a, this cell line has very low endogenous expression of *KLF6*, and previous studies have shown that this line is monosomic for chromosome 10 with wild-type p53 alleles (Kruse *et al.*, 1992). Western blot analysis of marker-selected mass cultures revealed that *KLF6* was expressed at a level below those of DI TNC1 astrocytes (Figure 2a). The low level of ectopically expressed *KLF6* in the stable lines thus provides a near-physiological system to study the effects of *KLF6*. Additionally, a mutant form of *KLF6*, *KLF6*- Δ N, which has the majority of the transactivation domain deleted was used as a negative control. This protein was undetectable, which we believe reflects the loss of major immunogenic epitopes recognized by the polyclonal antibody raised against the

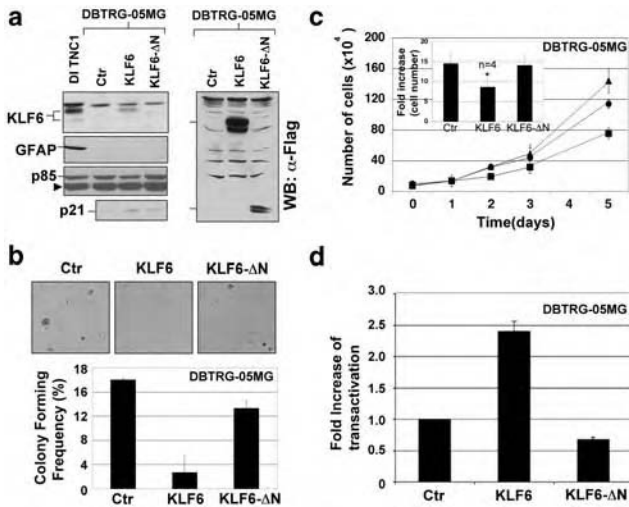


Figure 2 (a) Suppression of transformed phenotypes by *KLF6*. Stable cell lines created by retroviral infection of DBTRG-05MG with either a control virus (Ctr), *KLF6*, or a *KLF6* mutant with a truncated transactivation domain (*KLF6*-ΔN) were analysed by Western blot using the anti-*KLF6* antibody. The same blot was also probed with an antibody to the glial fibrillary acidic protein (GFAP) to determine the differentiation state of the cells, as well as the anti-p85 antibody to normalize protein loading (left panel). Cell lysates from transiently transfected DBTRG-05MG were analysed for the expression of the FLAG-tagged full-length *KLF6* and the *KLF6*-ΔN mutant by an anti-FLAG antibody (right panel). (b) DBTRG-05MG glioblastoma cells transduced with a control plasmid, *KLF6*, or the *KLF6*-ΔN mutant were seeded in soft agar and colonies were allowed to form. Representative fields from a single experiment are depicted (mag. × 4). The lower panel shows the number of colonies formed from an experiment performed in triplicate with standard deviations and similar data were obtained in a separate experiment. (c) The proliferation of cells harboring control vector (●), *KLF6* (■), and *KLF6*-ΔN (▲) expression plasmids was determined by counting cell numbers with results over a 5-day period are plotted. Error bars represent the standard deviation of a single assay performed in triplicate. The inset represents statistical analysis of the fold increase in cell number on day 5. Values are means ± s.e.m. where * indicates $P < 0.05$. (d) DBTRG-05MG cells were transiently transfected with *KLF6* expression plasmids along with a p21 promoter-luciferase reporter. Results are expressed as a fold over control-transfected cells, with all values normalized to total protein levels from an assay performed in triplicate. Similar results were obtained in an additional experiment

amino terminus of the protein. To confirm that the truncated protein could be expressed in this tumor, we transiently transfected expression constructs of FLAG-tagged full-length *KLF6* and *KLF6*-ΔN in DBTRG-05MG. Indeed, protein species of ~40 and ~17 kDa corresponding to the full-length and N-terminal truncated *KLF6* were detected with an anti-FLAG antibody (Figure 2a, right panel).

Most astrocytic cells express glial fibrillary acidic protein (GFAP), a marker of differentiated glial cells. DBTRG-05MG, on the other hand, represents a highly dedifferentiated tumor cell line and unlike the DI TNC1 astrocytes, do not express GFAP (Figure 2a, left panel). Expression of *KLF6* did not, however, upregulate GFAP in these tumor cells. It is, therefore, unlikely that *KLF6* can alter the differentiation state of DBTRG-

05MG. In addition, we observed a ~3.0-fold increase in the level of *p21/CIP1/WAF1* in the *KLF6* transfectant (Figure 2a). This is consistent with the previous finding that *KLF6* activates the transcription of this cell cycle inhibitor.

To examine if *KLF6* could modify the transformed phenotype of DBTRG-05MG cells, we assayed the ability of these transfectants to grow in an anchorage-independent manner. As shown in Figure 2b, whereas vector- and *KLF6*-ΔN-transduced cells were able to form large colonies, the growth of *KLF6*-expressing cells in semisolid agar was markedly impaired by approximately 5.0–7.0 fold. In addition, these cells also displayed a slower proliferative rate than their control counterparts (Figure 2c). *KLF6* expressing DBTRG-05MG showed a 43% reduction in cell numbers over a 5-day period when cultured in 5% serum (Figure 2c, inset). Next, we examined if both the reduction of colony formation in soft-agar growth as well as the slower cell growth correlated with the ability of *KLF6* to transactivate the p21 promoter. When transiently cotransfected in DBTRG-05MG cells with a luciferase reporter plasmid containing the p21 promoter, *KLF6* increased luciferase activity by ~2.5-fold when compared to vector-transfected cells (Figure 2d). Interestingly, the *KLF6*-ΔN construct appeared to slightly diminish basal transactivation of the promoter, which could explain its ability to moderately increase the proliferative rate *in vitro*.

To demonstrate that the growth-suppressive effects of *KLF6* were not limited to a single cell line, an additional GBM line was infected with the same *KLF6* retroviruses under similar experimental conditions. For this, we used the malignant glioma cell line, U87MG, which has a moderate level of *KLF6* expression and similar to DBTRG-05MG, possesses wild-type p53 gene. U87MG cells transduced with *KLF6* virus were able to express the ~40 kDa *KLF6* protein in a stable manner (Figure 3a). Expression of the truncated *KLF6*-ΔN mutant was also monitored by transient transfection as described for DBTRG-05MG previously (Figure 3a, right panel). In addition, we did not observe any significant increases in levels of either GFAP (data not shown) or p21/CIP1/WAF1 in the *KLF6* transfectant (Figure 3a, left panel). Next, their *in vitro* growth rates were assessed, which were significantly attenuated by *KLF6* by ~36% (Figure 3b, inset). Furthermore, a significant fraction of the *KLF6*-expressing U87MG cells reverted from a highly refractile to an overtly flattened cell morphology (dark arrows, Figure 3c). In addition, some cells displayed striking cellular protrusions reminiscent of neurite outgrowth (white arrowheads, Figure 3c). Thus, we conclude that *KLF6* is capable of suppressing the *in vitro* growth properties of glioblastoma cell lines.

KLF6 inhibits cellular transformation induced by oncogenes

Several human oncogene products have been implicated in glial tumor progression. These include the increased

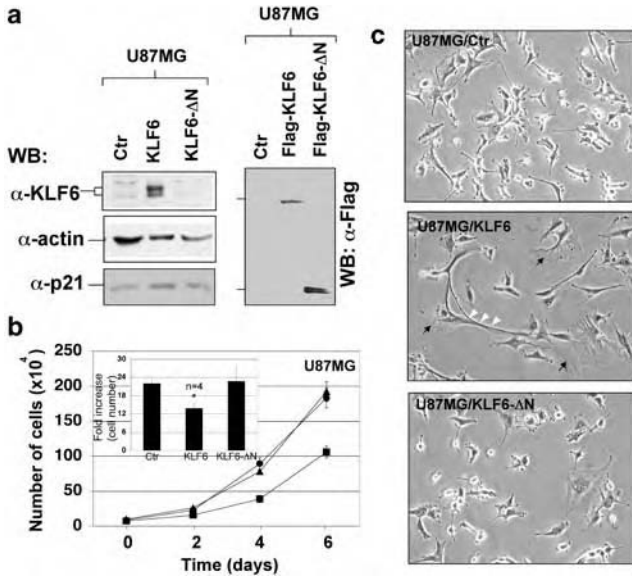


Figure 3 (a) *KLF6* induces morphological changes in a glioblastoma cell line. Stable cell lines were established by retroviral infection of U87MG as described in Figure 2. Cell lysates derived from transfectants were subjected to Western blot analysis using the anti-*KLF6* antibody, as well as an anti-actin antibody to normalize protein loading. Expression of the *KLF6* protein species was also confirmed by transient transfection of FLAG-tagged cDNAs as described in the legend of Figure 2a. (b) The proliferation of these cells was determined as described in Figure 2c. (c) Cell morphology of marker-selected U87MG transfectants was visualized by light photomicroscopy. *KLF6* induced a marked flattening of cell bodies (dark arrows) in U87MG as well as the extension of long cellular processes (white arrowheads) (mag. $\times 10$)

expression/activation of receptors for epidermal growth factor (EGF) and platelet-derived growth factor (PDGF) (Maher *et al.*, 2001). In addition, conditional expression of a *RAS* oncogene in glial cell lineages led to the formation of glioblastomas in an animal model (Ding *et al.*, 2001). Finally, animals harboring a *v-src* transgene underwent an early induction of angiogenesis in gliomas (Theurillat *et al.*, 1999). To analyse whether *KLF6* was capable of blocking these oncogenic signals, focus-forming assays were performed in NIH 3T3 cells. To induce transformed foci, NIH 3T3 cells were transfected with plasmids expressing *c-sis*/PDGF-B, *v-src*, H-Ras R12, or EGFR. Cells were either cotransfected with a control vector, a *KLF6* expression plasmid, or the *KLF6*-ΔN mutant. As shown in Figure 4, *KLF6* expression was able to significantly block morphological transformation by PDGF-B, *v-src*, H-Ras R12 by ~60%. *KLF6* was, however, relatively less effective in inhibiting the transforming effect of EGFR. As expected, the ability of *KLF6*-ΔN mutant to produce similar inhibitory effect was markedly diminished.

KLF6 attenuates glioblastoma tumorigenicity in vivo

Based on its inhibitory activity *in vitro*, we assessed whether the expression of *KLF6* in DBTRG-05MG affected tumorigenicity *in vivo*. Cells harboring either

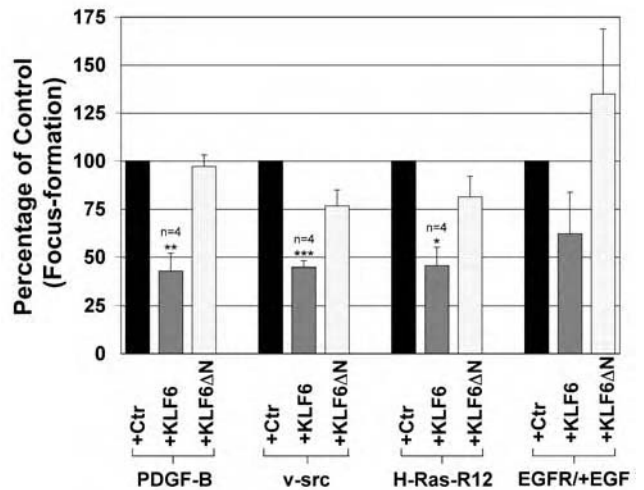


Figure 4 Suppression of oncogene transformation by *KLF6*. Around 1×10^5 NIH 3T3 cells were cotransfected using the indicated oncogenes with either a control plasmid, *KLF6* or *KLF6*-ΔN, and focus forming assays were performed. Data are expressed as percent of foci of control with results expressed as means \pm s.e.m. * $P < 0.05$; ** $P < 0.01$; *** $P < 0.001$

control or *KLF6* expression plasmid were injected subcutaneously into nude mice and tumors were allowed to form. Tumor volume was measured on a weekly basis for 7 weeks prior to sacrificing. As depicted in Figure 5a, the majority of animals injected with tumor cells expressing *KLF6* had decreased tumor volumes when compared to animals inoculated with cells expressing the vector control. Additionally, when grouped according to tumor volume, 60% of mice injected with control cells fell within the intermediate (3000–6000 mm³) to largest (>6000 mm³) volumes, while only 10% of animals injected with *KLF6*-transduced cells induced tumors in these volume ranges (Figure 5a, right panel). In fact, 90% of the mice injected with *KLF6*-expressing cells produced tumors with volumes smaller than 3000 mm³. These data were reproduced by using stable lines from an independent infection experiment (Figure 5b). In this case, while 4/7 of the animals injected with control cells harbored tumors of >10 000 mm³ in size, only 1/7 of mice inoculated with *KLF6*-expressing cells managed to achieve this tumor volume. Thus, the expression of *KLF6* in DBTRG-05MG glioblastoma cells leads to the attenuation of tumorigenic phenotypes both *in vitro* and *in vivo*.

Discussion

This report provides the first biological evidence that *KLF6* possesses tumor-suppressing activity *in vivo*. We have shown that *KLF6* expression is attenuated in a variety of glial tumor cell lines when compared with primary astrocytes. Expression of *KLF6* in two GBM lines inhibits their transformed phenotypes *in vitro* and reduces their ability to form tumors in mice. Additionally, *KLF6* may block proliferative signals associated

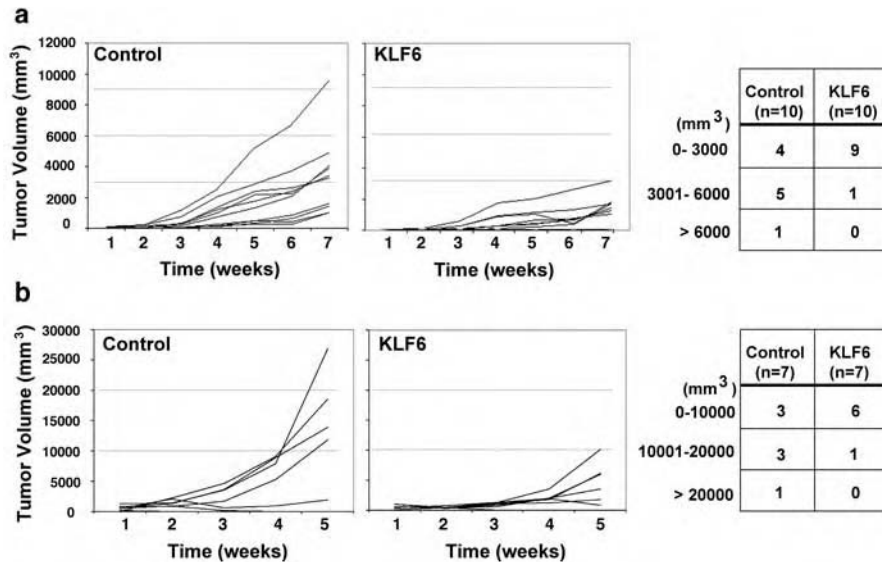


Figure 5 (a) Suppression of tumor formation *in vivo* by *KLF6*. DBTRG-05MG cells transduced with either the control vector (left panel) or *KLF6* (right panel) were injected subcutaneously into 10 nude mice. Individual lines representing total tumor volume ($L \times W \times H$ in mm³) of each animal measured over a 7-week period are shown. The horizontal bars (dotted line) demarcate the tumor groups based on the indicated size range. The number of mice with tumors of the indicated size range is tabulated on the right to illustrate the suppression of the number of animals possessing larger tumors by *KLF6*. An additional tumorigenicity assay was performed using the same transfectants with similar data being obtained. (b) A similar experiment was also repeated with independently infected DBTRG-05MG cells. A total of seven animals were used for each cell line and total tumor volume was measured weekly for up to 5 weeks

with specific lesions found in glial tumors such as PDGFR or EGFR amplification, and the constitutive activation of the Ras-dependent signaling pathways. Our work complements the recent finding that *KLF6* is mutated in 11.8% (9/76) of primary GBM samples (Jeng and Hsu, 2003). The fact that 85% of tumors with *KLF6* mutations have lost the remaining wild-type allele strongly suggests that *KLF6* is a classical tumor-suppressor gene.

GBM can occur as a primary (*de novo*) tumor or derived from the progression of anaplastic astrocytoma (Maher *et al.*, 2001). The loss of 10p is frequently associated with primary GBM, which are characterized by EGFR overexpression and the lack of p53 mutations (Maher *et al.*, 2001). Since *KLF6* can upregulate p21 independent of p53, this suggests that the loss of *KLF6* and p53 in GBM may be mutually exclusive.

Additionally, the tumor suppressor PTEN, which is located on the long arm of chromosome 10, is mutated in a significant fraction of GBM (Kato *et al.*, 2000). Therefore, it will be interesting to analyse *KLF6*-deficient mice alone or in combination with other genetic backgrounds, such as *PTEN* (-/+) or p53 (-/+), for the development of glial tumors. Of note, *PTEN* heterozygous mice, while susceptible to tumors such as lymphomas, do not develop glial tumors, although the gene is found to be mutated in approximately 12% of gliomas (Podsypanina *et al.*, 1999). It is also interesting to note that chromosome 10 is monosomic in >60% and partially lost in up to 90% of higher-grade gliomas (Maher *et al.*, 2001). In addition, using flanking microsatellite markers localized within 1 cm of the

KLF6 gene, the frequency was observed to be as high as 70% (J Martignetti and B Feuerstein, unpublished observations). Therefore, it is very likely that the inactivation of *KLF6*, *PTEN* as well as several other tumor-suppressor genes on this chromosome contribute to tumor progression. The availability of a knockout mouse model for *KLF6* will allow these possibilities to be tested.

Functional loss of *KLF6* may occur on several levels, as we failed to detect genetic alterations of this transcription factor in the limited number of cell lines examined (data not shown). We speculate that the reduced expression of *KLF6* may occur either by the loss of an entire or portion of chromosome 10 at loci flanking *KLF6*, while subsequent alterations leading to the abolition of *KLF6* expression could reflect epigenetic mechanisms. For example, the reduced transcription from Apaf-1 due to promoter methylation has been observed in some melanomas (Soengas *et al.*, 2001). Alternatively, overexpression of Mdm2, which is an E3 ubiquitin ligase, promotes the degradation of the p53 tumor suppressor through a proteasome-dependent pathway (Honda *et al.*, 1997). Finally, it is also possible that the loss of the single allele of *KLF6* may lead to tumor progression through a haploinsufficiency mechanism. However, a more extensive analysis of primary glial tumors and additional GBM cell lines is necessary to ascertain the frequency of *KLF6* loss and/or inactivation in GBM.

The ability of *KLF6* to suppress the transforming activity of several oncogenes in NIH 3T3 cells is potentially important. This observation is unlikely due

to a general toxic effect of *KLF6* on NIH3T3 cells since it does not significantly reduce the number of marker-selectable colony in conventional colony-forming assays (data not shown). Most receptor tyrosine kinase oncogenes such as PDGFR and EGFR are dependent on Ras and Src for their signaling events (Satoh *et al.*, 1990; Broome and Hunter, 1996). Interestingly, *p21/CIP1/WAF1*, a *KLF6* target gene, blocks cellular transformation by a variety of oncogenes, which could provide a mechanism through which *KLF6* inhibits tumor cell growth (Givol *et al.*, 1995). Whether *KLF6* could directly block components of signaling pathways emanated from these oncogenes in GBM is by far unknown.

Attenuation of GBM growth by *KLF6* could potentially be an avenue for therapeutic intervention. Indeed, since only a modest level of *KLF6* is necessary to suppress tumor growth, this gene is an attractive candidate for gene therapy approaches. More importantly, the frequent genomic loss in this region in multiple tumor types implies that *KLF6* may represent an important tumor suppressor for a broad range of human cancers.

Materials and methods

Cell culture, generation of stable lines, and tumor specimens

GBM cell lines were obtained from either American Type Culture Collection (ATCC) or Dr Stuart Aaronson (Mt Sinai, New York, NY, USA) and maintained in Dulbecco's modified Eagle's medium (D-MEM) supplemented with 10% (v/v) fetal calf serum (FCS). DI TNC1 was obtained from ATCC and propagated in DMEM supplemented with 10% FCS. NIH 3T3 was maintained in DMEM supplemented with 10% (v/v) calf serum (CS). The procedures for generating stable lines by retroviral-mediated gene transfer have been described previously (Osada *et al.*, 1999). Primary cultures of mouse astrocytes were prepared from postnatal day 4 pups as previously described (Banker and Goslin, 1998). Primary human astrocytes were purchased from Cambrex Corp. (East Rutherford, NJ, USA). All tumor specimens were obtained from the University of Toronto Nervous System Tumor Bank at The Toronto Hospital. Resected tumors were placed in cryovials and immediately flash-frozen in liquid nitrogen in the operating room. A random cohort of 13 GBM specimens was processed for protein extraction in a buffer containing 50 mM HEPES, pH 7.0, 150 mM NaCl, 10% glycerol, 1% Triton X-100, 1.5 mM MgCl₂, 1 mM EGTA, 100 mM NaF, 10 mM NaPPi, 1 mM PMSF, 2 mM leupeptin, and 2 mM aprotinin.

Expression plasmids

The *pBabepuro* expression constructs were generated by inserting the full-length and truncated (aa 184–283) human *KLF6* cDNA (*KLF6*-ΔN) in the *Bam*HI site of the *pBabepuro* vector. The *pCIneo-KLF6* expression construct was created by fusing a full-length *KLF6* cDNA in the *Eco*RI and *Xba*I sites of the *pCIneo* vector. The *c-sis*/PDGF-B expression plasmid has previously been described (LaRochelle *et al.*, 1990). The *pBabepuro-v-src* (Osada *et al.*, 1999), *pCEV29-H-Ras* R12 (Chan *et al.*, 1994), and *pLTR2-EGFR* (Di Fiore *et al.*, 1987) plasmids have been described previously.

Antibodies

The polyclonal anti-*KLF6* (R-173), anti-actin, and anti-p21 antibodies were obtained from Santa Cruz, Santa Cruz, CA, USA. The anti-p85 polyclonal antibody was purchased from Upstate Biotech, Lake Placid, NY, USA. The anti-GFAP monoclonal antibody was a gift from Dr David Colman (Mt Sinai, New York, NY, USA). The anti-FLAG M2 monoclonal antibody was purchased from Sigma, St Louis, MO, USA.

Western blot analysis

Unless otherwise indicated all cell solubilization steps were performed using the standard RIPA buffer. For standard Western blot analysis, 50–100 μg of total cell extracts were resolved on a 12.5% SDS-PAGE and following transfer onto nitrocellulose membranes, proteins of interest were detected by incubating with primary antibodies (α-*KLF6*, 1:400; α-actin, 1:2000; α-p21, 1:500; α-p85, 1:1000; α-GFAP, 1:1000, and α-Flag, 1:1000) and processed by the standard ECL detection method under conditions recommended by the manufacturer (Amersham, Piscataway, NJ, USA). Filters were then subjected to autoradiography.

Cell proliferation assays

For analysis of proliferation in semisolid medium, ~1 × 10⁴ cells were suspended in 0.5% agarose (Noble agar, Difco, Becton-Dickinson, Franklin Lakes, NJ, USA) in 10% CS in triplicate as described elsewhere (Chan *et al.*, 1994). Colonies were stained with *p*-iodonitrotetrazolium violet (Sigma, St Louis, MO, USA) and scored after 2 weeks. Proliferation of stably transfected cells were determined over a 5–6 day period by counting the number of cells by a hemacytometer at regular intervals.

p21 transactivation assays

DBTRG-05MG cells were plated at ~80% confluence in six-well plates and transfected using lipofectamine 2000 (Invitrogen, Carlsbad, CA, USA) with 1 μg of the *p21* promoter reporter construct (Narla *et al.*, 2001) and 2 μg of either *KLF6*, *KLF6*-ΔN, or a control vector. Approximately 48 h after transfection, cells were solubilized in the supplied lysis buffer and luciferase assays were performed according to the manufacturer's instructions (Promega, Madison, WI, USA).

NIH 3T3 focus forming assay

Approximately 1.5 × 10⁵ NIH3T3 cells were plated in triplicate onto a 100-mm culture dish and DNA transfection was performed by the standard calcium phosphate precipitation method (Chan *et al.*, 1994). Transformed foci were induced by using *c-sis*/PDGF-B (65 ng), *v-src* (30 ng), H-Ras R12 (50 ng), or EGFR (1 μg). Each oncogene plasmid was cotransfected with 2 μg of either *pBabepuro*, *pBabepuro-KLF6*, or *pBabepuro-KLF6*-ΔN. After transfection, medium was changed twice a week with 5% CS in DMEM, and the number and quality of foci were scored every week for up to 3 weeks. All plates were then fixed in 70% cold methanol and stained with Giemsa solution for detailed quantitative analysis.

In vivo tumorigenicity assays

Around 2.5 × 10⁶ marker-selected cells were injected subcutaneously into both flanks of nude mice. Tumor growth was monitored every 7 days at the sites of injection. A caliper was used to determine the length, width, and height of each tumor. The volume was calculated by multiplying the length, width,

and height. After approximately 5–7 weeks, each tumor was dissected and weighed. Tumor growth was presented as the total tumor volume for each animal in mm³.

Statistical analysis

Statistical significance was determined by Student's *t* test. Results are expressed as means ± s.e. Statistical significance was considered to be $P < 0.05$.

References

- Banker G and Goslin K. (1998). *Culturing Nerve Cells*. MIT Press: Cambridge, MA.
- Botella LM, Sanchez-Elsner T, Sanz-Rodriguez F, Kojima S, Shimada J, Guerrero-Esteo M, Cooreman MP, Ratziu V, Langa C, Vary CP, Ramirez JR, Friedman S and Bernabeu C. (2002). *Blood*, **100**, 4001–4010.
- Broome MA and Hunter T. (1996). *J. Biol. Chem.*, **271**, 16798–16806.
- Chan AM, Miki T, Meyers KA and Aaronson SA. (1994). *Proc. Natl. Acad. Sci. USA*, **91**, 7558–7562.
- Di Fiore PP, Pierce JH, Fleming TP, Hazan R, Ullrich A, King CR, Schlessinger J and Aaronson SA. (1987). *Cell*, **51**, 1063–1070.
- Ding H, Roncari L, Shannon P, Wu X, Lau N, Karaskova J, Gutmann DH, Squire A, Nagy A and Guha A. (2001). *Cancer Res.*, **61**, 3826–3836.
- Givol I, Givol D, Rulong S, Resau J, Tsarfaty I and Hughes SH. (1995). *Oncogene*, **11**, 2609–2618.
- Harada K, Nishizaki T, Maekawa K, Kubota H, Harada K, Suzuki M, Ohno T, Sasaki K and Soeda E. (2000). *Genomics*, **67**, 268–272.
- Holland EC. (2000). *Proc. Natl. Acad. Sci. USA*, **97**, 6242–6244.
- Honda R, Tanaka H and Yasuda H. (1997). *FEBS Lett.*, **420**, 25–27.
- Jeng YM and Hsu HC. (2003). *Int. J. Cancer*, **105**, 625–629.
- Kato H, Kato S, Kumabe T, Sonoda Y, Yoshimoto T, Kato S, Han SY, Suzuki T, Shibata H, Kanamaru R and Ishioka C. (2000). *Clin. Cancer Res.*, **6**, 3937–3943.
- Kimmelman AC, Ross DA and Liang BC. (1996). *Genomics*, **34**, 250–254.
- Kleihues P and Cavenee WK. (2000). *World Health Organization. IARC/WHO*: Lyon.
- Kojima S, Hayashi S, Shimokado K, Suzuki Y, Shimada J, Crippa MP and Friedman SL. (2000). *Blood*, **15**, 1309–1316.
- Kon H, Sonoda Y, Kumabe T, Yoshimoto T, Sekiya T and Murakami Y. (1998). *Oncogene*, **16**, 257–263.
- Kruse CA, Mitchell DH, Kleinschmidt-DeMasters BK, Franklin WA, Morse HG, Spector EB and Lillehei KO. (1992). *In Vitro Cell Dev. Biol.*, **28A**, 609–614.
- LaRochelle WJ, Giese N, May-Siroff M, Robbins KC and Aaronson SA. (1990). *Science*, **248**, 1541–1544.
- Maher EA, Furnari FB, Bachoo RM, Rowitch DH, Louis DN, Cavenee WK and DePinho RA. (2001). *Genes Dev.*, **15**, 1311–1333.
- Narla G, Heath KE, Reeves HL, Li D, Giono LE, Kimmelman AC, Gluckman MJ, Narla J, Eng FJ, Chan AM, Ferrari AC, Martignetti JA and Friedman SL. (2001). *Science*, **294**, 2563–2566.
- Osada M, Tolkacheva T, Li W, Chan TO, Tschlis PN, Saez R, Kimmelman AC and Chan AM. (1999). *Mol. Cell. Biol.*, **19**, 6333–6344.
- Podsypanina K, Ellenson LH, Nemes A, Gu J, Tamura M, Yamada KM, Cordon-Cardo C, Catoretti G, Fisher PE and Parsons R. (1999). *Proc. Natl. Acad. Sci. USA*, **16**, 1563–1568.
- Radany EH, Brenner M, Besnard F, Bigornia V, Bishop JM and Descheppe CF. (1992). *Proc. Natl. Acad. Sci. USA*, **15**, 6467–6471.
- Ratziu V, Lalazar A, Wong L, Dang Q, Collins C, Shaulian E, Jensen S and Friedman SL. (1998). *Proc. Natl. Acad. Sci. USA*, **95**, 9500–9505.
- Satoh T, Endo M, Nakafuku M, Akiyama T, Yamamoto T and Kaziro Y. (1990). *Proc. Natl. Acad. Sci. USA*, **87**, 7926–7929.
- Soengas MS, Capodici P, Polsky D, Mora J, Esteller M, Opitz-Araya X, McCombie R, Herman JG, Gerald WL, Lazebnik YA, Cordon-Cardo C and Lowe SW. (2001). *Nature (London)*, **409**, 207–211.
- Theurillat JP, Hainfellner J, Maddalena A, Weissenberger J and Aguzzi A. (1999). *Am. J. Pathol.*, **154**, 581–590.
- Turner J and Crossley M. (1999). *Trends Biochem. Sci.*, **24**, 236–240.
- Voesten AM, Bijleveld EH, Westerveld A and Hulsebos TJ. (1997). *Genes Chromosomes Cancer*, **20**, 167–172.
- Zhang W, Geiman DE, Shields JM, Dang DT, Mahatan CS, Kaestner KH, Biggs JR, Kraft AS and Yang VW. (2000). *J. Biol. Chem.*, **16**, 18391–18398.

Transcriptional Activation of the Insulin-Like Growth Factor I Receptor Gene by the Kruppel-Like Factor 6 (KLF6) Tumor Suppressor Protein: Potential Interactions between KLF6 and p53

MORAN RUBINSTEIN, GILA IDELMAN, STEPHEN R. PLYMATE, GOUTHAM NARLA, SCOTT L. FRIEDMAN, AND HAIM WERNER

Department of Clinical Biochemistry, Sackler School of Medicine, Tel Aviv University (M.R., G.I., H.W.), Tel Aviv 69978, Israel; Department of Medicine, University of Washington (S.R.P.), Seattle, Washington 98195; and Division of Liver Diseases, Mount Sinai School of Medicine (G.N., S.L.F.), New York, New York 10029

The IGF system plays an important role in prostate cancer initiation and progression. Most of the biological actions of IGF-I and IGF-II are mediated by activation of the IGF-I receptor (IGF-IR). Evidence accumulated in recent years indicates that acquisition of the malignant phenotype is initially IGF-IR dependent, but progression toward metastatic stages is usually associated with a decrease in IGF-IR levels. The Kruppel-like factor 6 (KLF6) is a zinc finger-containing transcription factor that was shown to be mutated in a significant portion of prostate and other types of cancer. To examine the potential regulation of IGF-IR gene expression by KLF6, we measured KLF6 levels in prostate-derived cell lines displaying different levels of IGF-IR. The results of Western analysis showed that KLF6 levels were higher in nontumorigenic P69 cells expressing high IGF-IR levels than in metastatic M12 cells containing reduced IGF-IR levels. Transient coexpression of wild-type, but not mutated, KLF6 together with an IGF-IR promoter-luciferase reporter plasmid resulted in an approximately 3.4-fold stimulation of IGF-IR promoter activity. Furthermore, KLF6 expression induced a significant in-

crease in endogenous IGF-IR levels. Deletion analysis of the IGF-IR promoter revealed that a cluster of four GC boxes located between nucleotides –399 and –331 mediates a significant portion of the transactivating effect of KLF6. KLF6, although unable to stimulate IGF-IR promoter activity in Sp1-null *Drosophila*-derived Schneider cells, significantly enhanced the effect of Sp1. To assess the potential interactions between KLF6 and p53 in the regulation of IGF-IR gene expression, transfections were performed in the colorectal cancer cell line HCT116^{+/+}, which expresses p53, and its HCT116^{-/-} derivative, which lacks p53. KLF6 exhibited an enhanced activity in p53-containing, compared with p53-null, cells. In addition, we were able to detect a physical interaction between KLF6 and p53. In summary, we have identified the IGF-IR gene as a novel downstream target for transcription factor KLF6. The regulation of IGF-IR gene expression by KLF6 may have significant implications in terms of cancer initiation and/or progression. (*Endocrinology* 145: 3769–3777, 2004)

THE IGF-I RECEPTOR (IGF-IR) mediates the mitogenic, transforming, differentiating, and antiapoptotic actions of IGF-I and IGF-II (1–3). Most primary tumors and transformed cell lines display augmented numbers of IGF-IRs on their cell surface as well as increased levels of IGF-IR mRNA that confer upon the malignant cell an enhanced survival capacity. The involvement of the IGF-IR in transformation of prostate epithelium has been the subject of intensive investigation. Thus, acquisition of the malignant phenotype is initially IGF-IR dependent, but as the disease advances and the tumor becomes androgen independent, there is a significant decrease in IGF-IR mRNA and protein levels (4, 5). IGF-IR expression is also extinguished in a majority of human cancer bone marrow metastases (6), although a recent study showed sustained up-regulation of the IGF-IR

in metastases (7). The molecular mechanisms that are responsible for regulation of the IGF-IR gene in prostate cancer, however, remain largely unidentified. It is, therefore, of considerable interest to further characterize the mechanisms underlying control of IGF-IR gene expression.

Molecular characterization of the IGF-IR gene regulatory region revealed that the promoter region lacks TATA or CAAT elements (8, 9). Transcription is initiated from a single start site contained within an initiator motif, a promoter element that directs accurate transcription initiation in the absence of a TATA box (10). Like many TATA-less promoters, the proximal 5'-flanking region of the IGF-IR gene is highly GC-rich and contains multiple binding sites for members of the Sp1 family of zinc finger transcription factors (11, 12). Analysis of physical and functional interactions of Sp1 at the IGF-IR promoter revealed that Sp1 is a potent transactivator of the IGF-IR gene. Thus, basal IGF-IR promoter activity was extremely low in Sp1-null, *Drosophila*-derived, Schneider cells, whereas cotransfection of an Sp1 expression vector significantly enhanced promoter activity (12, 13).

The Kruppel-like factor 6 (KLF6; Zf9, core promoter binding protein) is a ubiquitous transcription factor that includes

Abbreviations: CHO, Chinese hamster ovary; CMV, cytomegalovirus; FBS, fetal bovine serum; HA, hemagglutinin; IGF-IR, IGF-I receptor; KLF6, Kruppel-like factor 6; LOH, loss of heterozygosity; LUC, luciferase; nt, nucleotide.

Endocrinology is published monthly by The Endocrine Society (<http://www.endo-society.org>), the foremost professional society serving the endocrine community.

a proline- and serine-rich N-terminal activation domain, and three C₂H₂ zinc finger motifs at its C-terminal domain (14, 15). The KLF6 gene is located at 10p, a chromosomal region that is deleted in a large portion of sporadic prostate cancers (16, 17). Using specific microsatellite markers flanking KLF6, some of us have demonstrated that of a collection of 22 prostate tumor samples, 77% displayed loss of heterozygosity (LOH) of the KLF6 locus (18). Furthermore, 71% of tumor specimens exhibiting LOH had mutations in the remaining KLF6 allele. No mutations were seen in the patient's normal adjacent prostate tissue or in germline DNA from unaffected individuals. More recent data suggested a potential role for KLF6 in tumorigenesis of other tissues, including nasopharyngeal carcinomas, colorectal cancer, and astrocytic gliomas (19–22).

Although the mechanism of action and the biological role of KLF6 have not yet been established, it has been demonstrated that KLF6 interacts with GC boxes located in putative target promoters, including those of the keratin 4 (23), TGF- β 1 (24), 47-kDa heat shock protein (25), inducible nitric oxide synthase (26), and endoglin (27) genes. Furthermore, the expression of KLF6 in NIH-3T3 cells resulted in a significant decrease in DNA synthesis that was associated with increased expression of p21, a negative regulator of the G₁/S transition, and enhanced activity of a cotransfected p21 promoter-luciferase reporter plasmid (18). In addition, results of electrophoretic mobility shift assays demonstrated that the transactivating effect of KLF6 was associated with specific binding to GC boxes located in the p21 promoter region.

In view of the important roles of tumor suppressor KLF6 and the IGF-IR in the etiology of prostate cancer and to extend our previous observations on regulation of IGF-IR gene expression by transcription factors of the Sp and Kruppel-like family, we have examined the potential transcriptional regulation of the IGF-IR gene by KLF6. The results obtained indicate that wild-type, but not tumor-derived mutated, KLF6 has a stimulatory effect on IGF-IR gene expression. The transactivating effect of KLF6 seems to involve functional interactions with the Sp1 zinc finger protein and with tumor suppressor p53. Impaired activation of the IGF-IR gene by a defective KLF6 may have profound implications in terms of cancer initiation and/or progression.

Materials and Methods

Cell cultures

The Chinese hamster ovary (CHO) cell line was obtained from the American Type Culture Collection (Manassas, VA). Cells were grown in Ham's F-12 nutrient mixture supplemented with 10% fetal bovine serum (FBS), 2 mM glutamine, and 50 μ g/ml gentamicin sulfate. P69 and M12 prostate-derived cell lines were provided by Dr. Joy L. Ware (Medical College of Virginia, Richmond, VA). The P69 line was obtained by immortalization of prostate epithelial cells with simian virus 40 T antigen, and M12 cells were derived by injection of P69 cells into athymic nude mice and serial reimplantation of tumor nodules into nude mice (28). P69 and M12 cells were cultured in RPMI 1640 medium supplemented with 10 ng/ml epidermal growth factor, 0.1 nM dexamethasone, 5 μ g/ml insulin, 5 μ g/ml transferrin, and 5 ng/ml selenium. The human colorectal cancer cell lines HCT116^{+/+}, which expresses wild-type p53, and HCT116^{-/-}, in which the p53 gene has been disrupted by targeted homologous recombination, were provided by Dr. Bert Vogelstein (Johns Hopkins University School of Medicine, Baltimore, MD) (29). HCT116 cells were grown in McCoy's 5A medium with 10% FBS. *Drosophila*

Schneider cells were grown in Schneider's *Drosophila* medium containing 10% FBS, 2 mM glutamine, and 20 μ g/ml gentamicin sulfate. Schneider cells were grown at room temperature in tightly closed, 80-cm² flasks. Cells were plated at a density of 1.5 \times 10⁶ cells/ml in 100-mm dishes 24 h before transfection.

Plasmids and DNA transfections

For transient cotransfection experiments an IGF-IR promoter luciferase reporter construct was employed that includes 476 bp of 5'-flanking and 640 bp of 5'-untranslated regions of the IGF-IR gene [p(-476/+640)luciferase (LUC)]. The promoter activity of this genomic fragment and the location of Sp1 binding sites (GC boxes) and of a CT box have been previously described (12, 13, 30). Transient transfections were also performed using deleted reporter constructs that include 188 or 40 bp of the IGF-IR 5'-flanking region [p(-188/+640)LUC and p(-40/+640)LUC, respectively]. Site-directed mutagenesis of the CT box was carried out directly within p(-476/+640)LUC, using a Transformer site-directed mutagenesis kit (Clontech Laboratories, Palo Alto, CA), as previously described (12). This mutation replaced the 24-bp homopurine/homopyrimidine motif that extends from +434 to +458 in the 5'-untranslated region with a nonspecific DNA sequence of equal size. The mutation in the resulting p(-476/+640 Δ CT)LUC plasmid was confirmed by DNA sequencing.

A KLF6 expression vector was constructed by inserting the full-length KLF6 cDNA into the *Eco*RI and *Xba*I sites of pCI-neo (18). An expression vector encoding the X137 truncation mutant of KLF6 was generated by site-directed mutagenesis of pCI-neo-KLF6 using the QuikChange kit (Stratagene, La Jolla, CA) (18). Expression plasmids containing actin promoter-driven KLF6/Zf9 (pP_{act}-Zf9) and Sp1 (pP_{act}-Sp1) have been previously described (12, 15). A wild-type p53 expression vector was provided by Dr. Edward Mercer (Thomas Jefferson University, Philadelphia, PA).

CHO and HCT116 cells were transfected with 0.8 μ g of the p(-476/+640)LUC plasmid and increasing amounts of the KLF6 expression vector (pCI-neo-KLF6), along with 0.4 μ g of a β -galactosidase expression plasmid [cytomegalovirus plasmid β (pCMV β), Clontech Laboratories] using Polyfect (Qiagen, Hilden, Germany), Metafectene (Biontex Laboratories, Munich, Germany), or Jet-PEI (Polyplus, Illkirch, France) transfection reagents. The total amount of transfected DNA was kept constant using pCI-neo DNA. Cells were harvested 48 h after transfection, and luciferase and β -galactosidase activities were measured as previously described (13). Promoter activities were expressed as luciferase values normalized for β -galactosidase activity. Schneider cells were transfected with calcium phosphate as previously described (12). In previous studies we found that the large amounts of β -galactosidase plasmid required to obtain detectable β -galactosidase activity in Schneider cells severely impaired Sp1 activation of IGF-IR promoter constructs. Therefore, luciferase data were normalized per micrograms of protein in each sample, as measured using the Bradford reagent (Bio-Rad Laboratories, Hercules, CA).

Western immunoblots

Cells were harvested with ice-cold PBS containing 5 mM EDTA and lysed in a buffer containing 150 mM NaCl, 20 mM HEPES (pH 7.5), 1% Triton X-100, 2 mM EDTA, 2 mM EGTA, 1 mM phenylmethylsulfonyl fluoride, 2 μ g/ml aprotinin, 1 mM leupeptin, 1 mM pyrophosphate, 1 mM vanadate, and 1 mM dithiothreitol. Protein content was determined using the Bradford reagent. Samples were electrophoresed through 10% SDS-PAGE, followed by blotting of the proteins onto nitrocellulose membranes. After blocking with 2.5% skim milk in T-TBS [20 mM Tris-HCl (pH 7.5), 135 mM NaCl, and 0.1% Tween 20], blots were incubated with rabbit polyclonal antihuman IGF-IR α -subunit or β -subunit antibodies (Santa Cruz Biotechnology, Inc., Santa Cruz, CA), washed with T-TBS, and incubated with a horseradish peroxidase-conjugated secondary antibody. Proteins were detected using the SuperSignal West Pico Chemiluminescent Substrate (Pierce Chemical Co., Rockford, IL). In addition, blots were probed with antibodies against KLF6/Zf9 (R-173; Santa Cruz Biotechnology, Inc.) and actin.

Physical interactions between KLF6 and p53

HCT116^{-/-} cells were transiently transfected with 3 μ g each of a KLF6 expression vector (or empty pCI-neo) and a hemagglutinin (HA)-tagged p53 expression vector (or empty pcDNA3-HA) (31), using the FuGene-6 reagent (Roche, Indianapolis, IN). The pcDNA3-HA-p53 plasmid was provided by Dr. William G. Kaelin (Harvard Medical School, Boston, MA). Forty-eight hours after transfection, formaldehyde was added to the cultures to a final concentration of 1% for 10 min at room temperature. At the end of the incubation period, cells were washed twice and harvested using ice-cold PBS. Pelleted cells were resuspended in a 1% sodium dodecyl sulfate-containing buffer, incubated on ice for 10 min, and sonicated with three sets of 10-sec pulses. Cell extracts were then immunoprecipitated using 1 μ g of an anti-HA antibody (HA.11, Covance, Inc., Princeton, NJ) for 18 h at 4 C, followed by incubation with 30 μ l protein A-G agarose for an additional 2 h. Immunoprecipitates were electrophoresed through 10% SDS-PAGE and immunoblotted with a KLF6 antibody. Membranes were then washed, and proteins were detected as described above.

Results

Activation of the IGF-IR constitutes a basic requirement for progression through the cell cycle. In addition, overexpression of the IGF-IR gene is a typical hallmark in most types of cancer. Certain malignancies, including prostate tumors, display high IGF-IR levels and activity at early stages of the disease, whereas progression to advanced, metastatic stages is associated with a significant decrease in IGF-IR gene expression (4). Although regulation of IGF-IR gene expression is primarily achieved at the transcriptional level (32), the specific transcription factors involved in pathological regulation of the IGF-IR gene have not yet been identified. KLF6 has been characterized as a candidate tumor suppressor whose mutation was correlated with the etiology of prostate, colorectal, and other cancers (18, 19, 21, 22). To begin to address the potential involvement of KLF6 in IGF-IR gene regulation, we employed the P69 and M12 prostate epithelial-derived cell lines. As previously shown, the poorly tumorigenic P69 cell line expresses high IGF-IR levels, whereas the tumorigenic and metastatic M12 derivative exhibits significantly reduced IGF-IR values (33). Western blot analysis using a KLF6 antibody revealed that KLF6 expression was approximately 2-fold higher in P69 than in M12 cells, whereas IGF-IR levels were 2.24-fold higher (Fig. 1).

To examine the mechanism(s) responsible for regulation of IGF-IR gene expression by KLF6, transient cotransfection experiments were performed in CHO cells using a KLF6 expression vector together with the reporter plasmid p(-476/+640)LUC, which contains most of the proximal region of the IGF-IR promoter. The results of coexpression experiments are presented in Fig. 2A. KLF6 induced a dose-dependent increase in IGF-IR promoter activity, with maximal stimulation occurring with 0.1 μ g expression vector (337 \pm 32% activation). Remarkably, KLF6 displayed a very potent activity even at input doses as low as 10 ng DNA (260 \pm 23% stimulation). At higher DNA doses, the transactivation effect of KLF6 was significantly diminished, although a stimulatory effect was observed at each concentration studied. To assess the effect of a tumor-derived mutant form of KLF6 (X137; C to A substitution at codon 3315, within the KLF6 transactivation domain, that results in the introduction of a premature stop codon), cotransfections were performed using an expression vector encoding the

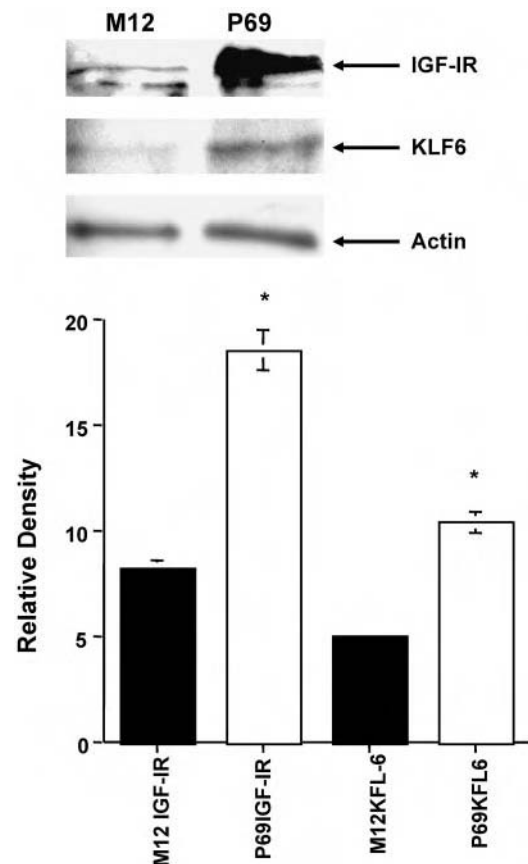


FIG. 1. Expression of endogenous IGF-IR and KLF6 in P69 and M12 prostate epithelial-derived cell lines. Untransfected M12 and P69 cells were lysed in the presence of protease inhibitors, as indicated in *Materials and Methods*. Equal amounts of protein (100 μ g) were separated by 10% SDS-PAGE, transferred to nitrocellulose filters, and blotted with anti-IGF-IR (*upper panel*), anti-KLF6 (*medium panel*), and antiactin (*lower panel*) antibodies. The positions of the 135-kDa IGF-IR α -subunit and approximately 35–37-kDa KLF6 proteins are indicated. The *bar graph* represents the densitometric scanning of three independent experiments. ■, M12 cells; □, P69 cells. Shown are the mean \pm SEM. *, $P < 0.01$ vs. M12 cells.

truncated KLF6/X137 protein. As shown in Fig. 2B, KLF6/X137 was unable to stimulate IGF-IR gene transcription.

To examine whether the transactivating effect of KLF6 was associated with corresponding changes in the levels of endogenous IGF-IR protein, Western blot analysis was performed. For this purpose, CHO cells were transiently transfected with 8 μ g wild-type or mutant KLF6 expression vectors (or empty pCI-neo plasmid), and after 48 h cells were lysed as described in *Materials and Methods*. Cell lysates (50 μ g) were electrophoresed through 10% SDS-PAGE, followed by blotting of the proteins onto nitrocellulose membranes. Western immunoblotting with an IGF-IR antibody revealed that KLF6, but not KLF6/X137, induced an approximately 1.3-fold increase in mature IGF-IR levels and an approximately 1.8-fold increase in IGF-IR precursor levels (Fig. 3A). No change was seen in the levels of actin. To verify that both wild-type and mutant forms of KLF6 were expressed in the cells, lysates were prepared from CHO cells that were transfected with increasing amounts of the appropriate expression vector,

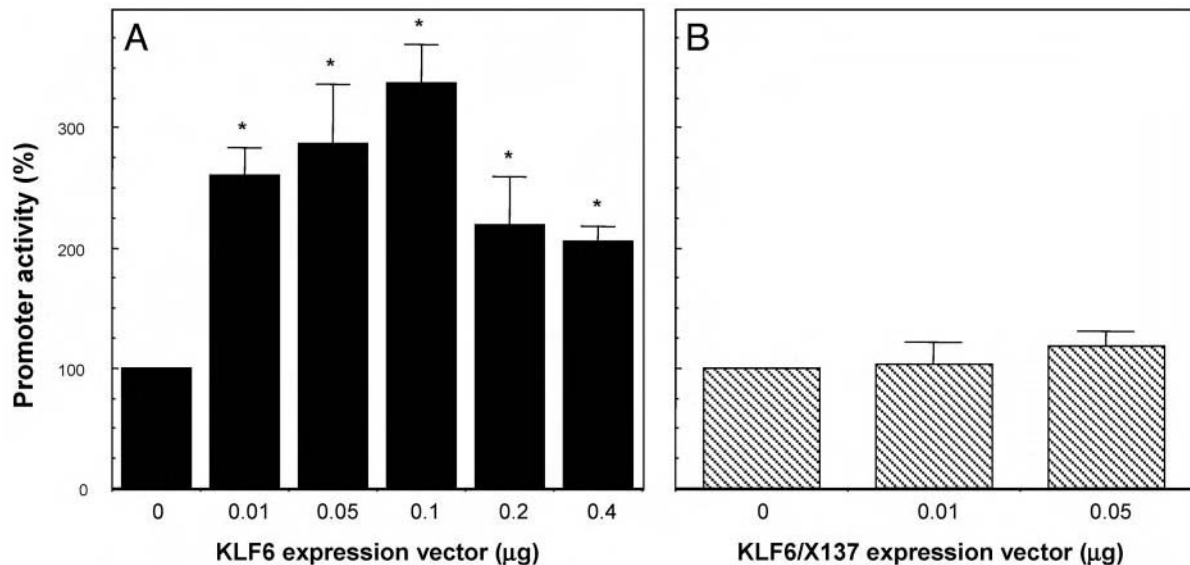


FIG. 2. Regulation of IGF-IR promoter activity by KLF6. The p(−476/+640)LUC reporter plasmid (0.8 µg) was cotransfected into CHO cells with increasing amounts of wild-type (A, ■) or truncated (X137; B, ▨) KLF6 expression vectors along with 0.4 µg of the pCMVβ plasmid using the Polyfect transfection reagent. Luciferase and β-galactosidase activities were measured after 48 h. Luciferase values, normalized for β-galactosidase, are expressed as a percentage of the luciferase activity of the reporter plasmid in the absence of KLF6 vector. Experiments were performed between three and five times, each time in duplicate. Shown are the mean ± SEM. *, $P < 0.01$ vs. controls.

and KLF6 abundance was assessed by Western analysis. As shown in Fig. 3B, both wild-type and mutant KLF6 proteins were produced by the cells, with apparent molecular weights of approximately 37-kDa (lanes 2 and 3) and approximately 21-kDa (lanes 4 and 5), respectively.

To more precisely map the IGF-IR promoter region responsible for mediating the effect of KLF6, cotransfections were performed in CHO cells using the reporter plasmids p(−188/+640)LUC and p(−40/+640)LUC (Fig. 4A) along with the KLF6 expression vector. Construct p(−188/+640)LUC lacks a cluster of four GC boxes localized between nucleotides −399 and −331 that appears to mediate the majority of Sp1 activation of the promoter (12). Two additional GC boxes are located at nucleotides (nt) −259/−253 and −193/−188, whereas no consensus GC boxes are located between nt −188 and −40. The transactivating effect of KLF6 on the p(−188/+640)LUC construct was significantly reduced compared to the p(−476/+640)LUC plasmid ($165.4 \pm 13.1\%$ stimulation vs. $286.8 \pm 49\%$ at 50 ng DNA; Fig. 4B). No further reduction was seen with the p(−40/+640)LUC construct ($195 \pm 34\%$ activation). Electrophoretic mobility shift assay analysis with nuclear extracts of KLF6-transfected cells, however, failed to reveal a specific KLF6 binding to a labeled fragment contained within the promoter region shown to mediate the effect of KLF6 (data not shown).

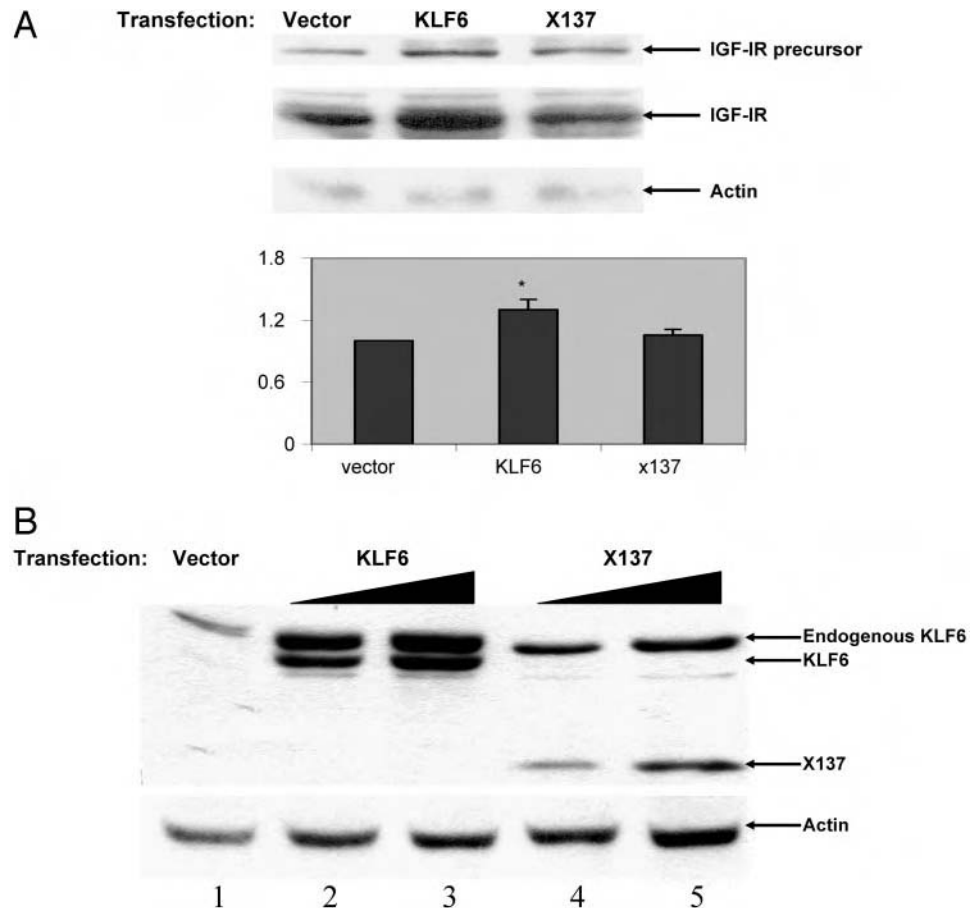
The fact that a significant level of KLF6 stimulation was retained in the p(−40/+640)LUC construct suggested that additional elements in the 5'-untranslated region can also mediate the response to KLF6. We have previously identified a homopurine/homopyrimidine motif or CT box (3'-CCTCCTCCTCCTCGGCCTCCTCCCC-5') located at nt +434 to +458 that was important for Sp1 activation of the IGF-IR promoter (Fig. 4A) (12). To examine the contribution of the CT element in KLF6 activation of the promoter, a mutation was made that replaced the 24-bp

homopurine/homopyrimidine box with a DNA sequence of similar size. Results of cotransfection experiments using wild-type [p(−476/+640)LUC] and mutant [p(−476/+640ΔCT)LUC] reporter constructs indicated that both plasmids were stimulated to a similar extent by a coexpressed KLF6 expression vector (not shown). Hence, these results indicate that, unlike Sp1, the CT box is not critical for KLF6 activation of the IGF-IR gene.

To compare the potency of KLF6 to that of Sp1 in transcriptional regulation of the IGF-IR gene, both zinc finger proteins were expressed in *Drosophila* Schneider cells along with the p(−476/+640)LUC reporter. The rationale for using Schneider cells lies in the fact that these cells lack endogenous Sp/KLF factors and therefore provide an optimal background for this type of experiments (11). As previously demonstrated, Sp1 induced a strong stimulation of IGF-IR promoter activity (~39-fold induction) (12, 34). KLF6, on the other hand, was unable to enhance IGF-IR gene transcription in this specific cellular environment (Fig. 5). Coexpression of both zinc finger proteins, however, resulted in synergistic transactivation of the IGF-IR promoter (~65-fold stimulation).

Although previous studies showed that KLF6 up-regulated p21 (WAF1/CIP1) in a p53-independent manner (18), we undertook a series of experiments aimed at establishing whether KLF6 and p53 functionally cooperate in the specific context of IGF-IR gene regulation. The P69 and M12 prostate-derived cell lines express wild-type p53 in equivalent concentrations (Plymate, S. R., unpublished observations). Therefore, we chose to perform cotransfections in the human colorectal cancer cell lines HCT116^{+/+}, containing wild-type p53, and HCT116^{-/-}, in which the p53 gene has been disrupted by targeted homologous recombination. In these cells the stimulatory effect of KLF6 was significantly reduced in p53-null (■) compared with

FIG. 3. Effect of KLF6 on endogenous IGF-IR gene expression. **A**, CHO cells were transfected with 8 μ g wild-type or mutant (X137) KLF6 expression vectors (or empty pCI-neo) using the Jet-PEI reagent, and after 48 h, cells were lysed in the presence of protease inhibitors. Equal amounts of protein (50 μ g) were electrophoresed through 10% SDS-PAGE, transferred to nitrocellulose filters, and blotted with an anti-IGF-IR antibody. The positions of the 97-kDa IGF-IR β -subunit and the approximately 205-kDa IGF-IR precursor are denoted. Membranes were reprobbed with an actin antibody. The *bar graph* represents the densitometric scanning of the IGF-IR bands normalized to the corresponding actin bands. *Bars* are the mean \pm SEM ($n = 3$ independent experiments). *, $P < 0.01$ vs. controls. **B**, CHO cells were transfected with 1.5 or 3 μ g KLF6 (lanes 2 and 3) or KLF6/X137 (lanes 4 and 5) expression vectors (or empty vector, lane 1), and after 48 h, the abundance of the approximately 37-kDa wild-type and approximately 21-kDa truncated forms was assessed by Western blotting using an anti-Zf9/KLF6 antibody.



p53-expressing (\square) cells ($149 \pm 6\%$ vs. $235 \pm 9\%$ at 10 ng DNA; $180 \pm 9\%$ vs. $283 \pm 33\%$ at 50 ng DNA) (Fig. 6). Mutant KLF6/X137 had no effect in either the absence (▨) or the presence (▩) of p53. Western blot analysis revealed no differences in endogenous IGF-IR and KLF6 levels between untransfected HCT116^{+/+} and HCT116^{-/-} cells. However, expression of KLF6 induced a 1.5- to 2-fold increase in IGF-IR levels in HCT116^{+/+} cells (data not shown).

To more rigorously examine the potential cooperation between KLF6 and p53 in modulation of IGF-IR gene expression, HCT116^{-/-} cells were transfected with 4 μ g each of expression vectors encoding KLF6, p53, or both (or empty vectors), and IGF-IR levels were measured by Western blotting. As shown in Fig. 7 (*upper panel*), transfection of KLF6 alone had no effect on endogenous IGF-IR levels in a p53-null background. However, the combined expression of both KLF6 and p53 vectors induced an approximately 1.5-fold increase in IGF-IR levels and an approximately 5.6-fold increase in IGF-IR precursor levels. Interestingly, coexpression of KLF6 and p53 induced a small reduction in p53 levels (*second panel*, lane 4).

Finally, we examined the potential physical interactions between KLF6 and p53 using a modified chromatin immunoprecipitation method. Specifically, HCT116^{-/-} cells were cotransfected with 3 μ g of a KLF6 expression vector (or empty pCI-neo) along with 3 μ g of an HA-tagged p53 vector (or empty pcDNA3-HA). After 48 h, transfected

cells were treated with formaldehyde to a final concentration of 1% for 10 min to induce cross-linking between interacting proteins. Cells were harvested, lysates were immunoprecipitated with an anti-HA antibody, and electrophoresed through 10% SDS-PAGE. After electrophoresis, complexes were transferred to nitrocellulose membranes and blotted with an anti-KLF6 antibody. As shown in Fig. 8, immunoblotting with the KLF6 antibody identified KLF6 in anti-HA immunoprecipitates of cells that were transfected with KLF6 and pcDNA3-HA-p53 (lane 4), but not in cells transfected with KLF6 and empty pcDNA3-HA (lane 2).

Discussion

The involvement of the IGF-IR in the initiation and/or progression of prostate cancer has been the subject of extensive investigation. Contradictory reports, however, have been presented regarding the pattern of expression of the IGF-IR throughout the various stages of the disease. Thus, although progression to androgen independence in prostate cancer xenografts was associated with a significant increase in IGF-IR mRNA expression (compared with the original androgen-dependent tumors) (35), levels of expression were much higher in the nonmetastatic prostate epithelial cell line P69, compared with its metastatic derivative, the M12 cell line (33). Furthermore, although IGF-IR mRNA levels were shown to be largely suppressed in bone marrow metastases

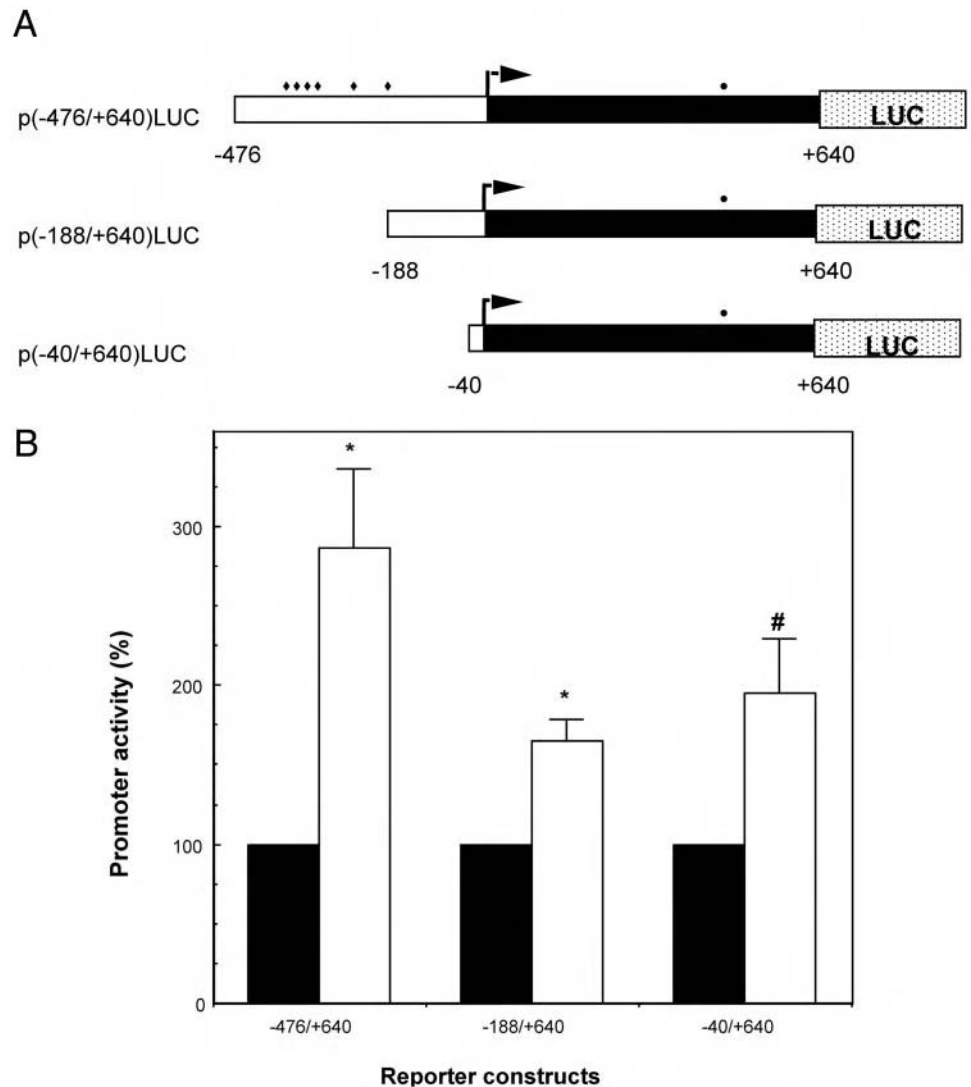


FIG. 4. Mapping of KLF6-responsive regions in the IGF-IR promoter. **A**, Schematic representation of reporter constructs. Plasmids p(-476/+640)LUC, p(-188/+640)LUC, and p(-40/+640)LUC contain, respectively, 476, 188, and 40 bp of the 5'-flanking region (□) and 640 bp of the 5'-untranslated region (■) of the IGF-IR gene, fused to a luciferase cDNA (LUC). The transcription start site is denoted by an arrow. The luciferase cDNA is not shown to scale. ♦, Consensus GC elements; ●, the CT motif. **B**, CHO cells were cotransfected with 0.8 μ g of the indicated reporter plasmid along with 0.05 μ g of the KLF6 expression vector (□) or empty pCI-neo (■) and 0.4 μ g pCMV β , as indicated in Fig. 1. Results are the mean \pm SEM of three to five experiments, performed in duplicate. *, $P < 0.01$; #, $P < 0.05$ (*vs.* cells transfected with empty vector).

(6), other studies reported a persistent expression of the IGF-IR gene in prostate metastases (7). Whereas these conflicting results may arise from the large heterogeneity of the tumors, sample selection, analytical techniques used, *etc.*, the seemingly paradoxical results may reflect the ability of the IGF-IR to mediate both differentiative and proliferative effects. The capacity of the IGF-IR to favor a particular biological pathway is dictated by multiple cellular and extracellular factors, many of whom remain to be identified.

This study identifies the IGF-IR gene as a potential downstream target for transcription factor KLF6 and suggests a potential functional link between these important players in the etiology of a subset of prostate and other types of cancer. Consistent with the postulated tumor suppressor role of KLF6, two recent studies have shown that KLF6 is inactivated in cases of prostate cancer, although the extent of LOH incidence differed between the studies (28% *vs.* 77% of the cases) (18, 36). Loss of function of the KLF6 gene resulted from three different events, including allelic loss, mutation, and gene silencing (37). Interestingly, epigenetic modifications such as promoter methylation may lead to KLF6 si-

lencing in cases of esophageal squamous cell carcinoma (38). In addition to prostate tumors, mutations in the KLF6 gene were reported in neurally derived cancers, including glioblastomas (11.8% of the cases) and astrocytomas (7%) (21), and in colorectal cancers (22).

The IGF-IR promoter has been characterized as a highly G-C-rich (>75%), initiator type of promoter. Multiple GC boxes, which constitute binding elements for zinc finger-containing transcription factors, were mapped to its proximal region (*i.e.* the region located immediately upstream of the transcription initiation site). Similar to Sp1, another member of the Sp/KLF family of zinc finger transcription factors, KLF6 exhibited a potent transactivating effect toward the IGF-IR promoter, even at very low input doses of expression vector (12). On the other hand, a prostate cancer-derived truncated mutant lacking the DNA-binding and part of the activation domains of KLF6 had no effect on IGF-IR promoter activity. Comparison of the effects of KLF6 with those of Sp1 revealed that KLF6, unlike Sp1, was unable to stimulate IGF-IR promoter activity in Sp/KLF-null *Drosophila*-derived Schneider cells. Coexpression of both zinc finger proteins,

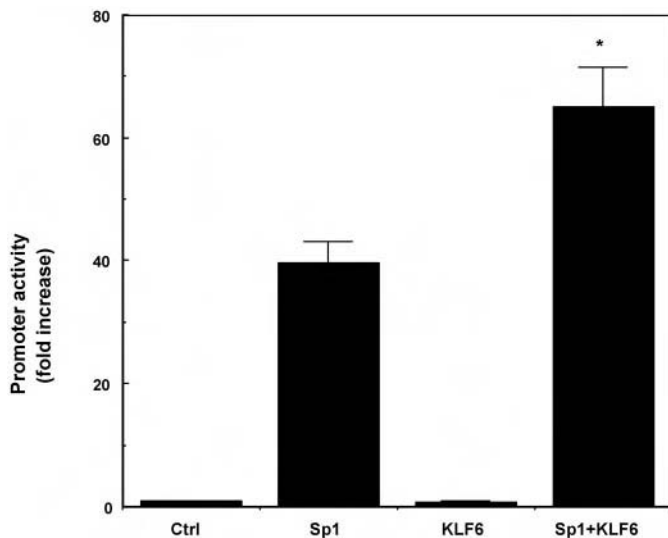


FIG. 5. Comparison of the transactivating effects of KLF6 and Sp1 in *Drosophila* Schneider cells. Schneider cells were cotransfected with 5 μ g of the IGF-IR promoter construct p(-476/+640)LUC along with 300 ng actin promoter-driven KLF6 (pP_{ac}Zf9) and/or Sp1 (pP_{ac}Sp1) expression vectors, using the calcium phosphate method. LUC activity was measured after 48 h. A value of 1 was given to the promoter activity in the absence of expression vectors. Shown are the results (mean \pm SEM) of a typical experiment, repeated three times. *, $P < 0.01$ vs. cells transfected with Sp1 alone.

however, enhanced IGF-IR promoter activity in a synergistic fashion, suggesting that Sp1 and KLF6 exhibit different mechanisms of action. Furthermore, these results seem to imply that the transactivating potentials of KLF6 and Sp1 toward the IGF-IR promoter depend, to a significant extent, on the cellular context.

In addition, the results of deletion analysis experiments revealed that a cluster of four GC boxes located between nt -399 and -331 appears to mediate a significant portion of KLF6 activation of this promoter. We were unable, however, to demonstrate a specific binding of KLF6 to this particular fragment. Because this region was previously shown to bind Sp1 with relatively high affinity (12, 34), our results are consistent with a model in which KLF6 binds (and, potentially, stabilizes) Sp1, thus enhancing its ability to bind and transactivate the IGF-IR promoter. Interestingly, a CT box in the 5'-untranslated region of the promoter, whose presence was critical for Sp1 transactivation of the IGF-IR promoter (12), had no major role in KLF6 action. Physical interactions between Sp1 and KLF6/Zf9 have been reported in the transcriptional activation of TGF- β 1 during stellate cell activation as well as in regulation of the endoglin promoter in response to vascular injury (24, 27). Together with our data, these studies underscore the important role of Sp/KLF family members in cell growth and, furthermore, suggest the existence of a transcriptional network that allows the fine-tuning of gene expression of target gene promoters (11). The participation of other DNA elements in stimulation of IGF-IR gene expression by KLF6 cannot be discounted. Furthermore, additional mechanisms, such as a KLF6-induced increase in IGF-IR mRNA stability or translational efficiency, may also contribute to the increase in IGF-IR expression.

In addition to its DNA sequence-dependent effects, the

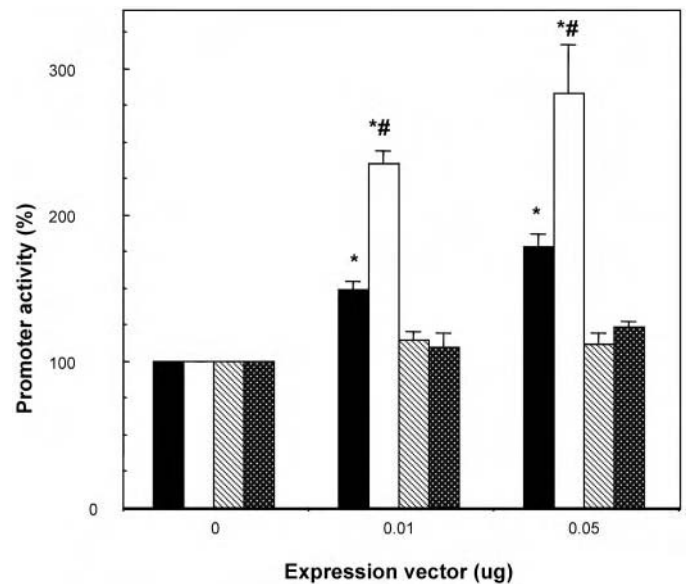


FIG. 6. Effect of p53 background on KLF6 action. Human colorectal cancer cell lines HCT116^{+/+}, containing wild-type p53, and HCT116^{-/-}, lacking p53, were cotransfected with 0.8 μ g of the p(-476/+640)LUC reporter plasmid and increasing amounts of wild-type or truncated (X137) KLF6 expression vectors along with 0.4 μ g pCMV β , using the Metafectene reagent. Promoter activities are expressed as luciferase normalized to β -galactosidase levels. A value of 100% was given to the IGF-IR promoter activity in the absence of expression vectors. The figure shows the results of three experiments, performed in duplicate dishes. ■, HCT116^{-/-} cells transfected with KLF6; □, HCT116^{+/+} cells transfected with KLF6; ▨, HCT116^{-/-} cells transfected with KLF6/X137. *, $P < 0.001$ vs. control cells transfected with empty pCI-neo; #, $P < 0.01$ vs. p53-lacking cells at the same dose of expression vector.

results of the present study suggest that a significant portion of the biological actions of KLF6 may result from protein-protein interactions with tumor suppressor p53. Specifically, we demonstrated that in HCT116^{+/+} cells, expressing a wild-type p53, the transactivating effect of KLF6 was approximately 1.6-fold higher than that in p53-null HCT116^{-/-} cells. In addition, coexpression of KLF6 and p53 induced a significant and consistent increase in endogenous IGF-IR and IGF-IR precursor levels, whereas the expression of KLF6 alone had no major effect. We may speculate that the enhanced capacity of KLF6 to stimulate IGF-IR gene expression in the presence of p53 results from its physical interaction with this protein, which may lead to an increased stability of the KLF6 molecule. These results are particularly intriguing in view of our early results showing that wild-type p53, in itself, strongly suppressed IGF-IR promoter activity, whereas a number of tumor-derived mutated p53 molecules stimulated IGF-IR gene transcription (39). The specific KLF6 and p53 domains involved in protein-protein interactions remain to be identified.

Consistent with these results, we recently demonstrated that the inhibitory activity of tumor suppressor WT1 (a member of the early growth response family of zinc finger transcription factors whose mutation was linked to the etiology of Wilms' tumor) was significantly enhanced in the presence of p53 (40). Similarly, tumor suppressor BRCA1 (breast can-

FIG. 7. Cooperation between KLF6 and p53 in stimulation of IGF-IR gene expression. HCT116^{-/-} cells were transfected with 4 μ g each of expression vectors encoding KLF6, p53, or both, using the FuGene-6 reagent. Cells were lysed after 48 h, and 50 μ g protein were separated through 10% SDS-PAGE gels. The resolved proteins were transferred to nitrocellulose membranes and blotted with IGF-IR, p53, KLF6, and actin antibodies.

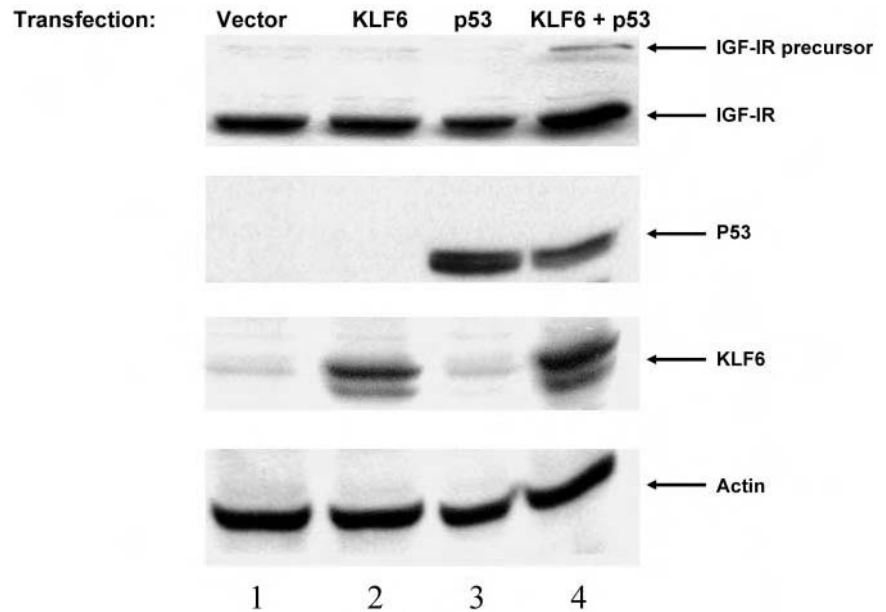
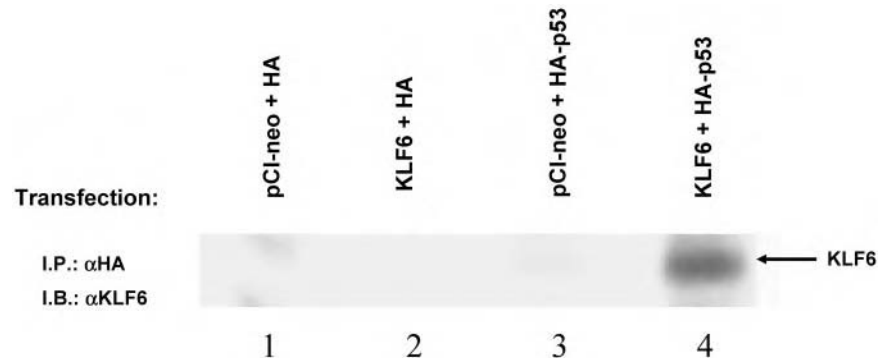


FIG. 8. Physical interaction between KLF6 and p53. HCT116^{-/-} cells were transfected with 3 μ g each of expression vectors encoding KLF6 (or empty pCI-neo) and pcDNA3-HA-p53 (or empty pcDNA3-HA). After 48 h cells were treated with formaldehyde (final concentration, 1%) for 10 min at room temperature, lysed in the presence of protease inhibitors, sonicated, and immunoprecipitated with an HA antibody. Precipitates were loaded onto 10% SDS-PAGE gels, electrophoresed, and transferred to nitrocellulose membranes that were blotted with an anti-KLF6 antibody. I.P., Immunoprecipitation; I.B., immunoblotting.



cer susceptibility gene) was able to suppress IGF-IR promoter activity in the presence of wild-type, but not mutant, p53 (41). Unlike the cooperative effect between p53 and KLF6 described in the present paper, we have previously reported that Sp1 counteracted the inhibitory effect of p53 on IGF-IR promoter in a dose-dependent manner (42). Together these data indicate that the IGF-IR gene promoter constitutes a molecular target to a number of transcription factors with tumor suppressor activity (32). The level of expression of the IGF-IR gene is the net result of complex interactions involving multiple DNA-binding as well as non-DNA-binding nuclear proteins.

In summary, we have demonstrated that the transcription factor KLF6 is an important activator of the IGF-IR gene. Regulation of the expression of this gene occurs primarily through a cluster of GC boxes in the 5'-flanking region. In addition, the ability of KLF6 to efficiently activate the IGF-IR promoter depends to a significant extent on the cellular status of p53. In the specific context of prostate cancer, we may assume that the decrease in IGF-IR gene expression that occurs in aggressive metastatic stages may result at least in part from impaired activation of the IGF-IR promoter by mutant KLF6. The concentration of cell surface IGF-I-binding sites in malignant cells will ultimately have a significant

impact on cell proliferation, differentiation, and sensitivity to apoptosis.

Acknowledgments

We thank Drs. D. Beitner-Johnson, J. L. Ware, E. Mercer, W. G. Kaelin, and B. Vogelstein for providing cell lines and reagents.

Received February 10, 2004. Accepted April 27, 2004.

Address all correspondence and requests for reprints to: Dr. Haim Werner, Department of Clinical Biochemistry, Sackler School of Medicine, Tel Aviv University, Tel Aviv 69978, Israel. E-mail: hwerner@post.tau.ac.il.

This work was supported by National Institutes of Health (NIH) Grant R01-DK-37340, Department of Defense Grant PC020770, and the Bendheim Foundation (to S.L.F.) and by NIH Grants R01-DK-52683 and P01-CA-85859 (to S.R.P.).

References

1. LeRoith D, Werner H, Beitner-Johnson D, Roberts Jr CT 1995 Molecular and cellular aspects of the insulin-like growth factor I receptor. *Endocr Rev* 16: 143–163
2. Baserga R, Hongo A, Rubini M, Prisco M, Valentini B 1997 The IGF-I receptor in cell growth, transformation and apoptosis. *Biochim Biophys Acta* 1332:F105–F126
3. Werner H, LeRoith D 1997 The insulin-like growth factor-I receptor signaling pathways are important for tumorigenesis and inhibition of apoptosis. *Crit Rev Oncog* 8:71–92

4. Tennant MK, Thrasher JB, Twomey PA, Drivdahl RH, Birnbaum RS, Plymate SR 1996 Protein and mRNA for the type 1 insulin-like growth factor (IGF) receptor is decreased and IGF-II mRNA is increased in human prostate carcinoma compared to benign prostate epithelium. *J Clin Endocrinol Metab* 81:3774–3782
5. Kaplan PJ, Mohan S, Cohen P, Foster BA, Greenberg NM 1999 The insulin-like growth factor axis and prostate cancer: lessons from the transgenic adenocarcinoma of mouse prostate (TRAMP) model. *Cancer Res* 59:2203–2209
6. Chott A, Sun Z, Morganstern D, Pan J, Li T, Susani M, Mosberger I, Upton MP, Bubleby GJ, Balk SP 1999 Tyrosine kinases expressed in vivo by human prostate cancer bone marrow metastases and loss of type 1 insulin-like growth factor receptor. *Am J Pathol* 155:1271–1279
7. Hellawell GO, Turner GD, Davies DR, Poulosom R, Brewster SF, Macaulay VM 2002 Expression of the type 1 insulin-like growth factor receptor is up-regulated in primary prostate cancer and commonly persists in metastatic disease. *Cancer Res* 62:2942–2950
8. Werner H, Stannard B, Bach MA, LeRoith D, Roberts Jr CT 1990 Cloning and characterization of the proximal promoter region of the rat insulin-like growth factor I (IGF-I) receptor gene. *Biochem Biophys Res Commun* 169:1021–1027
9. Cooke DW, Bankert LA, Roberts Jr CT, LeRoith D, Casella SJ 1991 Analysis of the human type I insulin-like growth factor receptor promoter region. *Biochem Biophys Res Commun* 177:1113–1120
10. Smale ST, Baltimore D 1989 The “initiator” as a transcription control element. *Cell* 57:103–113
11. Black AR, Black JD, Azizkhan-Clifford J 2001 Sp1 and Kruppel-like factor family of transcription factors in cell growth regulation and cancer. *J Cell Physiol* 188:143–160
12. Beitner-Johnson D, Werner H, Roberts Jr CT, LeRoith D 1995 Regulation of insulin-like growth factor I receptor gene expression by Sp1: physical and functional interactions of Sp1 at GC boxes and at a CT element. *Mol Endocrinol* 9:1147–1156
13. Werner H, Bach MA, Stannard B, Roberts Jr CT, LeRoith D 1992 Structural and functional analysis of the insulin-like growth factor I receptor gene promoter. *Mol Endocrinol* 6:1545–1558
14. Koritschoner NP, Bocco JL, Panzetta-Dutari GM, Dumur CI, Flury A, Patrito LC 1997 A novel human zinc finger protein that interacts with the core promoter element of a TATA box-less gene. *J Biol Chem* 272:9573–9580
15. Ratzu V, Lalazar A, Wong L, Dang Q, Collins C, Shaulian E, Jensen S, Friedman SL 1998 Zf9, a Kruppel-like transcription factor up-regulated in vivo during early hepatic fibrosis. *Proc Natl Acad Sci USA* 95:9500–9505
16. Trybus TM, Burgess AC, Wojno KJ, Glover TW, Macoska JA 1996 Distinct areas of allelic loss on chromosomal regions 10p and 10q in human prostate cancer. *Cancer Res* 56:2263–2267
17. Ittmann M 1996 Allelic loss on chromosome 10 in prostate adenocarcinoma. *Cancer Res* 56:2143–2147
18. Narla G, Heath KE, Reeves HL, Li D, Giono LE, Kimmelman AC, Glucksmann MJ, Narla J, Eng FJ, Chan AM, Ferrari AC, Martignetti JA, Friedman SL 2001 KLF6, a candidate tumor suppressor gene mutated in prostate cancer. *Science* 294:2563–2566
19. Vax VV, Gueorguiev M, Dedov II, Grossman AB, Korbonits M 2003 The Kruppel-like transcription factor 6 gene in sporadic pituitary tumours. *Endocrine Relat Cancer* 10:397–402
20. Chen HK, Liu XQ, Lin J, Chen TY, Feng QS, Zeng YX 2002 Mutation analysis of KLF6 gene in human nasopharyngeal carcinomas. *Ai Zhong* 21:1047–1050
21. Jeng Y-M, Hsu H-C 2003 KLF6, a putative tumor suppressor gene, is mutated in astrocytic gliomas. *Int J Cancer* 105:625–629
22. Reeves HL, Narla G, Ogunbiyi O, Haq AI, Katz A, Benzeno S, Hod E, Harpaz N, Goldberg S, Tal-Kremer S, Eng FJ, Arthur MJP, Martignetti JA, Friedman SL 2004 Kruppel-like factor 6 (KLF6) is a tumor-suppressor gene frequently inactivated in colorectal cancer. *Gastroenterology* 126:1090–1103
23. Okano J, Opitz OG, Nakagawa H, Jenkins TD, Friedman SL, Rustgi AK 2000 The Kruppel-like transcriptional factors Zf9 and GKLF coactivate the human keratin 4 promoter and physically interact. *FEBS Lett* 473:95–100
24. Kim Y, Ratzu V, Choi S-G, Lalazar A, Theiss G, Dang Q, Kim S-J, Friedman SL 1998 Transcriptional activation of transforming growth factor β 1 and its receptors by the Kruppel-like factor Zf9/core promoter-binding protein and Sp1. *J Biol Chem* 273:33750–33758
25. Yasuda K, Hirayoshi K, Hirata H, Kubota H, Hosokawa N, Nagata K 2002 The Kruppel-like factor Zf9 and proteins in the Sp1 family regulate the expression of HSP47, a collagen-specific molecular chaperone. *J Biol Chem* 277:44613–44622
26. Warke VG, Nambiar MP, Krishnan S, Tenbrock K, Geller DA, Koritschoner NP, Atkins JL, Farber DL, Tsokos GC 2003 Transcriptional activation of the human inducible nitric-oxide synthase promoter by Kruppel-like factor 6. *J Biol Chem* 278:14812–14819
27. Botella LM, Sanchez-Elsner T, Sanz-Rodriguez F, Kojima S, Shimada J, Guerrero-Esteo M, Cooreman MP, Ratzu V, Langa C, Vary CPH, Ramirez JR, Friedman SL, Bernabeu C 2002 Transcriptional activation of endoglin and transforming growth factor- β signaling components by cooperative interaction between Sp1 and KLF6: their potential role in the response to vascular injury. *Blood* 100:4001–4010
28. Bae VL, Jackson-Cook CK, Maygarden SJ, Plymate SR, Chen J, Ware JL 1998 Metastatic sublines of an SV40 large T antigen immortalized human prostate epithelial cell line. *Prostate* 34:275–282
29. Bunz F, Dutriaux A, Lengauer C, Waldman T, Zhou S, Brown JP, Sedivy JM, Kinzler KW, Vogelstein B 1998 Requirement for p53 and p21 to sustain G₂ arrest after DNA damage. *Science* 282:1497–1501
30. Werner H, Rauscher III FJ, Sukhatme VP, Drummond IA, Roberts Jr CT, LeRoith D 1994 Transcriptional repression of the insulin-like growth factor I receptor (IGF-I-R) gene by the tumor suppressor WT1 involves binding to sequences both upstream and downstream of the IGF-I-R gene transcription start site. *J Biol Chem* 269:12577–12582
31. Marin MC, Jost CA, Irwin MS, DeCaprio JA, Caput D, Kaelin WG 1998 Viral oncoproteins discriminate between p53 and the p53 homolog p73. *Mol Cell Biol* 18:6316–6324
32. Werner H, Roberts Jr CT 2003 The IGF-I receptor gene: a molecular target for disrupted transcription factors. *Genes Chromosomes Cancer* 36:113–120
33. Damon SE, Plymate SR, Carroll JM, Sprenger CC, Dechsukhum C, Ware JL, Roberts Jr CT 2001 Transcriptional regulation of insulin-like growth factor-I receptor gene expression in prostate cancer cells. *Endocrinology* 142:21–27
34. Abramovitch S, Glaser T, Ouchi T, Werner H 2003 BRCA1-Sp1 interactions in transcriptional regulation of the IGF-IR gene. *FEBS Lett* 541:149–154
35. Nickerson T, Chang F, Lorimer D, Smeekens SP, Sawyers CL, Pollak M 2001 In vivo progression of LAPC-9 and LNCaP prostate cancer models to androgen independence is associated with increased expression of insulin-like growth factor I (IGF-I) and IGF-I receptor (IGF-IR). *Cancer Res* 61:6276–6280
36. Chen C, Hyytinen E-R, Sun X, Helin HJ, Koivisto PA, Frierson Jr HF, Vessella RL, Dong J-T 2003 Deletion, mutation, and loss of expression of KLF6 in human prostate cancer. *Am J Pathol* 162:1349–1354
37. Narla G, Friedman SL, Martignetti JA 2003 Kruppel cripples prostate cancer: KLF6 progress and prospects. *Am J Pathol* 162:1047–1052
38. Yamashita K, Upadhyay S, Osada M, Hoque MO, Xiao Y, Mori M, Sato F, Meltzer SJ, Sidransky D 2002 Pharmacologic unmasking of epigenetically silenced tumor suppressor genes in esophageal squamous cell carcinoma. *Cancer Cell* 2:485–495
39. Werner H, Karnieli E, Rauscher III FJ, LeRoith D 1996 Wild type and mutant p53 differentially regulate transcription of the insulin-like growth factor I receptor gene. *Proc Natl Acad Sci USA* 93:8318–8323
40. Idelman G, Glaser T, Roberts Jr CT, Werner H 2003 WT1-p53 interactions in IGF-I receptor gene regulation. *J Biol Chem* 278:3474–3482
41. Abramovitch S, Werner H 2003 Functional and physical interactions between BRCA1 and p53 in transcriptional regulation of the IGF-IR gene. *Horm Metab Res* 35:758–762
42. Ohlsson C, Kley N, Werner H, LeRoith D 1998 p53 regulates IGF-I receptor expression and IGF-I induced tyrosine phosphorylation in an osteosarcoma cell line: interaction between p53 and Sp1. *Endocrinology* 139:1101–1107

Endocrinology is published monthly by The Endocrine Society (<http://www.endo-society.org>), the foremost professional society serving the endocrine community.

Frequent Inactivation of the Tumor Suppressor Kruppel-like Factor 6 (*KLF6*) in Hepatocellular Carcinoma

Sigal Kremer-Tal,^{1,2} Helen L. Reeves,^{1,3} Goutham Narla,¹ Swan N. Thung,⁴ Myron Schwartz,⁵ Analisa Difeo,⁶ Amanda Katz,¹ Jordi Bruix,⁷ Paulette Bioulac-Sage,⁸ John A. Martignetti,^{6, 9,10} and Scott L. Friedman^{1,10}

Hepatocellular carcinoma (HCC) is a leading cause of cancer death worldwide, reflecting incomplete characterization of underlying mechanisms and lack of early detection. Kruppel-like factor 6 (*KLF6*) is a ubiquitously expressed zinc finger transcription factor that is deregulated in multiple cancers through loss of heterozygosity (LOH) and/or inactivating somatic mutation. We analyzed the potential role of the *KLF6* tumor suppressor gene in 41 patients who had HCC associated with hepatitis C virus (16 patients), hepatitis B virus (12 patients, one of whom was coinfecting with hepatitis C virus), and other etiologies (14 patients) by determining the presence of LOH and mutations. Overall, LOH and/or mutations were present in 20 (49%) of 41 tumors. LOH of the *KLF6* gene locus was present in 39% of primary HCCs, and the mutational frequency was 15%. LOH and/or mutations were distributed across all etiologies of HCC evaluated, including patients who did not have cirrhosis. Functionally, wild-type *KLF6* decreased cellular proliferation of HepG2 cells, while patient-derived mutants did not. In conclusion, we propose that *KLF6* is deregulated by loss and/or mutation in HCC, and its inactivation may contribute to pathogenesis in a significant number of these tumors. (HEPATOLOGY 2004;40:1047–1052.)

Hepatocellular carcinoma (HCC) is the fifth most common cancer worldwide, typically arising within livers with cirrhosis in patients who have hepatitis B virus, hepatitis C virus, chronic alcohol abuse,

and/or nonalcoholic fatty liver disease.¹ The majority of HCCs are incurable, reflecting an incomplete understanding of pathogenic mechanisms and inadequate early detection.

Established genetic events in HCC include loss of tumor suppressor gene function through a combination of genetic and epigenetic events, including loss of an allele, mutation, or promoter methylation.^{2–4} Amplification and/or mutation of oncogenes such as *K-Ras* and *c-myc* have also been described, as has cyclin overexpression.⁵ Combined, these studies highlight many genetic alterations that have been associated with the development and/or progression of HCC; however, many key pathways and gene involvement remain to be elucidated.

Kruppel-like factor 6 (*KLF6*), a ubiquitously expressed zinc finger transcription factor,⁶ has been identified as a tumor suppressor gene in prostate,^{7,8} colon,⁹ and nasopharyngeal¹⁰ cancers, as well as astrocytic gliomas.¹¹ Moreover, downregulation of *KLF6* messenger RNA levels has been described in lung^{12,13} and esophageal¹⁴ cancers, the latter also being associated with promoter methylation. Reduced *KLF6* expression levels in lung and prostate cancers have been reported^{8,13}; the latter has also been correlated with increased likelihood of recurrence.¹⁵ *KLF6* also suppresses oncogenic transformation in glioblastoma.¹⁶ The principal aim of this study was to deter-

Abbreviations: HCC, hepatocellular carcinoma; *KLF6*, Kruppel-like factor 6; LOH, loss of heterozygosity.

From the ¹Division of Liver Diseases and ⁴Department of Pathology, ⁵Recanati-Miller Transplantation Institute; the Departments of ⁶Human Genetics and ⁹Pediatrics, and ¹⁰The Rutenberg Cancer Center, Mount Sinai School of Medicine, New York, NY; the ²Department of Internal Medicine D, Rabin Medical Center, Beilinson Campus, Petah-Tikva, Israel; ³Northern Institute for Cancer Research, University of Newcastle-upon-Tyne, Newcastle-upon-Tyne, United Kingdom; ⁷Barcelona Clinic Liver Cancer Group, Liver Unit, Hospital Clinic, University of Barcelona, IDIBAPS, Catalonia, Spain; and ⁸Groupe de Recherches pour l'Etude du Foie, INSERM E0362, Université Victor Segalen, Bordeaux, France.

Received March 29, 2004; accepted August 25, 2004.

This work was supported by grants from the National Institute of Diabetes and Digestive Kidney Diseases (RO1DK37340, RO1DK56621 [S.L.F.]; 1 K24 DK 60498-01 [M.S.]; T32 DK-07792 [S.T.K.]), the US Department of Defense (DAMD17-03-01-0100 [S.L.F.]; DAMD17-02-1-0720 and DAMD17-03-1-0129 [J.A.M.]), the Israeli Cancer Association (S.T.K.), the Bendheim Trust (S.L.F.), the American Association for the Study of Liver Disease/Schering Fellowship Award (H.L.R.), GlaxoSmithKline Senior Fellowship (H.L.R.), the Joint Research Executive Committee of Newcastle-upon-Tyne Hospitals (H.L.R.), and the Instituto de Salud Carlos II, no. C03/10 (J.B.).

Address reprint requests to: Scott L. Friedman, M.D., Division of Liver Diseases, Box 1123, Mount Sinai School of Medicine, 1425 Madison Avenue, Room 11-70F, New York, NY 10029. E-mail: scott.friedman@mssm.edu; fax: 212-849-2574.

Copyright © 2004 by the American Association for the Study of Liver Diseases.

Published online in Wiley InterScience (www.interscience.wiley.com).

DOI 10.1002/hep.20460

mine the incidence of loss and/or mutation of the *KLF6* gene in HCC.

Patients and Methods

Tumor Samples. All patient samples were collected and analyzed with written Institutional Review Board consent from each institution. In all cases, a 5- μ m section stained with hematoxylin-eosin was used as a histological reference for normal and tumor-derived tissue. Tumor DNA was isolated from 20- μ m sections of paraffin-embedded blocks using commercial reagents (Ambion, Austin, TX). Paired nontumoral DNA was isolated from either nontumorous liver tissue from the same patient—which in many cases was diseased—or gallbladder, xiphoid cartilage, or other extrahepatic tissue.

Loss of Heterozygosity Analysis. Fluorescent loss of heterozygosity (LOH) analysis using genomic DNA from paired control/tumor tissue was performed as described previously.^{7,9} *KLF6* is located 4.1 Mb from the telomeric end of chromosome 10p and is flanked by microsatellite markers D10S594 and D10S591, located 1.7 and 4.8 Mb, respectively, from the telomere (Table 1). The *KLF6*-specific markers *KLF6M1*, *M2*, and *M4* flank the *KLF6* locus by 40 kb centromerically and 10 kb and 20 kb telomerically, respectively. Data were analyzed using ABI Genescan and Genotyper software packages (Perkin Elmer, Boston, MA), and allelic loss was scored and confirmed by 2 independent observers. An X^{LOH} score of 0.7 or less was defined as LOH. All LOH analyses were performed at least twice.

DNA Sequence Analysis. *KLF6* exon 2 polymerase chain reaction products from normal and tumor-derived genomic DNA were generated using combinations of nine forward and reverse primers that generated overlapping amplicons as described previously.⁹ All mutations were confirmed via bidirectional sequencing in 2 independent polymerase chain reaction reactions, and, for the T179I mutation, further confirmed via restriction digest as described previously.⁹

Cell Culture and Transient Transfection. HepG2 cells were obtained from the American Tissue Culture Collection (ATCC, Manassas, VA). Cells were cultured in Dulbecco's Modified Eagle Medium (Gibco, Grand Island, NY) containing 10% fetal bovine serum (Hyclone Logan, UT) and antibiotics (penicillin, streptomycin 100 μ g/mL) (Gibco) and were supplemented with L-glutamine (30 μ g/mL) (Gibco). The medium was changed every 48 hours. Cells were passaged 1 to 2 times weekly and were split 24 hours prior to transient transfection experiments. Transient transfection was performed with

Fugene reagent according to the manufacturers' protocol (Roche, Indianapolis, IN).

***KLF6* Complementary DNA Constructs.** Full-length *KLF6* cloned into the *Eco*RI and *Xba*I sites of pCI-neo⁶ was used as the template for site-directed mutagenesis. Site-directed mutagenesis was performed using the Quick-Change mutagenesis kit (Stratagene, La Jolla, CA). All constructs were verified via DNA sequencing prior to expression studies.

Analysis of Proliferation. Measurement of proliferation was determined by assaying ³H-thymidine incorporation into DNA as described previously.⁶

Results

LOH of *KLF6* is Common in Hepatocellular Carcinoma. *KLF6* maps to chromosome 10p15, which has not been previously reported to be lost in HCC.^{17,18} We therefore analyzed possible LOH of the *KLF6* locus using several fluorescently labeled microsatellite markers, including 3 markers that tightly flank the gene (see Table 1).^{7,9} Using this approach, we have previously shown 50 to 100 kb minimal regions of *KLF6* loss in colorectal cancer.⁹

Of the 41 HCC cases studied, 16 (39%) had loss consistent with allelic imbalance in 10p15, the *KLF6* locus, 10 of which (24%) showed loss of flanking markers on both sides of the *KLF6* gene. The microsatellite markers in the additional 6 cases show unilateral loss very close to the gene, indicating LOH. Table 1 lists the tumor characteristics for all patients, the etiology of underlying liver disease, and LOH status.

Mutational Analysis of *KLF6* in HCC. Direct sequence analysis of the *KLF6* gene revealed that 6 (15%) of 41 HCCs harbored *KLF6* mutations. None of these changes were present in nontumorous tissue, confirming that they were somatic mutations. Sequence analysis was limited to exon 2. This exon encodes three quarters of the full-length protein, and the majority of *KLF6* mutations identified in other cancers have been localized to this exon.⁷⁻⁹ The mutations identified are shown in Table 1, and the corresponding sequence electropherograms are shown in Fig. 1A.

Four of the five *KLF6* mutations were missense mutations, predicting nonconservative amino acid substitutions within the *KLF6* activation domain. Two of these mutations—P149S (bases 3392 C>T) in patient 15 and P166S (3443 C>T) in patient 11—are predicted to disrupt proline residues, which could be important in proline-directed phosphorylation. One mutation (3483 C>T) predicts replacement of a threonine residue with an isoleucine (T179I) and was present in 3 distinct HCC

Table 1. 10p15 Locus and Microsatellite Markers; KLF6 LOH and Mutation Status, and Tumor Characteristics

Patient	D10S594	KLF6M4	KLF6M2	KLF6M1	D10S591	Mutation	Etiology	Differentiation	Tumor size (cm)
29							HBV, no cirr	WD	2.7
13	FAIL						HIV cirr	PD	5.5
16							HBV no cirr	MD	9
4						T179I	HBV cirr	PD	6
30	FAIL						Hemochromatosis, cirr	WD	4
12							HBV fibrosis	MD/PD	9
19							HCV, no cirr	MD	11.5
37							No cirr	WD	13
39							HBV fibrosis	PD	6.5
18		FAIL					HCV, cirr	WD	4.5
15	FAIL	FAIL				T179I; P149S	HCV cirr	WD/MD	24
38							HBV, in trans to cirr	PD	7.8
36		FAIL					No cirr	WD	10
5							HBV, no cirr	PD	23
41							No cirr	WD	6.5
10							HBV cirr	WD	7
9			SNP	FAIL		T179I	HCV cirr	WD/PD	4.5
33							No cirr	WD/MD	4.5
28							HCV cirr	WD	1.5
3							HBV cirr	MD	4.3
17							Cryptogenic cirr	MD	5
23							HCV cirr	WD	1.8
1							HCV, cirr	WD	6.5
25							HCV cirr	WD/MD	5
31				FAIL			HCV,alcohol, cirr	MD	4.5
6							No cirr	MD	12
21							HCV no cirr	PD	2.5
22							HCV cirr	MD	5
2							No cirr	WD	8.2
20							HCV cirr	WD,MD,PD	3.5
40							HBV cirr	WD	6.5
8					FAIL		No cirr	WD	8
32							No cirr	WD	8
35							HBV+HCV cirr	WD/MD	2.8
24						W162X	Autoimmune	WD/MD	1.5
27							HCV cirr	MD/PD	5
11		FAIL				P166S	HCV cirr	WD/MD	5.5
34						K182R	No cirr	WD/MD	19
7				FAIL			Alcohol cirr	MD/PD	4
14				FAIL			HBV in trans to cirr	MD	5
26							HCV cirr	WD	8.5

NOTE. LOH of the *KLF6* locus was analyzed using microsatellite markers for 10p15: D10S591 and D10S594. KLF6M1, M2 and M4 microsatellite markers were specifically designed to tightly flank the *KLF6* gene, as shown in diagram at the top of the Table. The relative position of the *KLF6* gene between the markers is indicated. The etiology of HCC, degree of tumor differentiation, as well as tumor sizes are listed for each case. Identified mutations are shown with predicted amino acid changes. Black cell—LOH; Grey cell—non-informative (NI) marker; White cell—no evidence of loss; Fail—represents a PCR reaction that failed three or more times; SNP—single nucleotide polymorphism. Cases are ranked according to degree of loss. HBV—hepatitis B virus, HCV—hepatitis C virus, cirr—cirrhosis, trans—in transition to cirrhosis; WD—well differentiated, MD—moderately differentiated, PD—poorly differentiated.

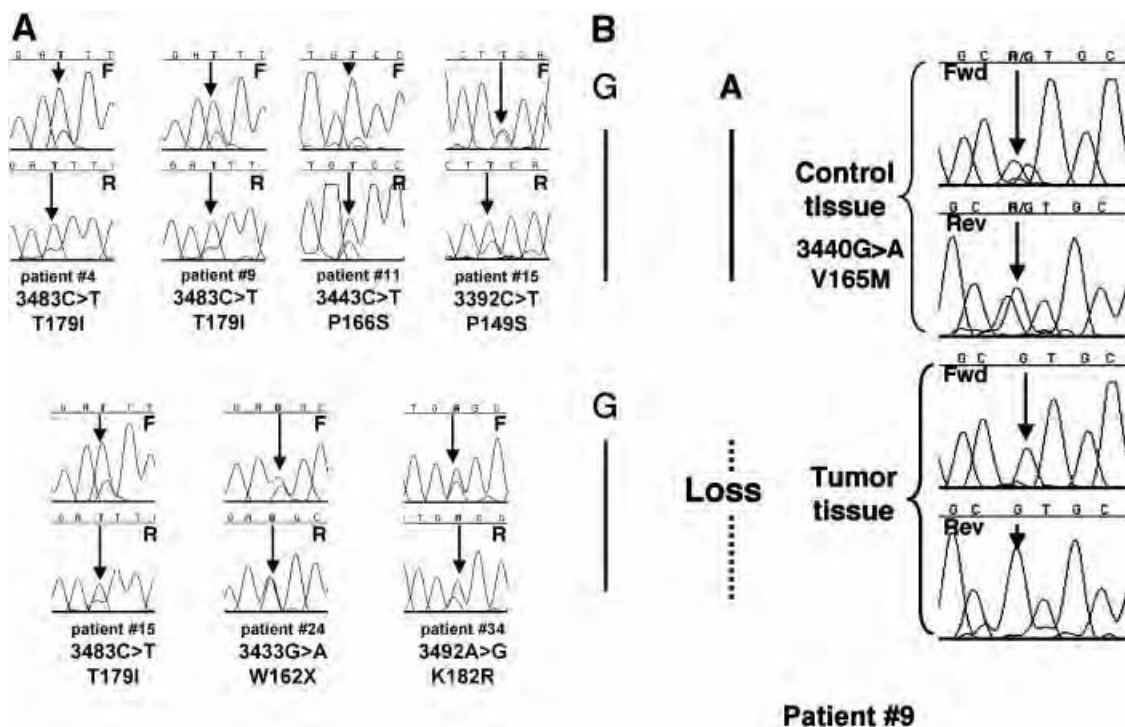


Fig. 1. (A) *KLF6* mutations identified in HCC. Bidirectional sequencing chromatograms are shown demonstrating 7 mutations from 6 patients. An arrow indicates each mutation. The base changes and the predicted amino acid changes are stated. Each mutation was confirmed in both directions. F, forward direction of sequence; R, reverse direction of sequence. (B) Allelic imbalance in a HCC patient identified by loss of a polymorphism. Sequencing chromatograms are shown for tumor and control tissue from patient 9, who was heterozygous for a V165M (nt 3440 G>A) polymorphism in the control tissue, while in the tumor DNA the A allele is lost, making it homozygous for G. This patient demonstrated no specific microsatellite marker loss and was noninformative for *KLF6M2* (see Table 1). Allelic imbalance, however, is suggested by the sequencing data. Arrows = base 3440. Fwd, forward direction of sequence; Rev, reverse direction of sequence.

cases (patients 4, 9, and 15). This mutation is predicted to disrupt a putative consensus phosphorylation site for three kinases: CaMII, p70s6k, and protein kinase A. The 3492 A>G mutation in patient sample 34 predicts a K182R substitution, which may potentially affect acetylation of the transcription factor. One further HCC case possessed a *KLF6* nonsense mutation predicting replacement of a tryptophan with a premature stop codon, W162X (G3433 TGG>TGA). These mutations—with the exception of K182R—have been previously detected in colorectal cancers.⁹

Interestingly, an additional patient (patient 9) had evidence of allelic imbalance demonstrated not by microsatellite analysis but instead by the loss in the tumor of a heterozygous polymorphism present in the corresponding normal genomic DNA (Fig. 1B). The normal DNA harbors both *KLF6* alleles, with both a G and an A nucleotide present at nucleotide position 3440 G>A. In the tumor, however, only the G nucleotide was present, suggesting loss of the allele containing the A nucleotide. Interestingly, *KLF6M2*—the marker closest to the *KLF6* gene locus (10 kb)—was noninformative for this patient, so LOH based on single nucleotide polymorphism instead of microsatellite analysis was identified.

***KLF6* But Not HCC-Derived *KLF6* Mutants Suppress Growth of HepG2 Cells.** Wild-type *KLF6* transcriptionally activates the cell cycle inhibitor p21 independently of TP53 and suppresses cell growth in fibroblast and cancer cell lines.^{7,9} We have previously shown increased p21 induction by wild-type *KLF6* but not by P149S, P166S, T179I, or W162X patient-derived mutants.⁹ Here we demonstrate a growth suppressive effect of the wild-type *KLF6* protein in the HepG2 hepatoblastoma cell line. Proliferation of HepG2 cells was inhibited by 15% ($P < .005$; $n = 4$) (Fig. 2) with the wild-type protein, but not by patient-derived mutant proteins. These results suggest that these HCC tumor mutations may functionally inactivate wild-type *KLF6* function.

Discussion

In this study, we established that *KLF6* is inactivated by loss and/or mutation in approximately 50% of hepatocellular cancers analyzed. Allelic imbalance in the *KLF6* region was confirmed using a combination of microsatellite markers and polymorphism analysis in approximately 41% (17 of 41) of patients. Individuals with evidence of

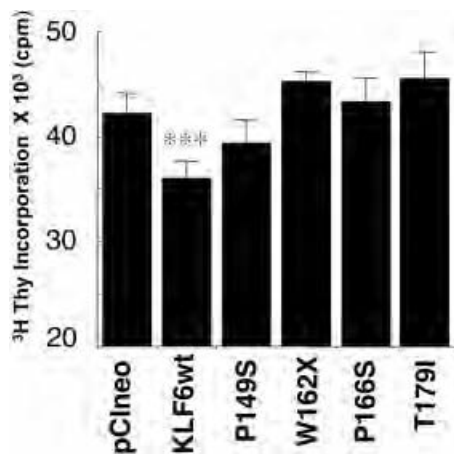


Fig. 2. Loss of growth suppression by HCC-derived *KLF6* mutations. Relative proliferation was assessed via [³H]-thymidine incorporation into DNA in the HepG2 cell line. Cells were grown in 10% fetal bovine serum and transfected with expression vector pCIneo (vector), *KLF6* wild-type, or mutants. At 24 hours, cells were incubated for 4 hours with 1 μ Ci/mL [³H]-thymidine, fixed and lysed, and disintegrations per minute were estimated via liquid scintillation counting. *KLF6* has a significant anti-proliferative effect relative to expression vector alone (***P* < .001; *n* = 4), while the mutant isoforms do not.

KLF6 flanking marker loss include those who had both hepatitis B virus- and hepatitis C virus-associated cirrhosis. Notably, 5 of these cases had *KLF6* allelic imbalance in tumors arising in viral hepatitis not associated with cirrhosis, possibly indicating a mechanism of loss associated with viral injury and/or prolonged inflammation rather than the presence of established cirrhosis. LOH in hepatitis B virus-related tumors may well arise as a result of genomic instability caused by viral integration into the genome.¹⁹ However, *KLF6* loss in HCC was also seen in 1 case of hepatitis C virus not associated with cirrhosis (case 19) and in 1 other nonviral case not associated with cirrhosis (patient 37). Tumors in these individuals who do not have cirrhosis are rare and are not associated with viral integration events. Because the majority of individuals in this study had viral hepatitis, additional studies are needed to determine the incidence of *KLF6* inactivation in HCCs associated with other etiologies. Of note, the mean tumor size of those HCCs harboring LOH tended to be larger (mean, 9.09) than in those without LOH (mean, 4.09) (*P* < .05). Nonetheless, whether *KLF6* deregulation is a late rather than early event in the development of HCC merits additional studies.

KLF6 mutations were identified in 15% of patients with HCC and were localized between amino acids 149 and 182 in the activation domain of *KLF6*. The mutation T179I found in 3 HCC cases was also particularly common in colorectal cancers⁹ and was further validated by a restriction digestion (data not shown). All the HCC-derived mutations identified to date failed to suppress

growth or induce p21 to the same extent as wild-type *KLF6* in HepG2 cells, offering a potential mechanism for their loss of tumor suppressor activity. The shared *KLF6* mutations identified in colorectal cancer⁹ and HCC, in particular a predicted T179I mutation, are noteworthy. These mutations occur within the cluster of amino acids 148 to 155, a region predicted to be a consensus phosphorylation site for GSK3 β . GSK3 β is a key regulator of the Wnt signaling pathway, which has a well-established role in colorectal cancer²⁰ as well as HCC pathogenesis.^{2,18}

Consistent with Knudson's two-hit hypothesis for a classic tumor suppressor gene,²¹ 3 of our patients had LOH in one *KLF6* allele and a mutation in the retained allele. Interestingly, given previous findings in esophageal cancer suggesting inactivation of *KLF6* by promoter methylation¹⁴ and other tumor suppressor genes by haploinsufficiency,²² the possibility that loss of 1 *KLF6* allele may lead to HCC development or progression warrants further study.

Although the role of *KLF6* in tumorigenesis is not completely characterized at present, it appears to be involved in many growth-suppressive pathways that might be abrogated following its inactivation or down-regulation in cancer. Here we demonstrate that *KLF6* mutations in HCC abolish its growth-suppressive activity, which has been associated with loss of induction of the p21 cdk/cyclin inhibitor as reported for prostate and colon cancers.^{7,9} Moreover, HCC mutations are predicted to affect consensus phosphorylation sites for GSK3 β , a Wnt signaling regulator whose role in HCC is well established.^{2,18} In addition, wild-type *KLF6* can transcriptionally induce transforming growth factor beta and its receptors.²³ Loss of transforming growth factor beta signaling frequently occurs in HCCs,²⁴ suggesting that *KLF6* inactivation or down-regulation could affect this pathway. Overexpression of cyclins has also been observed frequently in HCC cases,²⁵ and we recently demonstrated that *KLF6* can bind and inactivate cyclin D1 and converge with the Rb pathway.²⁶ *KLF6* may also up-regulate the insulin-like growth factor 1 receptor,²⁷ the loss of which could contribute to HCC.²⁸ Finally, apoptotic activity of *KLF6* has been reported in lung cancer cell lines,¹³ and down-regulation of this apoptotic potential could enable emergence of neoplastic cells.

KLF6 is a tumor suppressor gene involved in a growing number of neoplasms, including prostate, colon, glioma, lung, and esophageal cancers. Here we report evidence that this gene is also inactivated in a significant proportion of HCCs, some of the most common and least effectively treated malignant tumors worldwide. *KLF6* joins many other genes that are deregulated in HCC, albeit not in a

majority of cases, suggesting that accumulated abnormalities rather than a single gene defect underlie this neoplasm. Nonetheless, based on its inactivation in major human cancers and participation in converging pathways of growth control, *KLF6* deregulation may be an important event in HCC pathogenesis.

References

- Bruix J, Boix L, Sala M, Llovet JM. Focus on hepatocellular cancer. *Cancer Cell* 2004;5:215–219.
- Thorgeirsson SS, Grisham JW. Molecular pathogenesis of human hepatocellular carcinoma. *Nat Genet* 2002;31:339–346.
- Thorgeirsson SS. Hunting for tumor suppressor genes in liver cancer. *HEPATOLOGY* 2003;37:739–741.
- Laurent-Puig P, Legoix P, Bluteau O, Belghiti J, Franco D, Binot F, et al. Genetic alterations associated with hepatocellular carcinomas define distinct pathways of hepatocarcinogenesis. *Gastroenterology* 2001;120:1763–1773.
- Tannapfel A, Wittekind C. Genes involved in hepatocellular carcinoma: deregulation in cell cycling and apoptosis. *Virchows Arch* 2002;440:345–352.
- Ratziu V, Lalazar A, Wong L, Dang Q, Collins C, Shaulian E, et al. Z β , a Kruppel-like transcription factor up-regulated in vivo during early hepatic fibrosis. *Proc Natl Acad Sci U S A* 1998;95:9500–9505.
- Narla G, Heath KE, Reeves HL, Li D, Giono LE, Kimmelman AC, et al. KLF6, a candidate tumor suppressor gene mutated in prostate cancer. *Science* 2001;294:2563–2566.
- Chen C, Hyytinen ER, Sun X, Helin HJ, Koivisto PA, Frierson HF Jr, et al. Deletion, mutation, and loss of expression of KLF6 in human prostate cancer. *Am J Pathol* 2003;162:1349–1354.
- Reeves HL, Narla G, Oginbiyi O, Haq AI, Katz A, Benzeno S, et al. Kruppel-like factor 6 (KLF6) is a tumor suppressor gene frequently inactivated in colorectal cancer. *Gastroenterology* 2004;126:1090–1103.
- Chen HK, Liu XQ, Lin J, Chen TY, Feng QS, Zeng YX. Mutation analysis of KLF6 gene in human nasopharyngeal carcinomas. *Ai Zhong* 2002;21:1047–1050.
- Jeng YM, Hsu HC. KLF6, a putative tumor suppressor gene, is mutated in astrocytic gliomas. *Int J Cancer* 2003;105:625–629.
- Wikman H, Kettunen E, Seppanen JK, Karjalainen A, Hollmen J, Anttila S, et al. Identification of differentially expressed genes in pulmonary adenocarcinoma by using cDNA array. *Oncogene* 2002;21:5804–5813.
- Ito G, Uchiyama M, Kondo M, Mori S, Usami N, Maeda O, et al. Kruppel-like factor 6 is frequently down-regulated and induces apoptosis in non-small cell lung cancer cells. *Cancer Res* 2004;64:3838–3843.
- Yamashita K, Upadhyay S, Osada M, Hoque MO, Xiao Y, Mori M, et al. Pharmacologic unmasking of epigenetically silenced tumor suppressor genes in esophageal squamous cell carcinoma. *Cancer Cell* 2002;2:485–495.
- Glinsky GV, Glinskii AB, Stephenson AJ, Hoffman RH, Gerald WL. Gene expression profiling predicts clinical outcome of prostate cancer. *J Clin Invest* 2004;113:913–923.
- Kimmelman AC, Rui FQ, Narla N, Banno B, Lau N, Bos P, et al. Suppression of glioblastoma tumorigenicity by the Kruppel-like transcription factor, KLF6. *Oncogene* 2004;23:5077–5083.
- Nagai H, Pineau P, Tiollais P, Buendia MA, Dejean A. Comprehensive allelotyping of human hepatocellular carcinoma. *Oncogene* 1997;14:2927–2933.
- Buendia MA. Genetics of hepatocellular carcinoma. *Semin Cancer Biol* 2000;10:185–200.
- Brechot C, Gozuacik D, Murakami Y, Paterlini-Brechot P. Molecular bases for the development of hepatitis B virus (HBV)-related hepatocellular carcinoma (HCC). *Semin Cancer Biol* 2000;10:211–231.
- Grady WM, Markowitz SD. Genetic and epigenetic alterations in colon cancer. *Annu Rev Genomics Hum Genet* 2002;3:101–128.
- Knudson AG Jr. Mutation and cancer: statistical study of retinoblastoma. *Proc Natl Acad Sci U S A* 1971;68:820–823.
- Trotman LC, Niki M, Dotan ZA, Koutcher JA, Cristofano AD, Xiao A, et al. Pten dose dictates cancer progression in the prostate. *PLoS Biol* 2003;1:E59.
- Kim Y, Ratziu V, Choi SG, Lalazar A, Theiss G, Dang Q, et al. Transcriptional activation of transforming growth factor beta1 and its receptors by the Kruppel-like factor Z β /core promoter-binding protein and Sp1. Potential mechanisms for autocrine fibrogenesis in response to injury. *J Biol Chem* 1998;273:33750–33758.
- Enomoto A, Esumi M, Yamashita K, Takagi K, Takano S, Iwai S. Abnormal nucleotide repeat sequence in the TGF-betaRII gene in hepatocellular carcinoma and in uninvolved liver tissue. *J Pathol* 2001;195:349–354.
- Joo M, Kang YK, Kim MR, Lee HK, Jang JJ. Cyclin D1 overexpression in hepatocellular carcinoma. *Liver* 2001;21:89–95.
- Benzeno S, Narla G, Allina J, Cheng GZ, Reeves HL, Banck MS, et al. Cyclin-dependent kinase inhibition by the KLF6 tumor suppressor protein through interaction with cyclin D1. *Cancer Res* 2004;64:3885–3891.
- Rubinstein M, Idelman G, Plymate SR, Narla G, Friedman SL, Werner H. Transcriptional activation of the insulin-like growth factor I receptor gene by the Kruppel-like factor 6 (KLF6) tumor suppressor protein: potential interactions between KLF6 and p53. *Endocrinology* 2004;145:3769–3777.
- Scharf JG, Dombrowski F, Ramadori G. The IGF axis and hepatocarcinogenesis. *Mol Pathol* 2001;54:138–144.

Targeted Inhibition of the KLF6 Splice Variant, KLF6 SV1, Suppresses Prostate Cancer Cell Growth and Spread

Goutham Narla,¹ Analisa DiFeo,² Shen Yao,¹ Asoka Banno,³ Eldad Hod,¹ Helen L. Reeves,¹ Rui F. Qiao,³ Olga Camacho-Vanegas,² Alice Levine,¹ Alexander Kirschenbaum,^{1,4} Andrew M. Chan,³ Scott L. Friedman,^{1,3} and John A. Martignetti^{2,3,5}

Departments of ¹Medicine, ²Human Genetics, ³Oncological Sciences, ⁴Urology, and ⁵Pediatrics, the Mount Sinai School of Medicine, New York, New York

Abstract

Prostate cancer is a leading cause of cancer death in men. Risk prognostication, treatment stratification, and the development of rational therapeutic strategies lag because the molecular mechanisms underlying the initiation and progression from primary to metastatic disease are unknown. Multiple lines of evidence now suggest that KLF6 is a key prostate cancer tumor suppressor gene including loss and/or mutation in prostate cancer tumors and cell lines and decreased KLF6 expression levels in recurrent prostate cancer samples. Most recently, we identified a common KLF6 germ line single nucleotide polymorphism that is associated with an increased relative risk of prostate cancer and the increased production of three alternatively spliced, dominant-negative KLF6 isoforms. Here we show that although wild-type KLF6 (wtKLF6) acts as a classic tumor suppressor, the single nucleotide polymorphism-increased splice isoform, KLF6 SV1, displays a markedly opposite effect on cell proliferation, colony formation, and invasion. In addition, whereas wtKLF6 knockdown increases tumor growth in nude mice >2-fold, short interfering RNA-mediated KLF6 SV1 inhibition reduces growth by ~50% and decreases the expression of a number of growth- and angiogenesis-related proteins. Together, these findings begin to highlight a dynamic and functional antagonism between wtKLF6 and its splice variant KLF6 SV1 in tumor growth and dissemination. (Cancer Res 2005; 65(13): 5761-8)

Introduction

Disseminated prostate cancer is a leading cause of cancer death in men. Although gene loci, candidate genes, and risk factors for subsets of familial forms of prostate cancer development are increasingly being identified, the molecular mechanisms underlying the initiation and transition from localized to metastatic phenotype are poorly understood (1). Identification of individual genes and biomarkers which correlate with clinical behavior and metastatic spread is an urgent priority in order to define both therapeutic targets and improve patient stratification for future treatment. KLF6/COPEB is one of a number of candidate genes consistently emerging as a potentially relevant molecular target (2–7).

KLF6 is a member of the Kruppel-like family of zinc finger transcription factors which are DNA-binding proteins regulating growth-related signal transduction pathways, cell proliferation,

apoptosis, and angiogenesis (8, 9). We previously showed that KLF6, a ubiquitously expressed zinc finger transcription factor, is a tumor suppressor gene inactivated by allelic loss and somatic mutation in sporadic prostate cancers that can mediate growth suppression both by a p53-independent, up-regulation of p21 (2), and by disrupting the interaction between cyclin D1 and CDK4 (10). Independent studies, albeit not all (11), have also identified inactivation in both sporadic prostate cancer and prostate cancer cell lines (3). In support of its more general role as a tumor suppressor in a number of human cancers, KLF6 mutation and loss have also been described in colorectal cancer, hepatocellular and nasopharyngeal carcinomas, and in malignant gliomas (2–7). Moreover, in separate high-throughput array studies aimed at identifying novel risk stratification markers and predictive gene cluster fingerprints, decreased KLF6 expression has also been shown to predict poor clinical outcomes in both prostate cancer (12) and pulmonary adenocarcinoma (13).

Beyond these findings in tumor samples, we recently identified a germline KLF6 single nucleotide polymorphism (SNP), IVS1 –27 G>A/IVSΔA, that is significantly associated with increased prostate cancer risk in men (14). This intronic SNP, which is the first reported high-prevalence, low-penetrance prostate cancer susceptibility allele, generates a novel functional SRp40 DNA binding site, ablating two other overlapping SR-protein binding sites, and increasing transcription of three alternatively spliced KLF6 isoforms, KLF6 SV1, SV2, and SV3. These alternatively spliced KLF6 proteins, present in both normal and cancerous tissues, antagonize the ability of wild-type KLF6 (wtKLF6) to up-regulate p21 expression and suppress cell proliferation (14). Although alternative splicing is present in both normal and cancerous cells, expression of the KLF6 splice variants seems to be up-regulated in prostate cancer (14). These results suggested that the IVSΔA SNP effectively disrupts a regulated pattern of KLF6 splicing and through overexpression of splice variants, could lead to an increased relative risk of prostate cancer. Given that KLF6 SV1 and SV2 antagonize the ability of wtKLF6 to up-regulate p21 expression and suppress cellular proliferation (14), these isoforms may provide the physiologic and biological link between this KLF6 germ line SNP and increased risk of prostate cancer.

Thus, the present studies explore the biological relevance and implications of one of the recently identified KLF6 splice variants, KLF6 SV1, on a number of cancer-related phenotypes. In addition, this study provides the first demonstration that suppressing wtKLF6 expression increases prostate cell growth in culture and tumor growth *in vivo*.

Materials and Methods

Cell culture and transient transfection. All cell lines were obtained from the American Tissue Culture Collection (Rockville, MD). Polyclonal

Note: S.L. Friedman and J.A. Martignetti share senior authorship.

Requests for reprints: John A. Martignetti, Department of Human Genetics, Mount Sinai School of Medicine, 1425 Madison Avenue, New York, NY 10029. Phone: 212-659-6744; E-mail: john.martignetti@mssm.edu.

©2005 American Association for Cancer Research.

pools of stable cell lines were generated by cotransfection of the pSUPER-si-luc, si-wtKLF6, si-SV1, or si-SV2 with a puromycin expressing plasmid. Transfected cells were selected with 2 $\mu\text{g}/\text{mL}$ of puromycin. For each construct, three independent polyclonal pools of stable cell lines were generated and analyzed.

pSUPER plasmid construction and transfection. The pSUPER-siSV1 and pSUPER-siSV2 plasmids used to down-regulate KLF6 SV1 and KLF6 SV2 expression and the control pSUPER-luc construct were previously described (14). The pSUPER-si-wtKLF6 construct was generated as previously described using this pSUPER vector (ref. 15; generously provided by R. Agami). To insert the targeting sequence, DNA oligonucleotides were designed and cloned into the *BglII-HindIII* sites of the pSuper vector.

Si-wtKLF6-F: GATCCCCTGGCGATGCCTCCCCGACttcaagaga
GTCGGGGGAGGCATCGCCATTTTGGAAA

Si-wtKLF6-R: AGCTTTTCCAAAAATGGCGATGCCTCCCCGAC
tcctctgaaGTCGGGGGAGGCATCGCCAGG

Immunohistochemistry. Immunohistochemical staining for factor VIII-related antigen and proliferating cell nuclear antigen (PCNA) were carried out as previously described (16, 17) using a factor VIII-related antigen (DAKO, Carpinteria, CA) antibody for the detection of tumor microvessel density and a PCNA antibody (Santa Cruz Biotechnology, Santa Cruz, CA) for the detection of tumor cell proliferation, respectively. Measurements of PCNA staining and microvessel density were done as previously described (18). Briefly, microvessels that stained positive for factor VIII-related antigen were counted on four representative high-power fields ($400\times$) for each tumor. Data was expressed as the average number of microvessels per $400\times$ field for each experimental tumor group. PCNA staining was determined by counting the number of positive cells per $400\times$ field and dividing that number by the total number of cells in that particular field. For each tumor, four high-powered fields were counted and the average for each experimental tumor group was determined.

Colony formation assays. The ability of different transfectants to proliferate in an anchorage-independent manner was quantified by standard soft-agar assay. Approximately 10^5 cells were resuspended in 2 mL of 0.4% (w/v) Noble agar (Difco) and overlaid on top of 1% (w/v) agar as described previously (19). After 3 weeks of incubation at 37°C , continuously growing colonies were visualized by staining with 1 mg/mL of *p*-iodonitrotetrazolium violet. Colonies >2 mm in diameter were counted.

Tumorigenicity assay. Stable short interfering RNA (siRNA) PC3M cells (1×10^6) were injected into the left flank of 6- to 8-week-old female BALB/c *nu/nu* mice. Tumor volume was assessed every week and determined by the formula (length \times width \times width \times 0.4). The mice were sacrificed 8 weeks after inoculation and tumors were excised for RNA, protein, and immunohistochemical analysis. All animal work and protocols were approved by the Mount Sinai School of Medicine Institutional Animal Care and Use Committee.

Migration and invasion assays. Standard invasion assays were done in Boyden chambers by using a reconstituted basement membrane (Matrigel, 0.5 mg/mL; Becton Dickinson, Mountain View, CA; ref. 20). Coated membranes were first blocked with 0.5% bovine serum albumin (BSA) in DMEM and equilibrated in 0.1% BSA/DMEM. Approximately 10^5 cells in serum-free DMEM were added to the upper chamber and conditioned medium derived from NIH 3T3 fibroblasts was used in the lower chamber as a chemoattractant. Following incubation for 19 hours at 37°C , cells in the upper chamber were thoroughly removed by gentle suctioning. Cells invaded through the barrier were fixed in 10% formalin and stained with 4',6-diamidino-2-phenylindole in PBS. Nuclei were visualized under a fluorescence microscope and images of five randomly selected nonoverlapping fields were counted.

Generation of KLF6 monoclonal antibodies. A 67 kDa glutathione *S*-transferase fusion peptide containing amino acids 28 to 199 of the human KLF6 activation domain (*pGEX-2-PM*) and the following peptide: EKSLT-DAHGKGVSGVLQEVMS were purified and used to generate the 2A2 and 9A2 monoclonal KLF6 antibodies, respectively.

Western blot analysis. Cell extracts for Western blotting were harvested in radioimmunoprecipitation assay buffer (standard protocols, Santa Cruz Biotechnology). Tumor tissue extracts were harvested and prepared in the T-PER reagent (Pierce, Rockford, IL). Equal amounts of protein (50 μg) as determined by the Bio-Rad (Richmond, CA) DC Protein quantification assay were loaded and separated by PAGE and transferred to nitrocellulose membranes. Western blotting was done using a goat polyclonal antibody to actin and VE-cadherin (SC-1616 and SC-6458, respectively), and monoclonal antibodies to p21 (Santa Cruz Biotechnology) and the KLF6 2A2 and 9A2 antibodies (Zymed).

Densitometric analysis. Enhanced chemiluminescent images of immunoblots were analyzed by scanning densitometry and quantified with a BIOQUANT NOVA imaging system. All values were normalized to actin and expressed as fold changes relative to control.

Analysis of proliferation. Proliferation was determined by estimating [^3H]thymidine incorporation. PC3M stable cell lines expressing either si-luc, si-wtKLF6, si-SV1, or si-SV2 were plated at a density of 50,000 cells per well in 12-well dishes. Forty-eight hours after plating, 1 $\mu\text{Ci}/\text{mL}$ [^3H]thymidine (Amersham) was added. After 2 hours, cells were washed four times with ice-cold PBS and fixed in methanol for 30 minutes at 4°C . After methanol removal and cell drying, cells were solubilized in 0.25% sodium hydroxide/0.25% SDS. After neutralization with hydrochloric acid (1 N), disintegrations per minute were estimated by liquid scintillation counting.

RNA and quantitative real-time PCR analysis. Cell line and tumor RNA was extracted using the RNeasy Mini and Midi kit (Qiagen, Chatsworth, CA). All RNA was treated with DNase (Qiagen). A total of 1 μg of RNA was reverse-transcribed per reaction using first-strand complementary DNA synthesis with random primers (Promega, Madison, WI). Quantitative real-time PCR was done using the following PCR primers on an ABI PRISM 7900HT sequence detection system (Applied Biosystems, Foster City, CA): Ki-67 forward, 5'-GAA GAG TTG TAA ATT TGC TTC T-3'; and Ki-67 reverse, 5'-ATG TTG TTT TGA CAC AAC AGG A-3'. Primer sequences for total and wtKLF6, p21, and glyceraldehyde-3-phosphate dehydrogenase (14) as well as for markers of angiogenesis including *Flt-1*, *VE-cadherin*, *Ang-2*, *Tie-1*, and *PECAM* have all been previously described (21). All experiments were done in triplicate and repeated three independent times. All values were normalized to glyceraldehyde-3-phosphate dehydrogenase levels. Levels of KLF6 alternative splicing was determined as previously described (14).

Results

KLF6 alternative splicing is differentially regulated in prostate cancer cell lines. Prior to their experimental manipulation, we established the baseline level of KLF6 alternative splicing in two well-characterized prostate cell lines, the benign prostatic hyperplasia cell line, BPH1, and the metastatic prostate cancer-derived cell line, PC3M. The levels of wtKLF6 and alternative splicing in both of these cell lines was determined and compared at both the mRNA and protein levels. We chose these two cell lines because of their highly contrasting genotypic and phenotypic features. The nontumorigenic human prostatic epithelial cell line, BPH1, was originally immortalized using the large T antigen oncogene and fails to form tumors in nude mice (22). PC3M was originally derived from liver metastases produced in nude mice subsequent to intrasplenic injection of PC3 cells (23).

Similar to previous findings in patient-derived tissues (14), wtKLF6 levels were lower, whereas alternatively spliced isoforms of KLF6 were higher in the metastatic, cancer-derived cell line PC3M than those in BPH1 cells (Fig. 1A and B). Densitometric analysis of the KLF6 protein isoforms in PC3M cells showed an average 2.8-fold increase in the ratio of alternatively spliced KLF6 to wtKLF6.

Interestingly, the endogenous splicing preferences between wild-type and splice forms in these two cell lines were maintained following transfection of a KLF6 minigene construct. Each cell line

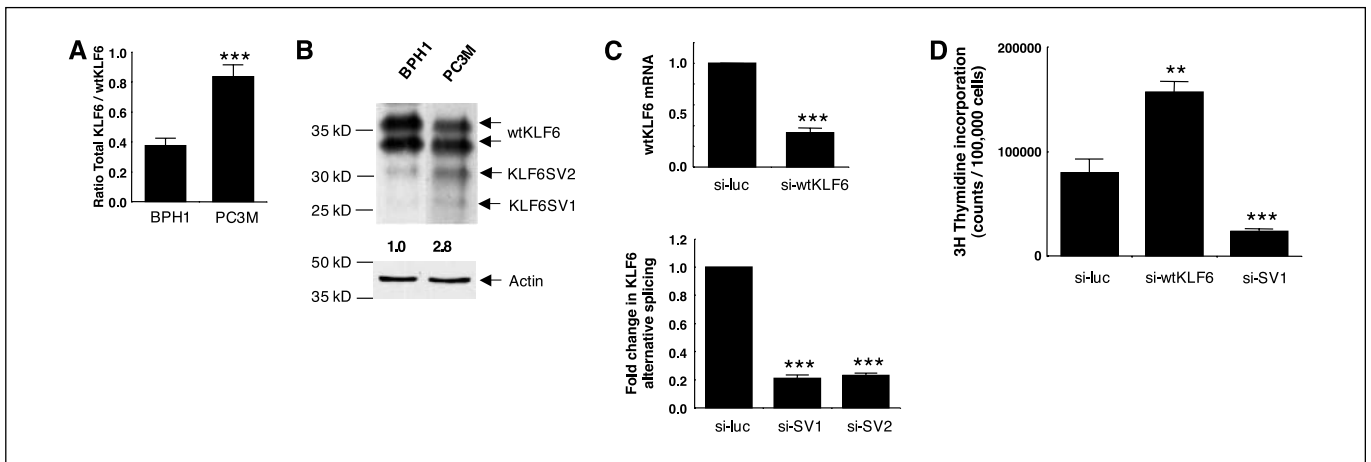


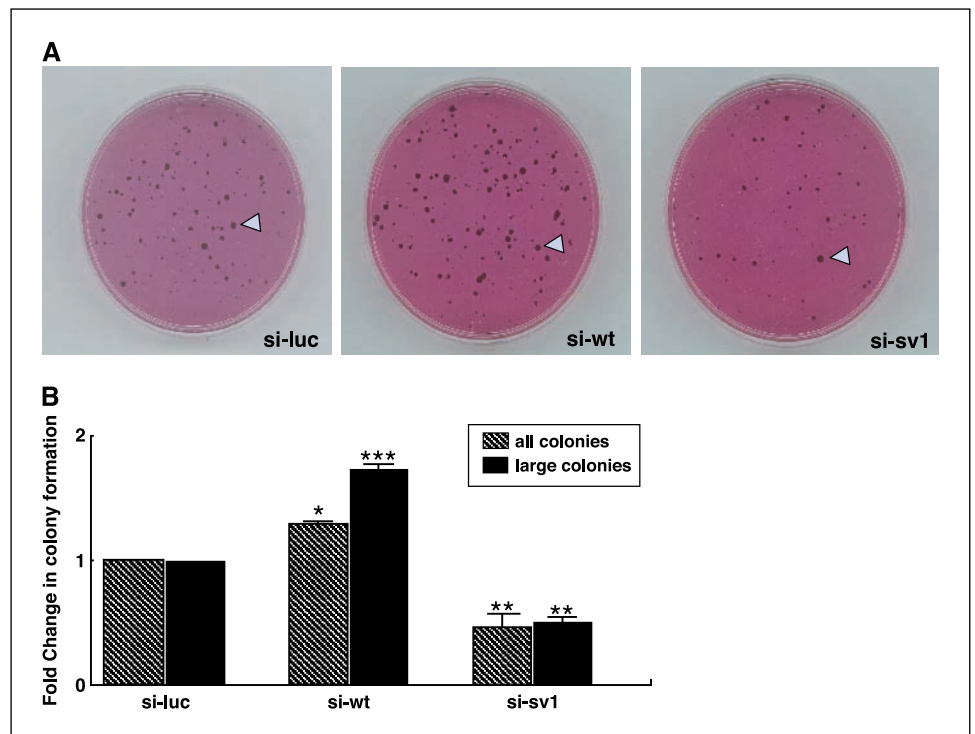
Figure 1. The *KLF6* gene is differentially spliced in prostate cell lines. *A*, quantitative real-time PCR was done on the benign prostatic hyperplasia cell line (BPH1) and the metastatic prostate cancer cell line (PC3M) to determine the baseline level of endogenous *KLF6* alternative splicing in these prostate-derived cell lines. The PC3M cell line had a significantly higher endogenous splicing ratio ($x = 0.83$) than did the BPH1 cell line ($x = 0.41$; $***, P < 0.0001$). *B*, Western blot analysis for *KLF6* expression in BPH1 and PC3M cells using the 2A2 *KLF6* monoclonal antibody. Consistent with the RNA findings, the PC3M cell line expresses increased levels of both *KLF6* variant proteins. The ratio of splice variants to wild-type protein was determined by densitometry to be ~ 2.8 -fold. *C*, transient expression of the pSUPER-si-wtKLF6, si-luc, si-SV1, and si-SV2 in PC3M cells. Three independent transfection experiments were done and analyzed for each pSUPER-siRNA construct. Transient si-wtKLF6 expression results in a 70% decrease in wtKLF6 mRNA ($***, P < 0.0001$), whereas targeted reduction of si-SV1 and SV2 expression results in an $\sim 80\%$ decrease in *KLF6* alternative splicing as measured by quantitative real-time PCR ($***, P < 0.0001$). *D*, cell proliferation analysis of transiently transfected PC3M cells. The pSUPER-si-wtKLF6 expressing cells proliferate 80% more than pSUPER-luc expressing cells ($**$, $P < 0.001$), whereas the pSUPER-si-SV1 expressing cells proliferate 65% less than control cells ($***, P < 0.0001$).

was transfected with an expression vector containing the entire *KLF6* gene including the 5' and 3' untranslated regions (14). Again, wtKLF6 levels were decreased, whereas alternatively spliced forms were increased in the PC3M cells when compared with the BPH1 cell line (Fig. 1A).

Targeted silencing of wtKLF6 and *KLF6* SV1 divergently affects cellular proliferation. Having shown differential regulation in *KLF6* alternative splicing levels in these two cell lines, we next examined the effect of targeted down-regulation of each

isoform specifically by RNAi-mediated gene silencing on growth- and metastasis-related features of the PC3M cell line. We have previously shown that both *KLF6* SV1 and *KLF6* SV2 proteins mislocalize to the cytoplasm and fail to either up-regulate endogenous p21 or suppress cell proliferation (14). Silencing of either the endogenous *KLF6* SV1 or SV2 transcripts increases p21 mRNA and protein levels (14). However, the isoforms are not biologically equivalent because silencing SV1, but not SV2, results in decreased cell proliferation in culture (14).

Figure 2. Stable abrogation of *KLF6* SV1 by siRNA decreases anchorage-independent growth of PC3M. Stable cell lines expressing siRNA to either luciferase (luc), wtKLF6 (si-wt), or SV1 (si-SV1) and were assessed for their ability to grow in soft agar (arrowheads), as described in Materials and Methods. *A*, targeted reduction of full-length *KLF6* (si-wtKLF6) results in increased colony formation in soft agar as compared with the control cell line, pSUPER-si-luc. Targeted reduction of *KLF6* SV1 results in a significant decrease in colony formation. *B*, the total number of all colonies and large colonies was counted by two independent observers in three independent experiments, each done in triplicate. Targeted reduction of wtKLF6 resulted in a 30% increase in the number of total colonies ($*, P < 0.01$) and a 90% increase in large colony formation compared with the si-luc control cell line ($***, P < 0.0001$). Furthermore, targeted reduction of *KLF6* SV1 leads to a 50% reduction in both the number of all colonies and large colonies formed compared with controls ($**$, $P < 0.001$).



First, we generated stable cell lines expressing siRNAs specific to either wtKLF6 (si-wtKLF6), KLF6 SV1 (si-SV1), or KLF6 SV2 (si-SV2). Each pSUPER-derived siRNA specifically targets the respective KLF6 mRNA, with no effect on the other isoforms (14). Multiple polyclonal cell line pools for each construct were generated and analyzed by quantitative real-time PCR and Western blotting. As shown in Fig. 1C, wtKLF6 levels were reduced ~50%, whereas each targeted KLF6 alternative splice form was reduced ~60% in the respective stable cell lines expressing pSUPER-si-SV1 and si-SV2 as compared with pSUPER-Luc expressing cell lines. Proliferation rates were drastically and divergently affected in two of the generated lines. Cell proliferation increased by almost 90% in the si-wtKLF6 cells but reduced by almost 60% in the si-SV1 cell lines when compared with controls (Fig. 1D). No changes in proliferation rates were noted in the pSUPER-si-SV2 stable cell lines (data not shown).

Differential effects of wtKLF6 and SV1 gene silencing on tumor cell colony formation, migration, and invasion. We next explored the effect of targeted reduction on the ability of different KLF6 siRNA stable cell lines to proliferate in an anchorage-independent manner as quantified by soft-agar assay. Consistent with its function as a tumor suppressor gene, targeted reduction of wtKLF6 (si-wtKLF6) led to a >50% increase in colony formation (Fig. 2A and B; $P < 0.01$). Reduction of KLF6 SV1, on the other hand, had exactly the opposite effect, resulting in a >50% decrease in colony formation (Fig. 2A and B; $P < 0.001$).

Given the role of cell migration and invasion in the progression of localized cancer to disseminated disease, we next analyzed these

phenotypes. Interestingly, these were only affected by one of the two KLF6 isoforms. Targeted reduction of the KLF6 SV1 protein resulted in a 60% decrease in both cell migration (Fig. 3A; $P < 0.01$) and invasion (Fig. 3B; $P < 0.001$) of this highly metastatic cell line. In contrast to its markedly opposite effects to SV1 on cellular proliferation and colony formation, reduction of the wtKLF6 protein had no effect on either cell migration or invasion (data not shown).

Inhibition of wtKLF6 and KLF6 SV1 differentially affect tumorigenicity *in vivo*. Based on the marked functional differences between the various KLF6 isoform siRNA cell lines, we next explored whether wtKLF6 or the splice variants affected tumorigenicity *in vivo*. Beyond the previous patient-derived tumor findings—that decreased wtKLF6 expression correlated with worse prognosis (12) and KLF6 SV1 expression is increased in prostate cancer tissue (14)—the tumorigenicity data provides the first experimental evidence that these isoforms differentially regulate tumor growth *in vivo*.

PC3M stable cell lines expressing specific siRNAs to either luciferase, wtKLF6, SV1, or SV2 were injected s.c. into nude mice and after 8 weeks, the mice were sacrificed and tumor mass was determined. Tumor take rates were consistent between the various groups, with less than two of the injected mice in each group failing to produce a measurable tumor after 8 weeks of growth. Consistent with its role as a tumor suppressor gene, reduction of wtKLF6 mRNA led to >2-fold increase in tumorigenicity (Fig. 4A and B; $P < 0.01$). In marked contrast, silencing of the KLF6 SV1 transcript resulted in a 40% reduction in tumorigenicity *in vivo* (Fig. 4A and B; $P < 0.001$). Targeted reduction of the KLF6 SV2 transcript had no effect on tumor growth (data not shown).

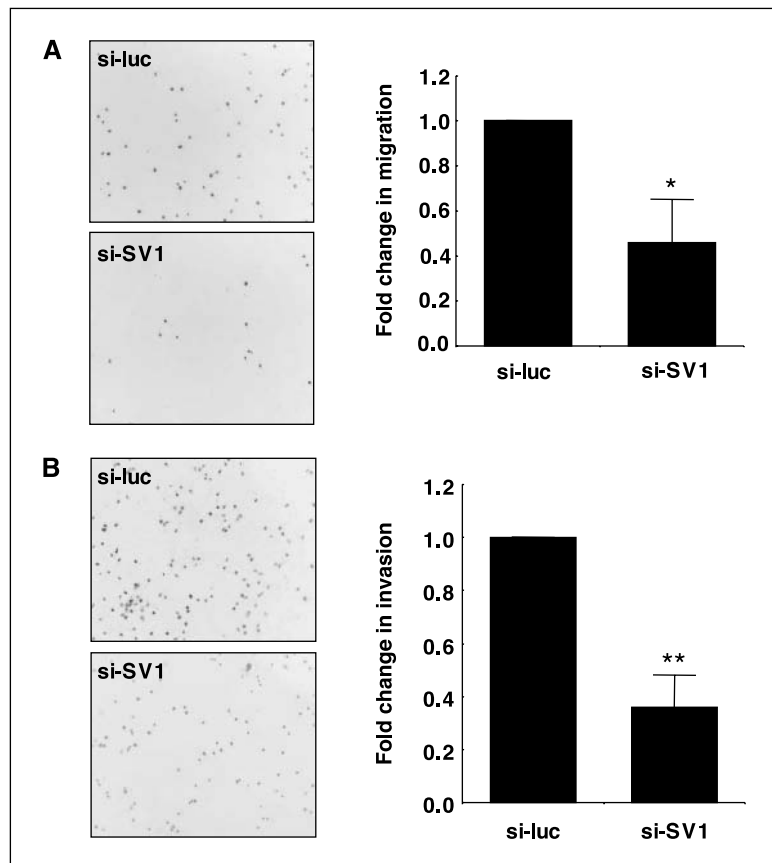


Figure 3. Reduced migration and invasion following abrogation of KLF6 SV1 by siRNA in PC3M cells. Cell lines stably expressing either siRNA to luciferase or KLF6 SV1 were assessed for their ability to either migrate and to invade through a Matrigel-coated insert, as described in Materials and Methods. Left, the underside of the insert stained with 4',6-diamidino-2-phenylindole; right, fold-change. A, targeted reduction of the KLF6 SV1 protein resulted in a 60% decrease in cell migration compared with the control luc cell line (*, $P < 0.01$). The number of cells that migrated were counted from four fields from three independent experiments done on two separate and independent polyclonal pools of si-luc, si-wtKLF6, si-SV1, and si-SV2 stable cell lines. B, si-SV1 stable cell lines were 50% less invasive through a Matrigel basement membrane (**, $P < 0.001$). The number of invasive cells were counted from four fields from four independent experiments on two separate and independent polyclonal pools of cells as described above.

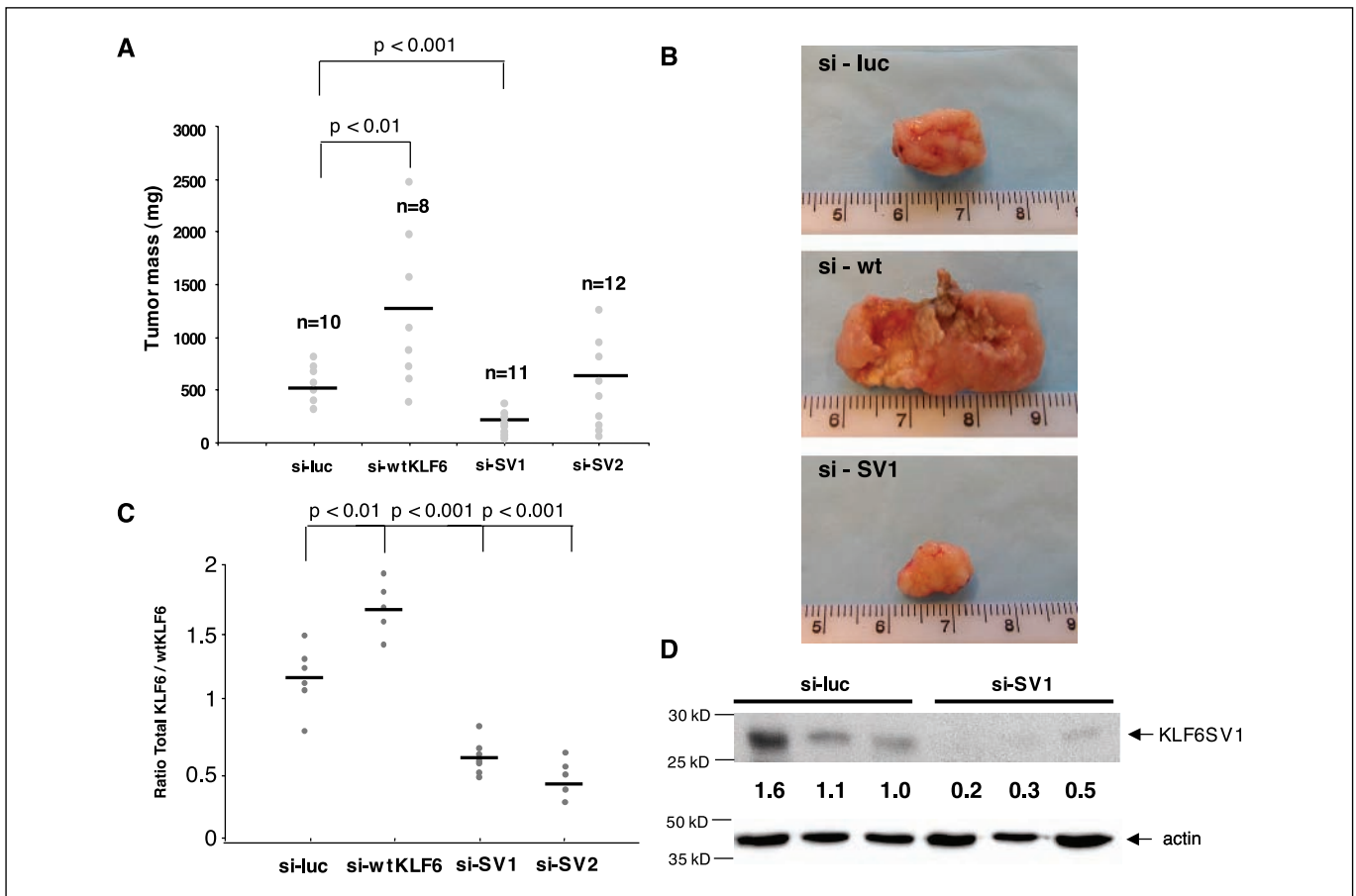


Figure 4. Divergent effects of stably expressed siRNAs to KLF6 wild-type and SV1 on PC3M xenograft growth *in vivo*. Stable cell lines expressing siRNAs to either luciferase wtKLF6, or splice forms SV1 or SV2 were injected into nude mice and their volume assessed as described in Materials and Methods. **A**, reduction of the full-length wtKLF6 mRNA resulted in >90% increase in tumorigenicity *in vivo* ($P < 0.01$); whereas PC3M cells expressing siRNA to KLF6 SV1 were 50% less tumorigenic *in vivo* ($P < 0.001$). **B**, a representative tumor from each group. **C**, KLF6 alternative splicing was quantified by quantitative real-time PCR as previously described (14) from RNA isolated from these tumors. The si-wtKLF6 derived tumors had 60% more alternative splicing relative to wtKLF6 mRNA than did control luc tumors ($P < 0.01$), whereas tumors derived from the si-SV1 and si-SV2 cell lines had a 50% and 70% decrease in KLF6 alternative splicing, respectively, compared with the control tumors ($P < 0.001$). **D**, Western blot analysis of tumor proteins extracted from independent animals injected with PC3M cells expressing pSUPER-luc ($n = 3$) and si-SV1 ($n = 3$) using the KLF6 9A2 monoclonal antibody specific to the KLF6 SV1 protein. Si-SV1 tumors expressed significantly less KLF6 SV1 protein than control si-luc tumors, as measured by densitometry relative to an actin-loading control.

To determine if the siRNA-derived tumors maintained their down-regulation of KLF6 isoforms *in vivo*, the ratio of alternatively spliced KLF6 transcripts to wtKLF6 levels was quantified by quantitative real-time PCR from tumor-isolated RNA at the end of the experimental time course. As predicted, tumors derived from the si-wtKLF6 cell line had decreased wtKLF6 levels compared with si-luc tumors (Fig. 4C). This resulted in a significant increase in the ratio of KLF6 splice variants to wtKLF6 mRNA (Fig. 4C; $P < 0.01$). On the other hand, tumors derived from the si-SV1 and si-SV2 cell lines had a reduction in KLF6 alternative splicing which effectively increased the wtKLF6 to total ratio of KLF6 (Fig. 4C; $P < 0.001$). Western blot analysis of the si-SV1 tumors with the KLF6 SV1 specific monoclonal (9A2) revealed a significant reduction in SV1 protein level *in vivo* (Fig. 4D). Interestingly, although si-SV2 tumors paralleled the significantly decreased ratio in KLF6 splice forms to wtKLF6 seen in the si-SV1 tumors, SV2 reduction had no effect on tumorigenicity (Fig. 4A-C).

Decreased si-SV1 tumor growth is associated with an antiproliferative and antiangiogenic gene expression profile. To explore potential mechanisms underlying the si-SV1-mediated reduction in tumorigenicity, we examined the expression patterns of a number of key genes regulating cell proliferation, angiogenesis,

and apoptosis in the stable cell-derived tumors. Consistent with our previous findings in patient-derived tumors (14), p21 mRNA and protein levels were increased over 2-fold in si-SV1-derived tumors (Fig. 5A and B; $P < 0.01$). This up-regulation of p21 was associated with decreased expression of markers of cellular proliferation as assessed by decreased PCNA staining and a ~30% reduction in Ki-67 mRNA levels (Fig. 5B-D). On the other hand, si-wtKLF6-derived tumors were significantly larger than control tumors and displayed higher PCNA staining, as well as a 50% increase in Ki-67 mRNA levels (Fig. 5C and D). Targeted reduction of the SV2 transcript had no effect on tumorigenicity or p21 levels (data not shown).

Tumor growth *in vivo* is known to be dependent on the ability of cancer cells to stimulate blood vessel growth through up-regulation of angiogenic mediators. Platelet/endothelial cell adhesion molecule-1 (PECAM-1)/CD31 is highly expressed by endothelial cells and is a reproducible marker of angiogenesis in transplanted tumor models. Given the relatively pallid appearance of the si-SV1-derived tumors (Fig. 4B), we analyzed the effects of SV1 silencing on a number of angiogenic markers, including CD31. Si-SV1-derived tumors had a >50% reduction in

CD31 expression compared with control tumors (Fig. 6A; $P < 0.0001$) consistent with an overall inhibition of *in vivo* angiogenesis. To broaden this finding, we then included an analysis of the expression levels of a panel of genes, *VEGF*, *Ang-1*, *Ang-2*, *Flt-1*, *KDR*, *Tie-1*, *VE-cadherin*, and *PECAM-1*, that together have been shown to more accurately reflect angiogenesis than any single marker gene alone (21). Consistent with the PECAM-1/CD31 protein immunohistochemical data, expression of five angiogenic genes, *Ang-2*, *Flt-1*, *Tie-1*, *VE-cadherin*, and *PECAM-1* was significantly reduced in si-SV1 tumors (Fig. 6B). *VEGF*, *Ang-1*, and *KDR* levels were not significantly changed. This potentially reflects the differences in the regulation of angiogenesis in different tumor types and tissues (21). Nonetheless, levels of VE-cadherin, a key molecule in endothelial cell-cell interaction and in the formation of mature, functional blood vessels, were decreased on average by >70% as assessed by Western blotting (Fig. 6C).

Discussion

A growing number of studies have highlighted the mechanisms by which the KLF6 tumor suppressor gene may be functionally inactivated in human cancer. Somatic KLF6 mutations and allelic

loss have been identified in several primary human neoplasms, including prostate (2, 3), colorectal (4), hepatocellular carcinoma (5), malignant glioma (6), and nasopharyngeal carcinoma (7). Additionally, KLF6 is transcriptionally silenced in esophageal cancer cells through promoter hypermethylation (24) and is significantly down-regulated in primary lung cancer samples and lung cancer cell lines (13, 25), as well as in some prostate cancer cell lines (3), whereas the mechanism(s) of inactivation in these cases have yet to be defined. Furthermore, KLF6 protein expression is absent in a number of glioblastoma cell lines and primary glioma patient samples and reconstitution of wtKLF6 protein expression reverts tumor growth both *in vitro* and *in vivo* (26).

Our experimental findings suggest an important role for the KLF6 tumor suppressor gene in regulating prostate cancer development and progression through two distinct yet complementary pathways. First, decreased expression of wtKLF6 leads to increased proliferation, colony formation, and tumorigenicity *in vivo*. This is the first report demonstrating the biological function of the KLF6 tumor suppressor gene by siRNA-mediated targeted gene silencing in culture and *in vivo*. These findings provide a biologically relevant link to independent studies

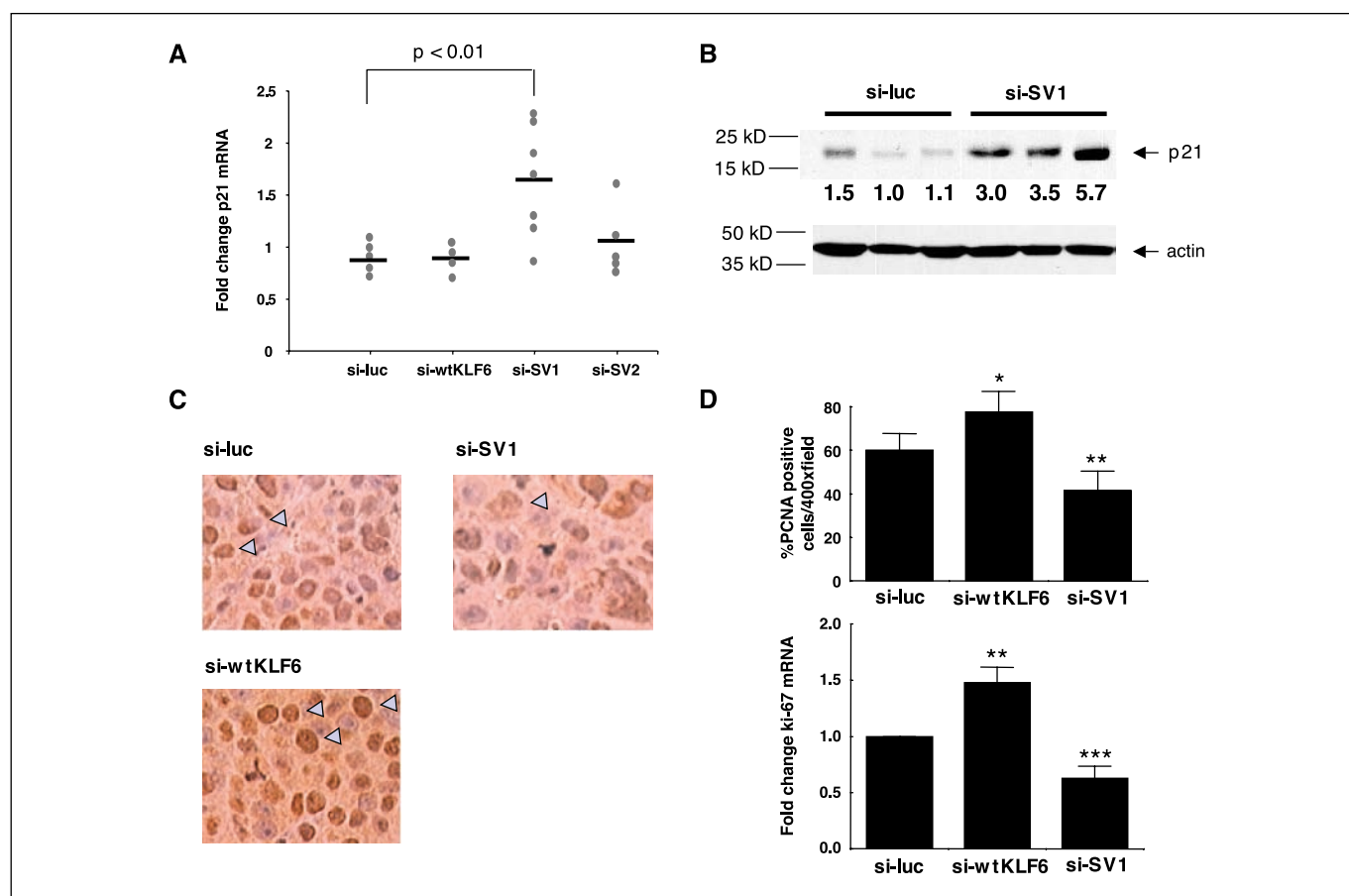


Figure 5. Correlation of cell growth effects with p21 and proliferation markers in tumors stably expressing siRNAs for wtKLF6 or KLF6 SV1. Tumors were analyzed for their expression of p21 mRNA or protein, PCNA, and Ki-67 in response to abrogation of wtKLF6 or KLF6 SV1. **A**, targeted reduction of the KLF6 SV1 protein results in a significant up-regulation of both p21 mRNA and protein as measured by quantitative real-time PCR and Western blotting, respectively. **B**, immunohistochemistry for PCNA in siRNA tumors. Targeted reduction of wtKLF6 results in increased PCNA staining *in vivo* ($P < 0.01$), whereas tumors derived from si-SV1 cells express significantly less PCNA ($P < 0.001$). For each group of tumors, si-luc ($n = 6$), si-wtKLF6 ($n = 5$), and si-SV1 ($n = 7$) six independent high-powered fields for each tumor were counted, assessing both the total number of cells and the number of PCNA-positive cells. The graph represents the average percentage of PCNA-positive cells for each group. **C**, quantitative real-time PCR analysis for Ki-67 mRNA levels in siRNA-derived tumors. Si-SV1 tumors ($n = 7$) expressed significantly less Ki-67 mRNA ($P < 0.0001$) than control luc ($n = 6$) controls, whereas targeted reduction of wtKLF6 ($n = 5$) *in vivo* resulted in an almost 50% increase in Ki-67 mRNA ($P < 0.001$).

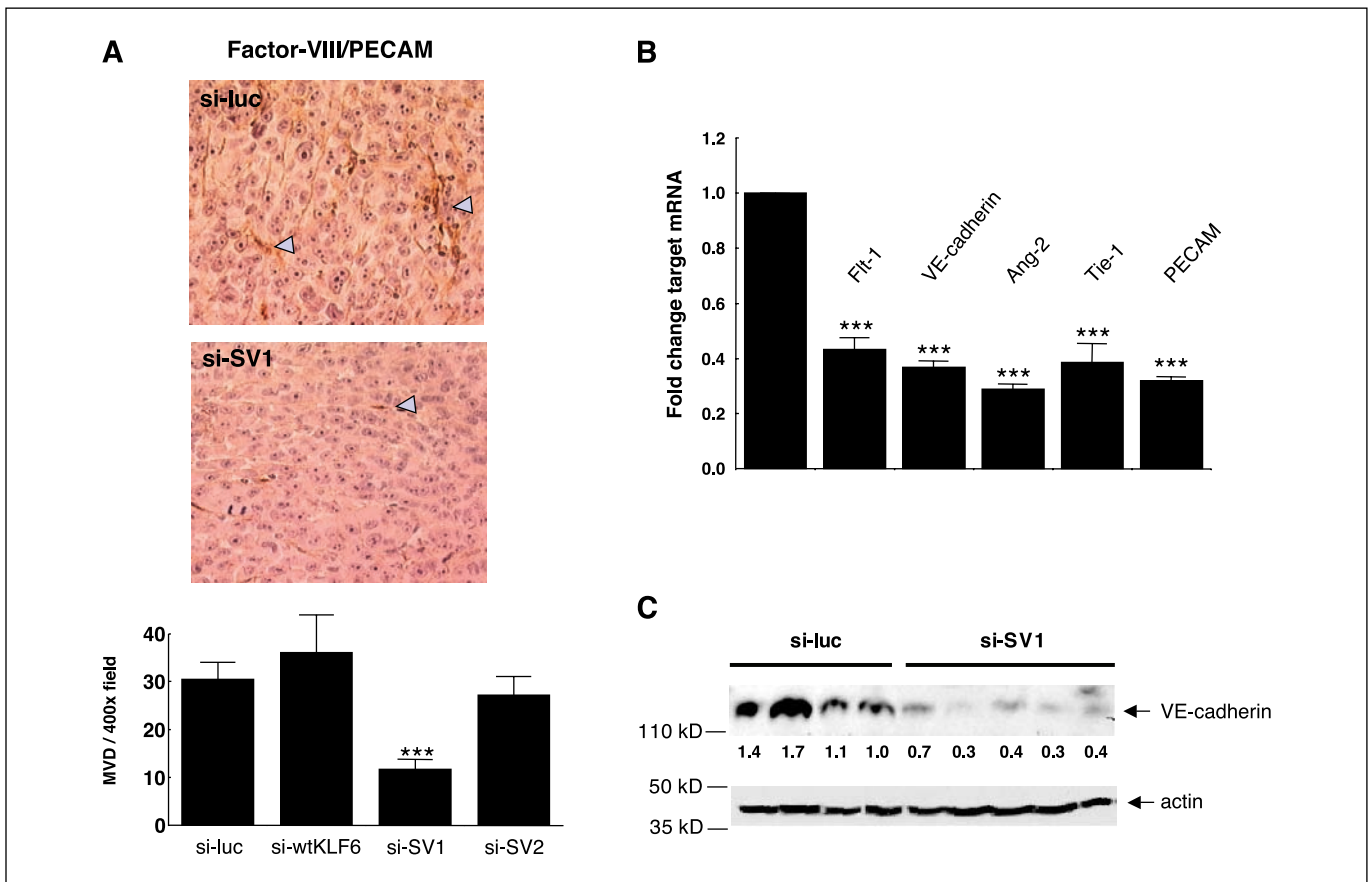


Figure 6. Reduced KLF6 SV1 expression leads to decreased angiogenesis by PC3M-derived tumors *in vivo*. Tumors generated as described in Fig. 5 were analyzed for expression of angiogenesis-related markers *in vivo*. **A**, CD31/PECAM staining of stable siRNA cell line-derived tumors. Targeted reduction of the KLF6 SV1 protein results in a 60% decrease in microvessel density ($P < 0.0001$) as measured by the number of CD31/PECAM-positive endothelial cells per 400 \times field. For each siRNA-derived tumor, four independent 400 \times fields were counted for CD31-positive endothelial cells. **B**, quantitative real-time PCR analysis of a panel of markers of angiogenesis. Si-SV1-derived tumors expressed significantly lower levels of Flt-1, VE-cadherin, Ang-2, Tie-1, and PECAM compared with luc control tumors ($P < 0.0001$). **C**, Western blot analysis of pSUPER-luc and si-SV1-derived tumor protein using a VE-cadherin antibody. Si-SV1 tumors expressed significantly less VE-cadherin protein than control si-luc tumors as measured by densitometry relative to an actin loading control. Three independent si-luc tumors compared with three independent si-SV1 tumors are shown.

demonstrating that decreased KLF6 expression correlates with poor outcomes in lung and prostate cancer (12, 13).

Second, enhanced alternative splicing in a metastatic-derived prostate cancer cell line leads to increased production of the dominant-negative splice variant KLF6 SV1. This isoform antagonizes the ability of wtKLF6 to suppress cell proliferation and tumorigenicity *in vivo*. siRNA-mediated gene silencing experiments suggest that the KLF6 SV1 variant significantly reduces colony formation, migration, invasion, and tumorigenicity. Complementing these studies and suggesting the global importance of these findings to prostate cancer, we have recently shown that the germ line *KLF6* gene IVSΔA polymorphism results in increased prostate cancer risk and increased production of KLF6 SV1 and SV2. Thus, the biological activity of KLF6 SV1 in these studies identifies a possible mechanistic basis for the association of the KLF6 SNP with increased lifetime prostate cancer risk. Indeed, enhanced generation of KLF6 alternative splice forms may contribute to a tumorigenic phenotype independent of either allelic loss, inactivating somatic mutation, or promoter methylation, possibly through a dominant-negative activity on wtKLF6 function. The molecular basis for this effect has yet to be determined.

Similarly, the mechanisms by which the KLF6 family regulates cancer development and progression are still being elucidated. Emerging cell cycle-related mechanisms include up-regulation of the cyclin-dependent kinase inhibitor p21 in a p53-independent manner (2) and disruption of the CDK4/cyclin D1 interaction (10). KLF6 may induce apoptosis and suppress colony formation independent of the p53 tumor suppressor gene (25). Of potential interest, KLF6 and p53 have also recently been shown to physically interact and to cooperate in the transcriptional up-regulation of the insulin-like growth factor-IR gene (27); however, the importance of this interaction in human cancer remains unknown. Combined, these studies highlight not only the general role of KLF6 in cancer pathogenesis but also the mechanisms of its action and regulation on key pathways regulating cell proliferation and angiogenesis in culture and *in vivo*.

The role of dysregulated alternative splicing in disease progression is now being shown in a range of human diseases (28) and cancer in particular (29). Similarly, genomic analysis suggests the existence of cancer-induced splice forms for a number of genes (29). Examples of other known tumor suppressor genes that are alternatively spliced include WT-1 (30), mdm-2

(31), WWOX (32), NF1 (33), Men1 (34), and PTEN (35). In general, dysregulated splicing of many genes and the subsequent generation of alternatively spliced transcripts may reflect a by-product of underlying defects in the genes regulating splice site selection and control and may therefore play little, if any role, in the development of cancer. No reports have suggested biological differences secondary to changes in these genes. In contrast, our findings suggest that cancer-induced/overexpressed splice forms can promote tumorigenesis rather than simply exist as by-products of cancer development.

Although KLF6 alternative splicing is present in both normal and cancerous tissue (14), we suggest that the KLF6 family tumor suppressor gene function is regulated by a critical balance between wild-type and alternatively spliced forms. We show that targeted and specific alterations of this ratio, combined with

specific regulation of KLF6 SV1 levels, have profound effects on many key processes regulating cancer cell growth and metastasis including colony formation, migration, invasion, proliferation, and angiogenesis.

Acknowledgments

Received 1/21/2005; revised 3/11/2005; accepted 4/13/2005.

Grant support: Prostate Cancer Foundation grants (to J.A. Martignetti and S.L. Friedman), DAMD17-02-1-0720 (to J.A. Martignetti and S.L. Friedman), DAMD17-03-1-0129 (to J.A. Martignetti), DAMD17-03-1-0100 (to S.L. Friedman), NIH grant DK37340 (to S.L. Friedman); by grants-in-aid from the T.J. Martell Foundation for Leukemia, Cancer, and Aids Research; and the Manfred Lehmann Cancer Research Foundation (A. Levine).

The costs of publication of this article were defrayed in part by the payment of page charges. This article must therefore be hereby marked *advertisement* in accordance with 18 U.S.C. Section 1734 solely to indicate this fact.

The authors are grateful to Linda Tringo (Mount Sinai School of Medicine) for technical assistance.

References

- Dhanasekaran SM, Barrette TR, Ghosh D, et al. Delineation of prognostic biomarkers in prostate cancer. *Nature* 2001;412:822-6.
- Narla G, Heath KE, Reeves HL, et al. KLF6, a candidate tumor suppressor gene mutated in prostate cancer. *Science* 2001;294:2563-6.
- Chen C, Hyytiäinen ER, Sun X, et al. Deletion, mutation, and loss of expression of KLF6 in human prostate cancer. *Am J Pathol* 2003;162:1349-54.
- Reeves HL, Narla G, Ogunbiyi O, et al. Kruppel-like factor 6 (KLF6) is a tumor-suppressor gene frequently inactivated in colorectal cancer. *Gastroenterology* 2004;126:1090-103.
- Kremer-Tal S, Reeves HL, Narla G, et al. Frequent inactivation of the tumor suppressor Kruppel-like factor 6 (KLF6) in hepatocellular carcinoma. *Hepatology* 2004 Nov;40:1047-52.
- Jeng YM, Hsu HC. KLF6, a putative tumor suppressor gene, is mutated in astrocytic gliomas. *Int J Cancer* 2003;105:625-9.
- Chen HK, Liu XQ, Lin J, Chen TY, Feng QS, Zeng YX. Mutation analysis of KLF6 gene in human nasopharyngeal carcinomas. *Ai Zheng* 2002;21:1047-50.
- Bieker JJ. Kruppel-like factors: three fingers in many pies. *J Biol Chem* 2001;276:34355-8.
- Black AR, Black JD, Azizkhan-Clifford J. Sp1 and Kruppel-like factor family of transcription factors in cell growth regulation and cancer. *J Cell Physiol* 2001;188:143-60.
- Benzeno S, Narla G, Allina J, et al. Cyclin dependent kinase inhibition by the KLF6 tumor suppressor protein through interaction with cyclin D1. *Cancer Res* 2004;64:3885-91.
- Muhlbauer KR, Grone HJ, Ernst T, et al. Analysis of human prostate cancers and cell lines for mutations in the TP53 and KLF6 tumour suppressor genes. *Br J Cancer* 2003;89:687-90.
- Glinksy GV, Glinkii AB, Stephenson AJ, Hoffman RM, Gerald WL. Gene expression profiling predicts clinical outcome of prostate cancer. *J Clin Invest* 2004;113:913-23.
- Kettunen E, Anttila S, Seppänen JK, et al. Differentially expressed genes in nonsmall cell lung cancer: expression profiling of cancer-related genes in squamous cell lung cancer. *Cancer Genet Cytogenet* 2004;149:98-106.
- Narla G, Difeo A, Reeves HL, et al. A germline DNA polymorphism associated with increased prostate cancer risk enhances alternative splicing of the KLF6 tumor suppressor gene. *Cancer Res* 2005;65:1213-22.
- Brummelkamp TR, Bernards R, Agami R. A system for stable expression of short interfering RNAs in mammalian cells. *Science* 2002;296:550-3.
- Weidner N, Carroll PR, Flax J, et al. Tumor angiogenesis correlates with metastasis in invasive prostate carcinoma. *Am J Pathol* 1993;40:143-6.
- O'Reilly MS, Boehm T, Shing Y, et al. Endostatin: an endogenous inhibitor of angiogenesis and tumor growth. *Cell* 1997;88:277-85.
- Igawa T, Lin FF, Rao P, et al. Suppression of LNCaP prostate cancer xenograft tumors by a prostate-specific protein tyrosine phosphatase, prostatic acid phosphatase. *Prostate* 2003;55:247-58.
- Chan AM, Miki T, Meyers KA, et al. A new human oncogene of the ras superfamily unmasked by expression cDNA cloning. *Proc Natl Acad Sci U S A* 1994;91:7558-62.
- Albini A, Iwamoto Y, Kleinman HK, et al. A rapid *in vitro* assay for quantitating the invasive potential of tumor cells. *Cancer Res* 1987;47:3239-45.
- Shih SC, Robinson GS, Perruzzi CA, et al. Molecular profiling of angiogenesis markers. *Am J Pathol* 2002;161:35-41.
- Hayward SW, Dahiya R, Cunha GR, et al. Establishment and characterization of an immortalized but non-transformed human prostate epithelial cell line: BPH-1. *In Vitro Cell Dev Biol Anim* 1995;31:14-24.
- Kozlowski JM, Fidler IJ, Campbell D, et al. Metastatic behavior of human tumor cell lines grown in the nude mouse. *Cancer Res* 1984;44:3522-9.
- Yamashita K, Upadhyay S, Osada M, et al. Pharmacologic unmasking of epigenetically silenced tumor suppressor genes in esophageal squamous cell carcinoma. *Cancer Cell* 2002;2:485-95.
- Ito G, Uchiyama M, Kondo M, et al. Kruppel-like factor 6 (KLF6) is frequently downregulated and induces apoptosis in non-small cell lung cancer cells. *Cancer Res* 2004;11:3838-43.
- Kimmelman AC, Qiao RF, Narla G, et al. Suppression of glioblastoma tumorigenicity by the Kruppel-like transcription factor KLF6. *Oncogene* 2004;29:5077-83.
- Rubinstein M, Idelman G, Plymate SR, et al. Transcriptional activation of the insulin-like growth factor I receptor gene by the Kruppel-like factor 6 (KLF6) tumor suppressor protein: potential interactions between KLF6 and p53. *Endocrinology* 2004;145:3769-77.
- Faustino NA, Cooper TA. Pre-mRNA splicing and human disease. *Genes Dev* 2003;15:419-37.
- Venables JP. Aberrant and alternative splicing in cancer. *Cancer Res* 2004;64:7647-54.
- Hastie ND. Life, sex, and WT1 isoforms—three amino acids can make all the difference. *Cell* 2001;106:391-4.
- Sigalas I, Calvert AH, Anderson JJ, Neal DE, Lunec J. Alternatively spliced mdm2 transcripts with loss of p53 binding domain sequences: transforming ability and frequent detection in human cancer. *Nat Med* 1996;8:912-7.
- Driouch K, Prydz H, Monese R, Johansen H, Lidereau R, Frengen E. Alternative transcripts of the candidate tumor suppressor gene, WWOX, are expressed at high levels in human breast tumors. *Oncogene* 2002;21:1832-40.
- Vandenbroucke I, Callens T, De Paeppe A, Messiaen L. Complex splicing pattern generates great diversity in human NF1 transcripts. *BMC Genomics* 2002;3:13.
- Forsberg L, Zablewska B, Pielh F, et al. Differential expression of multiple alternative spliceforms of the Men1 tumor suppressor gene in mouse. *Int J Mol Med* 2001;8:681-9.
- Sharrard RM, Maitland NJ. Alternative splicing of the human PTEN/MMAC1/TEP1 gene. *Biochim Biophys Acta* 2000;1494:282-5.

**In vivo Regulation of p21 by the KLF6 Tumor Suppressor Gene in
Mouse Liver and Human Hepatocellular Carcinoma**

Goutham Narla*, Sigal Kremer-Tal*, Nobuyuki Matsumoto, Xiao Zhao, Shen Yao,
Kevin Kelley, Mirko Tarocchi, and Scott L. Friedman

From the Departments of Medicine (G.N. S.T.K, S.L.F., N.M, M.T, and X.Z.), Human Genetics (G.N), Oncological Sciences (S.Y.), Brookdale Department of Molecular, Cell, and Developmental Biology (KK), and the Divisions of Liver Diseases (G.N. S.T.K, S.L.F., N.M, M.T, and X.Z.), and Hematology / Oncology (G.N), the Mount Sinai School of Medicine, New York, N.Y.

*These authors contributed equally to the work

Keywords

KLF6, Kruppel-like factor, tumor suppressor gene, p21, haploinsufficiency

Corresponding author:

Scott Friedman, M.D.

Department of Medicine, Box 1123

Mount Sinai School of Medicine

1425 Madison Ave, Room 11-70

New York, NY 10029

Tel 212 659 9501

Email: Scott.Friedman@mssm.edu

Abbreviations:

KLF6 – Kruppel-like factor 6; *wtKLF6* – wild type KLF6, *qRT-PCR* – quantitative real time PCR, WT – wild type, TG - transgenic

Abstract

KLF6 is a tumor suppressor gene functionally inactivated by loss of heterozygosity (LOH), somatic mutation, and/or alternative splicing that generates a dominant negative splice form, KLF6-SV1. Wild type KLF6 expression is also decreased in many human malignancies, which correlates with reduced patient survival. Additionally, loss of the KLF6 locus in the absence of somatic mutation in the remaining allele occurs in a number of human cancers, raising the possibility that haploinsufficiency of the KLF6 gene alone contributes to cellular growth dysregulation and tumorigenesis. Our earlier studies identified the cyclin dependent kinase inhibitor p21 as a transcriptional target of the KLF6 gene in cultured cells, but not *in vivo*. To address this issue, we have generated two genetic mouse models to define the *in vivo* role of KLF6 in regulating cell proliferation and p21 expression. Transgenic over-expression of KLF6 in the liver resulted in a runt phenotype with decreased body and liver size, with evidence of decreased hepatocyte proliferation, increased p21, and reduced PCNA expression. In contrast, mice with targeted deletion of one *KLF6* allele (*KLF6* +/-) display increased liver mass with reduced p21 expression, compared to wild type littermates. Moreover, in primary hepatocellular carcinoma (HCC) samples, there is a significant correlation between *wtKLF6*

and *p21* mRNA expression. Combined, this data suggest that haploinsufficiency of the *KLF6* gene may regulate cellular proliferation *in vivo* through decreased transcriptional activation of the cyclin dependent kinase inhibitor p21.

Main Text

Kruppel-like factor 6 (KLF6) belongs to the Kruppel-like family of transcription factors, which play roles in the regulation of diverse cellular processes including development, differentiation, proliferation, and apoptosis (Bieker, 2001). Functional inactivation of the KLF6 gene occurs through several mechanisms, including loss of heterozygosity (LOH), somatic mutation, and/or increased alternative splicing that yields a dominant negative splice isoform, KLF6-SV1. KLF6 dysregulation has been demonstrated in a number of human cancers including prostate (Chen et al., 2003; Narla et al., 2001), colorectal (Reeves et al., 2004), non-small cell lung (Ito et al., 2004), gastric (Cho et al., 2005), nasopharyngeal (Chen et al., 2002), hepatocellular (Kremer-Tal et al., 2004), and ovarian carcinomas (DiFeo et al., 2006) as well as glioma (Jeng et al., 2003). Furthermore, decreased *KLF6* mRNA expression is associated with reduced patient survival in prostate (Glinsky et al., 2004; Singh et al., 2002) and lung cancers (Kettunen et al., 2004). Interestingly, reconstitution of KLF6 decreases cell proliferation and reverts tumorigenicity in glioblastoma cell lines (Kimmelman et al., 2004).

Depending on cell type and context, KLF6's growth suppressive properties have been associated with key pathways disrupted in human cancer, including p53-independent

upregulation of p21(Narla et al., 2001), reduced interaction of cyclin D1 with CDK4 (Benzeno et al., 2004), induction of apoptosis (Ito et al., 2004), and inhibition of c-jun (Slavin et al., 2004). Recently, a single nucleotide polymorphism (SNP) in the KLF6 gene has been associated with increased prostate cancer risk (Narla et al., 2005).

Overall, the majority of the published data to date report frequent loss of heterozygosity (LOH) of the KLF6 gene locus in primary HCC patient-derived samples. KLF6 LOH was reported in 36% of 14 informative HCC patient samples and somatic mutations were detected in 3 patient samples (Wang et al., 2004). These findings complement our original report describing frequent loss and somatic mutation in primary HCC tumor samples (Kremer-Tal et al., 2004). In a separate study, somatic mutations were identified in 8.7% of patient samples (Pan et al., 2006). In addition, LOH was reported in 6.8% of tumors with no mutation or promoter methylation in a Korean cohort of HCCs (Song et al., 2006). On the other hand, two reports have either failed to identify KLF6 mutations in HCC samples (Boyault et al., 2005) or did not find a decrease in KLF6 mRNA expression in HCCs (Wang et al., 2004), however methodologic differences may account for these discrepant results (Narla et al., 2003). We and others, however, have demonstrated significant downregulation of wtKLF6 expression by both quantitative real time PCR analysis and microarray studies in both HBV and HCV derived HCC patient samples (Kremer-Tal et al., 2006; Lee et al., 2004). Although the frequency of somatic mutation in the KLF6 gene is quite variable, the bulk of evidence from published studies supports a role for the KLF6 tumor suppressor gene in the development and progression of HCC, through either KLF6 loss and / or somatic mutation and decreased wtKLF6 expression.

Interestingly, there are a number of tumor types in which loss of one KLF6 allele

occurs in the absence of somatic mutation in the remaining allele, including glioblastoma, ovarian, gastric and head and neck squamous cell cancers. This finding raises the possibility that haploinsufficiency of the KLF6 gene alone might contribute to increased cellular proliferation and tumor development *in vivo*. To explore this possibility, and to investigate the *in vivo* biologic activity of KLF6, we generated transgenic mice with hepatocyte-specific overexpression of KLF6 by using a well validated transgenic construct (Wu et al., 1996) in which the human KLF6 cDNA was cloned downstream of the transthyretin promoter. Three independent lines of mice, TTR1-KLF6, TTR4-KLF6, and TTR9-KLF6 were generated with modest (~2-3 fold) but reproducible expression of KLF6. Expression of the transgene is confined specifically to hepatocytes with variable expression in the choroid plexus of the brain at high transgene copy number (Wu et al., 1996)(data not shown). Transgenic mice were analyzed at 6 weeks of age since this is the period of rapid murine liver growth and differentiation (Walthall et al., 2005), and studies of mice with hepatocyte specific overexpression of p21 (Wu et al., 1996) demonstrated a significant phenotype during this time period. Compared to wild type littermates, KLF6 transgenic mice had diminished body weight and liver mass, with reduced serum albumin levels; serum ALT and AST levels were normal, however, indicating a lack of hepatocyte injury, as documented also by lack of inflammatory infiltrates within the liver (Table 1). Interestingly, the liver/total body ratio was not different between transgenic and wild type mice suggesting that both are reduced equally in KLF6 transgenic mice. There was no distortion of liver architecture, although the length of portal triades-hepatic plates was greatly reduced (Figure 1a,b). This is nearly identical to the phenotype originally identified in mice in which hepatocyte specific p21 expression was generated using the same promoter (Wu et al., 1996). Expression of proliferating cell nuclear

antigen (PCNA) in hepatocytes of 4-week-old transgenic pups was markedly diminished, consistent with reduced hepatocyte proliferation (Fig 1c,d). There was no increase in cellular apoptosis as assessed by TUNEL (data not shown). Correlating with the decreased liver mass, transgenic mice yielded ~50% fewer hepatocytes than their non-transgenic littermates following cell isolation using standard methods – this difference was a result of decreased cellular proliferation, as assessed by ³H thymidine incorporation and PCNA staining. No differences in apoptosis or cellular viability were noted between transgenic and wild type-derived hepatocytes, as measured by TUNEL staining and FACS analysis. Of note, the altered weight, histology and KLF6 expression were confined to the liver, and there were no differences in these features in any other tissues.

Because an anti-proliferative effect of KLF6 was apparent in the hepatocytes of transgenic mice, and since we had previously established that KLF6 transactivates p21 independent of p53 (Narla et al., 2001), we examined the expression of p21, an inhibitor of several cyclin-dependent kinases and a key regulator of the G1/S transition (el-Deiry et al., 1993). By Western blot there was a 3-fold increase in KLF6 and a 10-fold increase in p21 in transgenic hepatocytes, which was associated with an ~80% reduction in PCNA expression (Figure 1f) and a 50% reduction in DNA synthesis, as assessed by ³H thymidine incorporation compared to hepatocytes isolated from wild type mice (data not shown).

In light of the mounting number of studies reporting *KLF6* involvement in HCC through LOH and / or mutation, and to further establish a direct relationship between KLF6 and p21 *in vivo*, we characterized the livers of *KLF6* heterozygous mice that had been generated by homologous recombination and targeting of KLF6 exon 2, as previously described (Matsumoto et al., 2006). Two independent lines of mice, AH2 and CH2 were

generated and heterozygous AH2 mice were examined. KLF6 heterozygous mice were analyzed between the ages of 50-70 weeks. This time was selected because previous studies describing haploinsufficiency of other tumor suppressor genes including p53, PTEN, and SMAD4 demonstrated growth-relevant phenotypes during this time period. Specifically, mice heterozygous for p53 (Venkatachalam et al., 2001), PTEN (Kwabi-Addo et al., 2001), and SMAD4 (Alberici et al., 2006) demonstrate significant tumorigenic phenotypes within a similar time interval. Compared to wild type littermates, *KLF6* heterozygous mice weighed more and their livers were larger (Figure 2a). Hepatic *KLF6* mRNA levels were reduced by 70% in *KLF6* +/- mice compared to wild type littermates, which were associated with equal reductions in *p21* mRNA, as assessed by quantitative real-time PCR (qRT-PCR) (Figure 2b). These findings were further verified by semi quantitative RT-PCR, as illustrated in Figure 2c. In parallel with the mRNA expression levels from the *KLF6* heterozygous mice, both wt*KLF6* and *p21* protein levels were significantly reduced compared to wild type littermates (Figure 2d and Table 2). Of note, there was no change in the hepatic expression of E-cadherin or iNOS in the heterozygous mice compared to wild type littermates (data not shown), both of which have been previously shown to be regulated by KLF6 in other tissues or cell types (Difeo et al., 2006; Warke et al., 2003). Combined, these results suggest that *KLF6* is a critical regulator of hepatocyte proliferation and liver size *in vivo* at least in part through up-regulation of the cyclin dependent kinase inhibitor *p21*.

We have previously described decreased wt*KLF6* expression in primary HCC samples compared to matched surrounding tissue (ST)(Kremer-Tal et al., 2006). ST were either cirrhotic or non cirrhotic livers (Lee et al., 2004). Based upon our findings in the *KLF6*

mouse models, we examined the levels of KLF6 and p21 expression in a set of 33 of matched HCC-derived tumors (Kremer-Tal et al., 2006) to establish a correlation between p21 and KLF6 expression in patient-derived tumor samples. Real time PCR using wild type KLF6- and p21-specific primers demonstrated a significant correlation between decreased KLF6 and p21 expression in primary tumors compared to matched ST (p value < 0.001) (Figure 3), suggesting that decreased expression of p21 in primary tumors result in part from the down-regulation of the KLF6 tumor suppressor gene.

Previous reports in both ovarian and prostate cancer demonstrated that increased KLF6 alternative splicing into the dominant negative isoform KLF6-SV1 results in functional inactivation of wild type KLF6 tumor suppressive function. Detailed analysis of KLF6 in the HCC samples demonstrated a relatively low prevalence of increased KLF6 splicing (data not shown). In addition, analysis of mouse tissue derived from both transgenic and wild type mice revealed that although the KLF6 gene is alternatively spliced in the mouse, the dominant negative KLF6-SV1 isoform is not expressed.

Our data reveal a unique role for KLF6 in regulating cell growth *in vivo* and suggest that upregulation of the cyclin dependent kinase inhibitor p21 accounts for much of KLF6's growth suppressive properties. In addition, loss of one KLF6 allele, a frequent event in human cancer, leads to decreased wtKLF6 and p21 expression *in vivo* suggesting that haploinsufficiency of the KLF6 gene may also contribute to tumorigenesis. Our results further establish p21 as a transcriptional target of KLF6. In addition to a direct anti-proliferative effect mediated by p21, KLF6 may also indirectly inhibit cell growth through its ability to upregulate the antiproliferative cytokine TGF β 1 and its receptors (Kim et al., 1998) and to stimulate

plasmin mediated activation of latent TGF β 1 by driving transcription of the urokinase type plasminogen activator gene (Botella et al., 2002).

The decrease in hepatic synthetic function in KLF6 transgenic mice may reflect an indirect effect of impaired cellular growth, similar to that observed in transgenic mice with hepatocyte-specific expression of p21(Wu et al., 1996). Alternatively, KLF6 might directly impair hepatocyte differentiation through transactivation of target genes not yet identified. The current studies further enumerate the biologic pathways and mechanisms of KLF6 tumor suppressor gene, and extend previous findings of KLF6 regulation of p21 to mouse models and human cancer *in vivo*. In addition, these current studies highlight the potential for haploinsufficiency of the KLF6 gene in the regulation of cellular proliferation *in vivo*. Combined, these findings highlight not only the general role of KLF6 in cancer pathogenesis, but also the mechanisms of its action and regulation on key pathways regulating cell proliferation *in vivo*.

Acknowledgements

Grant Support: SLF: NIH DK37340, the Bendheim Foundation and the Department of Defense, DAMD17-03-1-0100

Xiao Zhao and Goutham Narla were each supported by a Howard Hughes Medical Institute Medical Student Research Fellowship.

Competing interests statements: The authors disclose that they have no competing financial interests.

Correspondence and requests for materials should be addressed to Scott Friedman (Scott.Friedman@mssm.edu)

References

- Alberici P, Jagmohan-Changur, S, De Pater, E, Van Der Valk, M, Smits, R, Hohenstein, P, et al. (2006). Smad4 haploinsufficiency in mouse models for intestinal cancer. *Oncogene* 25: 1841-1851.
- Benzeno S, Narla, G, Allina, J, Cheng, GZ, Reeves, HL, Banck, MS, et al. (2004). Cyclin-dependent kinase inhibition by the KLF6 tumor suppressor protein through interaction with cyclin D1. *Cancer Res* 64: 3885-3891.
- Bieker J.J. (2001). Kruppel-like factors: Three fingers in many pies. *J Biol Chem* 276: 34355-34358.
- Bissell DM, Guzelian, P.S. (1980). Phenotypic stability of adult rat hepatocytes in primary monolayer culture. *Ann N Y Acad Sci* 349: 85-98.
- Botella LM, Sanchez-Elsner T, Sanz-Rodriguez F, Kojima S, Shimada J, Guerrero-Esteo, M, et al. (2002). Transcriptional activation of endoglin and transforming growth factor-beta signaling components by cooperative interaction between sp1 and KLF6: Their potential role in the response to vascular injury. *Blood* 100: 4001-4010.
- Boyault S , Herault, A , Balabaud, C , Zucman-Rossi, J. (2005). Absence of KLF6 gene mutation in 71 hepatocellular carcinomas. *Hepatology* 41: 681-682; author reply 682-683.
- Chen C , Hyytinen, E R , Sun X , Helin H J, Koivisto PA, Frierson HF, et al. (2003). Deletion, mutation, and loss of expression of KLF6 in human prostate cancer. *Am J Pathol* 162: 1349-1354.

- Chen HK, Liu XQ, Lin J, Chen TY, Feng QS, Zeng, Y.X. (2002). Mutation analysis of KLF6 gene in human nasopharyngeal carcinomas. *Ai Zheng* 21: 1047-1050.
- ChoYG, Kim CJ, Park CH, Yang, YM, Kim SY, Nam SW, et al. (2005). Genetic alterations of the KLF6 gene in gastric cancer. *Oncogene* 24: 4588-4590.
- Difeo A, Narla, G, Camacho-Vanegas O, Nishio H, Rose SL, Buller RE, et al. (2006). E-cadherin is a novel transcriptional target of the KLF6 tumor suppressor. *Oncogene* 25: 6026-31.
- DiFeo A, Narla G, Hirshfeld J, Camacho-Vanegas O, Narla, J, Rose SL, et al. (2006). Roles of KLF6 and KLF6-SV1 in ovarian cancer progression and intraperitoneal dissemination. *Clin Cancer Res* 12: 3730-3739.
- el-Deiry WS, Tokino T, Velculescu VE, Levy DB, Parsons R, Trent, JM, et al. (1993). Waf1, a potential mediator of p53 tumor suppression. *Cell* 75: 817-825.
- Glinsky GV, Glinskii AB, Stephenson AJ, Hoffman RH, Gerald W.L. (2004). Gene expression profiling predicts clinical outcome of prostate cancer. *J Clin Invest* 113: 913-923.
- Ito G, Uchiyama, M., Kondo, M., Mori, S., Usami, N., Maeda, O., et al. (2004). Kruppel-like factor 6 is frequently down-regulated and induces apoptosis in non-small cell lung cancer cells. *Cancer Res* 64: 3838-3843.
- Jeng YM, Hsu H.C. (2003). KLF6, a putative tumor suppressor gene, is mutated in astrocytic gliomas. *Int J Cancer* 105: 625-629.
- Kettunen E, Anttila S, Seppanen JK, Karjalainen A, Edgren H, Lindstrom I, et al. (2004). Differentially expressed genes in nonsmall cell lung cancer: Expression profiling

- of cancer-related genes in squamous cell lung cancer. *Cancer Genet Cytogenet* 149: 98-106.
- Kim Y, Ratziu V, Choi SG, Lalazar A, Theiss G, Dang Q, et al. (1998). Transcriptional activation of transforming growth factor beta1 and its receptors by the Kruppel-like factor Zf9/core promoter-binding protein and Sp1. Potential mechanisms for autocrine fibrogenesis in response to injury. *J Biol Chem* 273: 33750-33758.
- Kimmelman AC, Qiao RF, Narla G, Banno A, Lau N, Bos PD, et al. (2004). Suppression of glioblastoma tumorigenicity by the Kruppel-like transcription factor KLF6. *Oncogene* 23: 5077-5083.
- Kremer-Tal S, Narla G, Chen Y, Hod E, DiFeo A, Yea, S, et al. (2006). Downregulation of KLF6 is an early event in hepatocarcinogenesis, and stimulates proliferation while reducing differentiation. *Journal of Hepatology*, in press.
- Kremer-Tal S, Reeves HL, Narla G, Thung SN, Schwartz M, Difeo A, et al. (2004). Frequent inactivation of the tumor suppressor Kruppel-like factor 6 (KLF6) in hepatocellular carcinoma. *Hepatology* 40: 1047-1052.
- Kwabi-Addo B, Giri D, Schmidt K, Podsypanina K, Parsons R, Greenberg N, et al. (2001). Haploinsufficiency of the PTEN tumor suppressor gene promotes prostate cancer progression. *Proc Natl Acad Sci U S A* 98: 11563-11568.
- Lee JS, Chu IS, Heo J, Calvisi DF, Sun Z, Roskams T, et al. (2004). Classification and prediction of survival in hepatocellular carcinoma by gene expression profiling. *Hepatology* 40:667-676.

- Matsumoto N, Kubo A, Liu H, Akita K, Laub F, Ramirez, F, et al. (2006). Developmental regulation of yolk sac hematopoiesis by Kruppel-like factor 6. *Blood* 107: 1357-1365.
- Narla G, Difeo A, Reeves HL, Schaid DJ, Hirshfeld J, Hod E, et al. (2005). A germline DNA polymorphism enhances alternative splicing of the KLF6 tumor suppressor gene and is associated with increased prostate cancer risk. *Cancer Res* 65: 1213-1222.
- Narla G, Friedman, SL, Martignetti J.A. (2003). Kruppel cripples prostate cancer: KLF6 progress and prospects. *Am J Pathol* 162: 1047-1052.
- Narla G, Heath KE, Reeves HL, Li D, Giono LE, Kimmelman AC, et al. (2001). KLF6, a candidate tumor suppressor gene mutated in prostate cancer. *Science* 294: 2563-2566.
- Pan XC, Chen Z., Chen F, Chen XH, Jin HY, Xu, X.Y. (2006). Inactivation of the tumor suppressor Kruppel-like factor 6 (KLF6) by mutation or decreased expression in hepatocellular carcinomas. *J Zhejiang Univ Sci B* 7: 830-836.
- Reeves HL, Narla G, Ogunbiyi O, Haq AI, Katz A, Benzeno S, et al. (2004). Kruppel-like factor 6 (KLF6) is a tumor-suppressor gene frequently inactivated in colorectal cancer. *Gastroenterology* 126: 1090-1103.
- Singh D, Febbo PG, Ross K, Jackson DG, Manola J, Ladd C, et al. (2002). Gene expression correlates of clinical prostate cancer behavior. *Cancer Cell* 1: 203-209.

- Slavin DA, Koritschoner NP, Prieto CC, Lopez-Diaz FJ, Chatton B, Bocco, J.L. (2004).
A new role for the Kruppel-like transcription factor KLF6 as an inhibitor of c-jun
proto-oncoprotein function. *Oncogene* 23: 8196-8205.
- Song J, Kim CJ, Cho YG, Kim SY, Nam SW, Lee SH, et al. (2006). Genetic and
epigenetic alterations of the KLF6 gene in hepatocellular carcinoma. *J
Gastroenterol Hepatol* 21: 1286-1289.
- Venkatachalam S, Tyner SD, Pickering CR, Boley S, Recio L, French JE., et al. (2001).v
Is p53 haploinsufficient for tumor suppression? Implications for the p53+/- mouse
model in carcinogenicity testing. *Toxicol Pathol* 29 (Suppl): 147-154.
- Walthall K, Cappon GD, Hurtt ME, Zoetis T. (2005). Postnatal development of the
gastrointestinal system: A species comparison. *Birth Defects Res B Dev Reprod
Toxicol* 74: 132-156.
- Wang SP, Chen X P, Qiu F.Z. (2004). A candidate tumor suppressor gene mutated in
primary hepatocellular carcinoma: Kruppel-like factor 6. *Zhonghua Wai Ke Za
Zhi* 42: 1258-1261.
- Warke VG, Nambiar MP, Krishnan S, Tenbrock K, Geller DA, Koritschoner NP, et al.
(2003). Transcriptional activation of the human inducible nitric-oxide synthase
promoter by Kruppel-like factor 6. *J Biol Chem*, 278, 14812-14819.
- Wu H, Wade M, Krall L, Grisham J, Xiong Y, Van Dyke T. (1996). Targeted in vivo
expression of the cyclin-dependent kinase inhibitor p21 halts hepatocyte cell-
cycle progression, postnatal liver development and regeneration. *Genes Dev*
10:245-260.

Table 1. Features of Wild type (WT) and KLF6 Transgenic (TG) Mice

	Wt (n=6)	<u>TG</u> (n=6)
Albumin (g/dL)	2.7 ± 0.1	2.1 ± 1.0
Total Protein (g/dL)	5.2 ± 0.1	3.8 ± 0.5
ALT (units/L)	25 ± 6	21 ± 4
AST (units/L)	62 ± 3	65 ± 6
Weight (g)	11 ± 0.7	8 ± 1

Table 1: Clinical parameters of KLF6 transgenic mice vs. control littermates

Clinical parameters, including serum analysis and body weight for transgenic mice (TG) (6) and wild type (wt) littermates (6) are provided. Serum protein and albumin levels are reduced in the TG compared to wt. In addition, there was no evidence of inflammation in either of the groups to account for these changes as there is no difference in ALT and AST levels. Body weight is reduced in the TG mice compared to WT. ($p < 0.01$)

Table 2. Correlation between wtKLF6 and p21 expression in 33 HCC patient tumor samples compared to matched surrounding tissue (ST)

	High KLF6 levels	Low KLF6 levels	Total
High p21 levels	11	5	16
Low p21 levels	5	12	17
Total	16	17	33

mRNA levels for both KLF6 and p21 in HCC patient samples were categorized as either higher or lower than their matched ST. There was a significant correlation between tumors expressing low levels of p21 and wtKLF6 ($p < 0.05$).

Figure Legends

Figure 1. KLF6 transgenic mice have runted phenotype with increased levels of wtKLF6 and p21. **a.** KLF6 transgenic mice are runted compared to wild type littermates; **b,c.** H&E staining of 5 um sections of livers derived from wild type (b) and KLF6 transgenic mice (c). No distortion of liver architecture or injury is noted, however the length of cell hepatic plates between the ~~portal triads~~ the central vein and the portal triad is greatly reduced. Arrows indicate the hepatic plates. ~~the distance between the portal~~ ~~portal triads~~ **d, e.** Immunohistochemistry using a proliferating cell nuclear antigen (PCNA) antibody on sections of liver derived from wild type (d) and transgenic (e) mice. Decreased or absent PCNA staining is seen in transgenic KLF6 mice consistent with its anti-proliferative effect. **f.** Primary hepatocytes isolated by standard methods (Bissell et al., 1980) were characterized from both transgenic and wild type littermates. Western blotting was performed on cell extracts harvested from three KLF6 transgenic and wild type mice in RIPA buffer (Santa Cruz Biotechnology, Santa Cruz, CA, USA). Equal amounts of protein (50 µg; BioRad, Hercules, CA, USA) DC Protein quantification assay, BioRad) were loaded, separated by polyacrylamide gel electrophoresis, transferred to nitrocellulose membranes and probed with KLF6 (SC-7158), p21 (SC-6246) (Santa Cruz Biotechnology) and PCNA (DAKO) antibodies. KLF6 transgenic mice demonstrated a significant upregulation of the cyclin dependent kinase inhibitor p21, with concomitant decreases in PCNA expression.

Figure 2. KLF6 heterozygous mice have larger livers, with decreased expression of wtKLF6 and p21. **a.** A total of 10 wild type (wt) and 14 KLF6 heterozygous (*Het*) were analyzed. The body and liver weights of the *Het* mice were significantly increased

compared to wt littermates. Error bars represent SEM. **b.** *KLF6* mRNA levels were analyzed in liver samples by qRT-PCR. Livers were homogenized in RLT buffer (Qiagen) and RNA was extracted using RNEasy kit (Qiagen) with DNase. For quantitating target gene expression, one μg of RNA was reverse transcribed for each reaction using first strand cDNA synthesis with random primers (Promega). mRNA levels were quantified by qRT-PCR using the following PCR primers on an ABI PRISM 7900HT (Applied Biosystems): wt*KLF6* Forward: 5'-CGG ACG CAC ACA GGA GAA AA-3' and Reverse: 5'- CGG TGT GCT TTC GGA AGT G-3'; GAPDH Forward: 5'-CAA TGA CCC CTT CAT TGA CC-3' and GAPDH Reverse: 5'- GAT CTC GCT CCT GGA AGA TG-3'; beta-actin Forward: 5' - CCC ACA CTG TGC CCA TCT AC-3' and beta-actin Reverse: 5' - GCT TCT CCT TAA TGT CAC GC-3'; p21 Forward: 5' – ACTCTCAGGGTCGAAAACGG-3' and p21 Reverse: 5' – CCTCGCGCTTCCAGGACTG-3'. All values were calculated by normalizing the levels of each target for each cDNA to both GAPDH and β -actin to determine the relative amount of wt*KLF6* in each sample. All experiments were performed in triplicate and repeated three independent times. In *KLF6* heterozygous mice There was a ~70% reduction in *KLF6* and *p21* mRNA levels compared to age-matched wild type littermate liver samples ($p < 0.001$). **c.** In order to confirm that the high cycle number obtained by qRT-PCR was a true representation of low mRNAs in the tissue and not a technical artifact due to the formation of primer dimers, cDNAs from liver samples were also amplified by conventional PCR using GAPDH, wt*KLF6* and p21 primers as indicated above. PCR reactions were performed for 25, 30, 35 and 40 cycles and the products were separated by agarose gel electrophoresis. While GAPDH expression was evident within

the 25-30 cycles and equal between the wild type and heterozygous derived liver RNA, wtKLF6 and p21 products were detected within the 35-40 cycle range in the livers of KLF6 heterozygous mice, compared to the 30-35 cycle range for wild type mice, indicating decreased wtKLF6 and p21 expression within the livers of KLF6 heterozygous mice. **d.** Mouse livers were homogenized using the T-PER buffer (Pierce, Rockford, IL) and the 60 μ g of each of the lysates were separated by polyacrylamide gel electrophoresis. Gels were transferred to a nitrocellulose membrane that was blotted for KLF6 (1:250; Rabbit 1:2500; Santa Cruz SC-7158), p21 (SC-6246) and GAPDH (SC-32233). KLF6 heterozygous mice had significantly reduced expression of KLF6 and p21 protein compared to wild type littermates.

Figure 3. KLF6 and p21 expression in primary HCC tumor samples is reduced compared to matched ST.

Patient samples were obtained with the approval of the Institutional Review Board (IRB) of all institutions involved, as described recently (Kremer-Tal et al., 2006). wtKLF6 and p21 mRNAs were assessed in 33 HCC and matched surrounding tissue (ST) by qRT-PCR and normalized to GAPDH. wtKLF6 and p21 were significantly reduced in the tumors compared to ST ($p < 0.001$). Error bars represent SEM.